

WL-TR-92-3069

AD-A258 470



ADD-ON DAMPING TREATMENT
FOR THE F-15 UPPER-OUTER
WING SKIN

VINCENT LEVRAEA
DR LYNN ROGERS
ARNEL PACIA

MIKE PARIN

STRUCTURAL DYNAMICS BRANCH
STRUCTURES DIVISION

STRUCTURES ADP BRANCH

JULY 1992

FINAL TECHNICAL REPORT FOR PERIOD 1 JANUARY 1989 TO 28 FEBRUARY 1991

APPROVED FOR PUBLIC RELEASE; DISTRIBUTION IS UNLIMITED.

FLIGHT DYNAMICS DIRECTORATE
WRIGHT LABORATORY
AIR FORCE MATERIEL COMMAND
WRIGHT PATTERSON AIR FORCE BASE, OH 45433-6553

DTIC
ELECTE
DEC 29 1992
S A D

92-33018



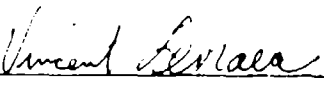
92 12 28 176

NOTICE


When Government drawings, specifications, or other data are used for any purpose other than in connection with a definitely Government-related procurement, the United States Government incurs no responsibility or any obligation whatsoever. The fact that the government may have formulated or in any way supplied the said drawings, specifications, or other data, is not to be regarded by implication, or otherwise in any manner construed, as licensing the holder, or any other person or corporation; or as conveying any rights or permission to manufacture, use, or sell any patented invention that may in any way be related thereto.

This report is releasable to the National Technical Information Services (NTIS). At NTIS, it will be available to the general public, including foreign nations.

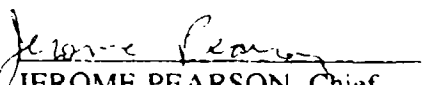
Prepared by:


VINCENT LEVRAEA, Captain, USAF
Project Engineer
Acoustics and Sonic Fatigue Group

Coordination:


RALPH M. SHIMOVETZ, GM-14
Technical Manager
Acoustics and Sonic Fatigue Group

This technical report has been reviewed and is approved for publication.


JEROME PEARSON, Chief
Structural Dynamics Branch

If your address has changed, if you wish to be removed from our mailing list, or if the addressee is no longer employed by your organization please notify WL/FIBGD, WPAFB, OH 45433-6553 to help us maintain a current mailing list.

Copies of this report should not be returned unless return is required by security considerations, contractual obligations, or notice on a specific document.

REPORT DOCUMENTATION PAGE			Form Approved OMB No. 0704-0188	
<small>Public reporting burden for this collection of information is estimated to average 2 hours per response, including the time for reviewing existing information, gathering additional information, reviewing the data needed, and completing and reviewing the collection of information. Send comments regarding this burden estimate or any other aspect of this collection of information, including suggestions for reducing this burden, to Washington Headquarters Office of Management and Budget, Paperwork Project (0704-0188), Washington, DC 20503.</small>				
1. AGENCY USE ONLY (Leave blank)		2. REPORT DATE 26 March 1992		3. REPORT TYPE AND DATES COVERED Final Jan 89 - Feb 91
4. TITLE AND SUBTITLE Add-on Damping Treatment for the F-15 Upper-Outer Wing Skin			5. FUNDING NUMBERS PE: 616200 PR: 2401 TA: 04 WA: 23	
6. AUTHOR(S) Vincent Levraea Arnel Pacia Lynn Rogers Mike Parin				
7. PERFORMING ORGANIZATION NAME(S) AND ADDRESS(ES) STRUCTURAL DYNAMICS BRANCH STRUCTURES DIVISION FLIGHT DYNAMICS DIRECTORATE WRIGHT LABORATORY (WL/FIBG) WRIGHT-PATTERSON AFB OH 45433-6553			8. PERFORMING ORGANIZATION REPORT NUMBER WL-TR-92-3069	
9. SPONSORING / MONITORING AGENCY NAME(S) AND ADDRESS(ES) F-15 Engineering LFLEA Warner-Robins Air Logistics Center Robins AFB GA			10. SPONSORING / MONITORING AGENCY REPORT NUMBER	
11. SUPPLEMENTARY NOTES				
12a. DISTRIBUTION / AVAILABILITY STATEMENT Approved for Public Release; Distribution is Unlimited.			12b. DISTRIBUTION CODE	
13. ABSTRACT (Maximum 200 words) The purpose of this investigation was to design, fabricate, and verify candidate add-on damping treatments for the F-15 upper-outer wing skin. The F-15 upper-outer wing skin has experienced high cycle fatigue cracks caused by separated flow on the upper wing surface. The separated flow results during high load factor maneuvers, and in turn induces large vibratory loads on the upper wing skin and associated substructure. The capability of the F-15 to sustain these maneuvers allows the excitation to occur for sufficiently long periods of time to result in damage. Damage accumulates due to the resonant vibration of local skin/stiffener modes. The cracks initiate at the fastener holes adjacent to the integrally machined "T" stiffeners and tend to propagate parallel to the stiffeners. Two damping treatments resulted from the investigation and were recommended for F-15 fleet retrofit. One was an external constrained-layer treatment and the other was an internal "stand-off" treatment. Laboratory vibration, corrosion, and thermal aging tests were conducted as part of the development of the add-on damping treatments. Estimates of the life extension factors for the external and internal damping treatments were 5 and 34, respectively.				
14. SUBJECT TERMS Aircraft Vibration Resonant Vibration Vibration Damping Constrained Layer Damping Viscoelastic Damping Fatigue			15. NUMBER OF PAGES 119	
			16. PRICE CODE	
17. SECURITY CLASSIFICATION OF REPORT UNCLASSIFIED	18. SECURITY CLASSIFICATION OF THIS PAGE UNCLASSIFIED	19. SECURITY CLASSIFICATION OF ABSTRACT UNCLASSIFIED	20. LIMITATION OF ABSTRACT UL	

FOREWORD

This report describes the development of candidate F-15 wing add-on damping treatments by personnel in the Structural Dynamics and Structures ADP Branches of the Structures Division, Flight Dynamics Directorate, Wright Laboratory, Wright-Patterson Air Force Base, Ohio, for the support project 24010423, "Viscoelastic Damping for the F-15 Wing."

This report covers the damping treatment development work performed between January 1989 and February 1991, including the laboratory vibration, corrosion, and thermal aging tests conducted on the damping treatments. The project supported the F-15 Engineering Office (LFLEA), Warner-Robins Air Logistics Center, Robins Air Force Base, Georgia. The authors wish to acknowledge the work contributed to this effort by Kevin Harris, Michael Banford, Earl Rogers, and Michael Hart. Their support led to the successful completion of this project.

1-1

1-1

Accession For	
NTIS CR81	
DTIC TAB	
Unannounced	
Justification	
By	
Distribution/	
Availability Codes	
Dist	Avail and/or Special
A I	

TABLE OF CONTENTS

SECTION	PAGE
FOREWORD	iii
List of Figures	v
I. INTRODUCTION	1
II. BACKGROUND	2
III. MODAL TESTS	4
A. <u>LASER VIDEO HOLOGRAPHY</u>	4
B. <u>MODAL TEST OF THE SKIN SURFACE</u>	4
C. <u>MODAL TEST ON THE STIFFENERS</u>	5
D. <u>RESULTS OF MODAL TESTING</u>	6
IV. DAMPING TREATMENTS	7
A. <u>DAMPING TREATMENT SELECTION</u>	8
B. <u>RECOMMENDED DESIGN</u>	9
C. <u>INSTALLATION</u>	9
V. FLIGHT DATA	11
VI. DISCUSSION	13
A. <u>LIFE EXTENSION</u>	13
B. <u>COST SAVINGS</u>	13
VII. CONCLUSIONS	15
VIII. RECOMMENDATIONS	16
APPENDIX A: DAMPING TREATMENT CONFIGURATIONS	17
APPENDIX B: METHODOLOGY FOR CALCULATION OF LIFE EXTENSION	18
APPENDIX C: CORROSION TESTS	22
APPENDIX D: THERMAL AGING TESTS	24
BIBLIOGRAPHY	119

List of Figures

Figure	Title	PAGE
1	F-15 Aircraft	26
2	F-15 Wing Substructure	27
3	Right Upper-Outer Wing Skin (UOWS)	28
4	Close-up of a Damaged UOWS	29
5	Detail of External Straps	30
6	Cracks in Rib 206 Fastener Holes Between Stiffeners 4 and 5	31
7	Cracks in Rib 206 Fastener Holes Between Stiffeners 7 and 8	32
8	Damaged F-15 Outer Torque Box Rib	33
9	Spar-Rib Bay Designation	34
10	Streamlines for an Airfoil at 12° AOA	35
11	Video Holography Equipment	36
12	F-15 Wing With Reflective Tape	37
13	Detail of Shaker Attachment	38
14	Video Holography Mode Shapes for UOWS	39
15	Video Holography Mode Shapes for UOWS cont'd	40
16	Video Holography Mode Shapes for UOWS cont'd	41
17	Video Holography Mode Shapes for UOWS cont'd	42
18	Video Holography Mode Shapes for UOWS cont'd	43

19	Video Holography Mode Shapes for UOWS cont'd	44
20	Video Holography Mode Shapes for UOWS cont'd	45
21	Video Holography Mode Shapes for UOWS cont'd	46
22	Accelerometer Locations on Wing	47
23	Accelerometer Grid Point Locations on Wing Skin	48
24	Accelerometer Grid Point Locations on Stiffeners	49
25	Accelerometer Locations on Stiffeners	50
26	Modal Indicator Function for Skin Response	51
27	Modal Indicator Function for Stiffener Response	52
28	Combined Skin and Stiffener Mode Shape at 299.1 Hz	53
29	Combined Skin and Stiffener Mode Shape at 306.3 Hz	54
30	Combined Skin and Stiffener Mode Shape at 314.3 Hz	55
31	Combined Skin and Stiffener Mode Shape at 333.4 Hz	56
32	Combined Skin and Stiffener Mode Shape at 346.0 Hz	57
33	Combined Skin and Stiffener Mode Shape at 371.2 Hz	58
34	Combined Skin and Stiffener Mode Shape at 395.5 Hz	59
35	F-15 Aircraft Performance Data	60
36	F-15 Load Factor Curves	61
37	"1980 Damping Treatment"	62
38	"1980 Damping Treatment" Installed on F-15 Wing	63
39	External Damping Treatment Design	64

40	External Damping Treatment	65
41	Internal Damping Treatment Design	66
42	Internal Damping Treatment	67
43	Placement of VELs in Rib Notches	68
44	VEL Locations	69
45	Application of the External Damping Treatment	70
46	External Treatment Installation	71
47	Strain Gage Locations for Flight Tests	72
48	Typical Flight Conditions	73
49	PSD of Strain Gage Flight Data	74
50	Comparison of the Baseline UOWS and the UOWS With External Damping Treatment	75
51	Comparison of the Baseline UOWS and the UOWS With Internal Damping Treatment	76
52	Life Extension Factor Calculation	77
A1	Four Basic Damping Treatment Lay-ups	78
A2	Details on Damping Treatment Lay-ups	79
A3	Tested Damping Treatment Configurations	80
A4	Test Configuration 2	81
A5	Test Configuration 3	82
A6	Test Configuration 4	83
A7	Test Configuration 5	84

A8	Test Configuration 6	85
A9	Test Configuration 7	86
A10	Test Configuration 8	87
A11	Test Configuration 9	88
A12	Test Configuration 10	89
A13	Test Configuration 11	90
A14	Damped Flow Fences	91
A15	Test Results for Damping Configurations	92
A16	Life Extension Factors	93
B1	Typical S-N Curve	94
B2	Life Extension Factor Calculation	95
C1	Damping System Cross-Selections	96
C2	Bare Test Panel After Corrosion Test	97
C3	"1980 Damping Treatment" With Edge Sealant After Corrosion Test	98
C4	Partially Removed "1980 Damping Treatment" With Edge Sealant After Corrosion Test	99
C5	"1980 Damping Treatment" After Corrosion Test	100
C6	Partially Removed "1980 Damping Treatment" After Corrosion Test	101
C7	External Treatment After Corrosion Test	102
C8	Partially Removed External Treatment After Corrosion Test	103

C9	External Treatment With Edge Sealant After Corrosion Test	104
C10	Partially Removed External Treatment With Edge Sealant After Corrosion Test	105
C11	Internal Treatment After Corrosion Test	106
C12	Partially Removed Internal Treatment After Corrosion Test	107
C13	Internal Treatment With Edge Sealant After Corrosion Test	108
C14	Exposed Stand-off Layer for Internal Treatment With Edge Sealant After Corrosion Test	109
C15	Partially Removed Internal Treatment With Edge Sealant	110
C16	Viscoelastic Link After Corrosion Test	111
C17	Partially Removed Viscoelastic Link After Corrosion Test	112
D1	"1980 Damping Treatment" Exposed to Actual Field Service	113
D2	"1980 Damping Treatment" Exposed to Laboratory Thermal Aging	114
D3	Cantilever Beam Test Set-up	115
D4	"1980 Damping Treatment" Thermal Aging Results	116
D5	Stand-off Damping Treatment Thermal Aging Results	117
D6	Viscoelastic Link Thermal Aging Results	118

I. INTRODUCTION

The requirement for high performance fighter aircraft places tremendous demands on the components and materials from which these aircraft are constructed. Inherent with high performance are high vibration levels. One possible cause of large vibratory loads is separated flow. Separated flow presents an unpredictable and complex environment. Within this environment it is often impossible to estimate the precise dynamic flow characteristics or loading conditions that aircraft components may experience during flight. If not properly accounted for in the design phase, large vibratory loads can result in high cycle fatigue and a substantial reduction in the useful service life of the component. Aircraft skins, in particular outboard wing skins, are relatively light weight structures which are extremely susceptible to vibration response induced by separated flow.

The F-15 upper-outer wing skin (UOWS) panel has experienced cracks resulting from high cycle fatigue. The F-15 aircraft, shown in Figure 1, has sufficient thrust to perform sustained, high load maneuvers. Consequent separated flow over the wing panel contains high-level broad-band random pressure fluctuations and induces large vibratory response in the UOWS panel and associated wing substructure. The resulting elevated stresses over time cause high cycle fatigue cracks to form in the wing skin. Historically, UOWS cracking dates to the late 1970s and early 1980s. At that time, the cracks were considered to occur only over a small portion of the skin closest to the wing tip. Later findings show that the entire UOWS is prone to cracking.

The UOWS was originally designed for a service life of 8,000 hours. Unfortunately, the initial service life realized was only 250 hours. Several modifications were incorporated by the contractor in the early 1980s to improve the fatigue life of the skin, including fortifying critical locations on the wing skin. The modifications were initially thought to have resolved the fatigue cracking problem. In reality these changes only increased the life of the skin to approximately 1,250 hours. The need still remained to increase the service life to the original design value of 8,000 hours. Dr. Rogers of the Structures Division contacted Warner-Robins Air Logistics Center (W-R ALC), initiating the Structural Dynamics and Structures ADP Branches study of the UOWS high cycle fatigue problem.

The purpose of this investigation was to design, fabricate, and verify candidate add-on damping treatments for the F-15 UOWS that would alleviate the fatigue cracks caused by separated flow on the upper wing surface and increase the UOWS service life to the desired 8,000 hours. Two candidate damping treatments resulted from the investigation and were recommended to W-R ALC for fleet retrofit. One treatment was a field installable external system, and the other was an internal depot installable system. Neither system required modifications to the existing wing structure.

II. BACKGROUND

The F-15 UOWS is machined from a single block of 2024 aluminum and consists of the skin, integrally machined "T" stiffeners, and chemically milled pockets between the stiffeners. The thickness of the UOWS varies from location to location on the panel, but averages approximately 0.080 inches thick. Figure 2 shows the major substructure for the left wing. The UOWS extends from rib 155 to rib 224, and from the front spar to the rear spar. There are intermediate ribs at locations 172, 188, and 206. At rib 188, the front, main, and rear spars are at 10%, 45%, and 65% chord, respectively. Collectively, these members constitute the outer wing torque box. The wing skin measures approximately 5 feet wide by 7 feet long measuring along rib 188 and the main spar, respectively. Inboard of rib 155 the wing is "wet," that is, the volume is used for fuel storage. The outer torque box is "dry." Blind threaded, flush fasteners are used to attach the skin to the rib and spar substructure. A right-hand UOWS, removed from active service due to cracking, is shown in Figure 3. Visible in Figure 3 are the integral stiffeners and their runouts, spar and rib fastener holes, and various panel access holes. Stiffeners are numbered consecutively starting at the UOWS leading edge. The stiffeners are not clipped to the ribs but are allowed to move freely within the rib notch. The cracks develop in the rib fastener holes adjacent to the stiffeners. Predominantly, the cracks initiate either perpendicular to the ribs or parallel to the stiffeners. A close-up of a damaged UOWS, showing the crack locations, is presented in Figure 4. Close inspection of Figure 4 reveals the extra holes in the skin used for fastening the external stainless steel straps on top of rib lines 188 and 206. The external straps, detailed in Figure 5, were an interim fix to extend the service life of cracked wing skins; this fix was abandoned several years ago. Figures 6 and 7 show close-ups of the cracks in the scrapped UOWS occurring in rib 206 fastener holes. Extra holes for the external straps are also visible. Based on the crack patterns and the unclipped stiffener design, it was concluded that the skin cracks were most likely induced by stiffener rotation. The flow induced vibration also results in damage to the outer torque box substructure. A photograph of a cracked rib is shown in Figure 8. Figure 9 gives a convenient shorthand designation for the spar-rib bays which will be used throughout the remainder of this report to aid the reader in locating specific portions of the UOWS.

The UOWS cracks are caused by high cycle fatigue. Damage accumulates due to resonant vibration of local skin/stiffener modes excited by external oscillatory pressure resulting from separated flow. The excitation occurs during high load factor maneuvers. The capability of the F-15 to sustain these maneuvers allows the excitation to result in significant cumulative damage. Figure 10 is a photo of smoke streamlines for a typical airfoil at 12° angle-of-attack (AOA) and shows separated air flow. Other investigations concerning the aerodynamic characteristics of the F-15 suggest that 12° angle-of-attack provides the most severe disturbances and consequently the most

damage.

The locations where UOWS fatigue cracks were observed evolved during the course of this investigation. Initially, the concern was for the web of stiffener 4 in bay L1 (see Figure 9) and over rib 206 between bays L1 and L2. Next, it was observed that cracks also occurred over rib 188 between bays L2 and L3. Finally, it was learned that cracks occur over ribs 188 and 206 between the main and rear spars. Ribs 188 and 206 themselves crack, but were not specifically addressed in this study. The reinforcements around the numerous access panels in bays L4 and R4 result in a significantly heavier structure and made this area less susceptible to fatigue cracking. Thus, with the exception of bays L4 and R4, high cycle fatigue cracks were observed over the entire UOWS panel.

III. MODAL TESTS

To ascertain the cause of the problem, modal tests were conducted on a full-scale F-15A wing in the laboratory. The modal tests were done in three phases. The first test used laser video holography, and the second and third phases used more traditional multi-accelerometer surveys.

A. LASER VIDEO HOLOGRAPHY

Laser video holography shows mode shapes right on a video monitor as the structure is being excited at discrete resonant frequencies. The video holography equipment is shown in Figure 11. The equipment consisted of a Retra 1000 holography unit, a variable phase digital synthesizer, a power amplifier, a freeze frame unit, and a video monitor.

For this test, the wing was leaned against a wall of the Branch's Large Acoustics Chamber as shown in Figure 12. Acoustic foam was inserted between the leading edge and the floor to dampen any noise transmitted from the floor. The wing was excited from the back by a Delta Dynamics 10 pound electrodynamic shaker. A suction cup was used to attach the shaker to the wing; see Figure 13. The shaker was placed where stiffener 6 and rib 224 of the wing intersect. Highly reflective tape was attached to the wing in order to better reflect the laser light. The mode shapes were recorded using a video cassette recorder. Both sine sweeps and sine dwells were used to extract the modes.

Numerous wing skin modes were found. They were found to be closely spaced in terms of frequencies; slight changes in the frequency of the excitation altered the mode shape, although the overall mode shapes over a range of frequencies remained relatively similar. Figures 14-21 shows the UOWS mode shapes for resonant frequencies between 200 and 850 Hz. The fringe patterns shown in these figures resemble a contour map of the deformed wing skin. Each successive fringe represents an additional displacement of one-half the wavelength of the laser light. This displacement is relative to the undeformed UOWS and therefore represents a peak displacement. For the HeNe laser used, one half of the wave length is about 12.46 microinches.

B. MODAL TEST OF THE SKIN SURFACE

The second phase of the modal test of the F-15 UOWS was a more conventional modal test employing roving accelerometers. For this test the wing was

laid horizontally with the UOWS panel facing up. One end was supported by the massive fuselage attachment structure while the wing tip was supported by a wooden 2 inch x 4 inch cribbing such that the area of interest was relatively horizontal and approximately 2 feet off the ground. It was assumed that the boundary conditions represented by this configuration, although hardly realistic, were inconsequential to the results, since we were only interested in the panel and stiffener modes of the UOWS.

Twelve PCB Structcel accelerometers were used to measure the response of the UOWS when exposed to 0-1000 Hz random noise excitation. The wing was excited using a Delta Dynamics 10 pound shaker. A grid consisting of 170 nodes was laid out to map the wing skin mode shapes. Figures 22 and 23 show the location of the grid points on the wing. Great care was used in spreading out the accelerometers on the structure to avoid mass loading. Accelerometers were moved 15 times to completely map the entire grid. A PCB 208A03 force gage measured the force input to the structure.

A Honeywell 101 magnetic tape recorder was used to record the acceleration response of the wing skin. Twelve tracks of the tape were used for the accelerometers, one track for the force gage, another for the time code and another for the voice. The runs were recorded at 7.5 ips (inches per second).

Before the data were recorded, the transducer signals were conditioned. Transducer signals were passed through Precision Devices model 744PB-3 antialiasing filters with their roll-off frequency set at 1,000 Hz. Next, the signals were passed through Intech auto gain ranging amplifiers to make sure there was good dynamic range before recording. Finally, before recording, each channel was examined with an oscilloscope, again to make sure of the quality of the data.

The analog data recorded on magnetic tape were digitized and analyzed by the Analysis Group of the Structural Dynamics Branch. A VAX computer and analysis software developed in-house were used to perform discrete Fast Fourier Transforms on the digitized time histories. The resulting transfer functions were stored in Universal file format, which the Structural Dynamics Research Corporation (SDRC) program Test Data Analysis System (TDAS) readily converted to Function Associated Data Files (ADFs). TDAS used the ADFs to extract the resonant frequencies, mode shapes, modal damping, modal assurance criteria, etc.

C. MODAL TEST ON THE STIFFENERS

Once the modal test on the skin surface was completed, the upper skin was removed and instrumented with 27 Vibrametrics M1000-8A accelerometers. For this

test the accelerometers were placed on the stiffeners. Figures 24 and 25 show the locations of the accelerometers on the stiffeners. The accelerometers were attached to the stiffeners with 5-minute epoxy. Rubber boots were placed over the accelerometers to insulate them, thus reducing the effects of temperature transients. With the change of accelerometers, the data acquisition system had to be changed; however, the Delta Dynamics 1016 shaker and the PCB 208A03 force gage were again employed.

The set-up using the PCB Structcels were not appropriate for the Vibrametrics M1000-8A because the latter required 15V DC excitation. Therefore, an alternative data acquisition system was used. This system used diodes to provide constant current to the accelerometers. Like the previous arrangement, the transducer signals were passed through Precision Devices model 744PB-3 antialiasing filters set at 1000 Hz cut-off frequency, and through Intech auto gain ranging amplifiers. The transducer output signals, along with the time code and voice, were stored using the Honeywell 96 FM analog magnetic tape recorder. Once again, the Analysis Group digitized and analyzed the data. TDAS was also used to obtain the modal parameters.

D. RESULTS OF MODAL TESTING

Mode shapes and other modal parameters were obtained from the transfer functions gathered during the modal surveys on the skin and stiffeners. Figures 26 and 27 contain modal indicator functions for the skin test data and the stiffener test data, respectively. The modal indicator function represents the relative strength of each mode plotted on a logarithmic scale. Figures 26 and 27 showed that a number of resonant frequencies were shared by the skin and stiffeners. This was expected because the skin and stiffeners are one structure. Mode shapes were generated of the skin by itself, the stiffeners by themselves, and the skin and stiffeners combined. Figures 28 through 34 show some of the skin and stiffener modes. The strong correlation between the stiffener and the skin motion led to a damping design applied to both the skin and stiffeners which yielded the necessary increase in the service life of the wing skin. The damping treatments developed are discussed in the next section.

IV. DAMPING TREATMENTS

This study investigated the performance of 13 different candidate add-on damping treatment configurations under laboratory conditions. For brevity, only the "1980 Damping Treatment" and the two new damping treatments which were recommended to W-R ALC are discussed in this section. A detailed description of the additional configurations tested is given in Appendix A.

Past damping experience suggested that a constrained-layer damping treatment would offer the most viable, cost effective solution. A constrained-layer damping system consists of a layer of viscoelastic material (VEM) which is constrained by a metal layer. Often this type of damping system will be constructed of multiple constrained layers to achieve the desired level of damping. Whenever the structure undergoes bending, the metal layer will constrain the viscoelastic material, resulting in shear deformation of the VEM. Energy is dissipated due to this shear deformation.

An important part of designing a damping treatment is determining the environmental condition to which the treatment will be exposed and ensuring that the selected treatment will withstand and perform properly under these conditions. Critical environmental considerations include the operational temperature range for which damping is desired, the effects of the damping treatment on corrosion of the structure, and the effects of thermal aging on the performance of the damping treatment. Recent laboratory corrosion testing showed no degradation in corrosion resistance caused by the application of the recommended damping treatments. The corrosion test panels were exposed to a standard 30-day humidity corrosion environment in the laboratory consisting of 120° F, 98% relative humidity, and salt spray. The addition of the damping treatments had no effect on corrosion, primarily because the UOWS paint was not disturbed during installation. Extensive service experience with similar damping treatments has not revealed any corrosion problems. For example, the "1980 Damping Treatment" has flown externally on approximately 300 aircraft for 10 years with no adverse effects on corrosion. Although the requirements used to develop the thermal aging tests were judged to be excessive, satisfactory thermal aging characteristics were demonstrated in the laboratory for all materials used in the new damping treatments. The temperature exposure of 8 hours at 340° F plus 48 hours at 270° F was intended to be a conservative design condition for the 8,000-hour life; however, these exposure levels are believed to be more severe than necessary. Thousands of hours of F-111 service data establish that the stagnation temperature exceeds 125° F less than 1% of the time. Laboratory tests confirmed that thermal aging caused the damping material to stiffen slightly, but did not adversely affect the effectiveness of the damping treatment. An additional issue of practicality is the ability to inspect the UOWS for structural integrity with the damping treatment installed. The damping treatment configurations in no instance covered up fasteners or locations where the cracks

initiate. Therefore, the damping treatments will not hinder inspection of the UOWS either visually or radiographically and the treatments also will not impact removal or installation of the UOWS or other maintenance functions. The details of the corrosion and thermal aging tests are deferred to Appendices C and D. A discussion on the selection of the damping treatment design temperature range follows.

A. DAMPING TREATMENT SELECTION

A plot of Mach number versus altitude is presented in Figure 35 for the F-15 aircraft. Figure 36 is extracted from the F-15 tech orders and substantiates the load factor curves of Figure 35. Included on the plot in Figure 35 are standard day constant value curves for the following parameters: dynamic pressure (q), stagnation temperature, and maneuver load factor. The load factor is for an F-15 with a gross weight of 42,000 pounds flying at a 12° AOA. The equilibrium temperature for the wing skin and the installed damping treatment will fall between the stagnation temperature and the ambient temperature. The large dash marks in Figure 35 indicate planned data gathering flight conditions. Because the ratio of oscillatory pressure to dynamic pressure tends to be a constant in the subsonic flight regime, the oscillatory pressure (thus the cumulative damage) increases as Mach 1.0 at sea level is approached from the upper left on the graph. The structural limit of the F-15 is approximately 8g. Based on this, a temperature range from 50° F to 75° F was selected for the damping design. No cumulative damage was expected below 0° F or above 125° F.

A previous attempt by MCAIR to correct the UOWS fatigue cracking included the application of a multiple constrained-layer damping treatment referred to as the "1980 Damping Treatment." The treatment was applied externally over bay L1 of the skin (see Figure 9) because at the time, the fatigue cracks were considered to occur only in this outer spar-rib bay. It consisted of three constrained layers, each containing a 0.002 inch layer of ISD-112 VEM and a 0.005 inch layer of aluminum. Figure 37 illustrates the "1980 Damping Treatment" which for this investigation was denoted Test Configuration 1 (TC1). Figure 38 is a photo of the "1980 Damping Treatment" installed on an F-15 wing. Note the ramp of sealant around the circumference of the treatment to protect the edge from the air flow and prevent moisture from getting under the treatment. After paint is applied to the top constraining layer and the sealant, the damping treatment is barely noticeable. The "1980 Damping Treatment" was installed and flown on numerous operational F-15 aircraft but it proved to be unsuccessful in eliminating the UOWS fatigue cracks.

As previously mentioned, the Flight Dynamics Directorate developed two new damping treatments which were recommended to W-R ALC for F-15 fleet retrofit. The treatments consisted of an externally applied, field installable system and an internally applied, depot installable system. Figure 39 shows the recommended

external multiple (4) constrained layer configuration. Two different constrained layers were used in the external treatment design. One consisted of a 0.002 inch layer of ISD-112 VEM constrained by a 0.005 inch layer of aluminum and the other was made of a 0.002 inch layer of ISD-113 VEM also constrained by a 0.005 inch layer of aluminum. Two each of these different constrained layers were used to build up the total of four constrained layers in the external treatment design. The use of two VEMs broadened the effective temperature range relative to the "1980 Damping Treatment." The six outer most spar-rib bays were covered (R1, R2, R3, L1, L2, and L3) by the external treatment. Figure 40 is a photo of the external treatment installed on an F-15 wing.

B. RECOMMENDED DESIGN

The recommended internal treatment design is summarized in Figure 41. Starting at the wing skin, there was a 0.004 inch layer of pressure sensitive adhesive (PSA) which performed as a VEM. Next there was an 0.080 inch stand-off layer of syntactic foam configured to maintain high shear stiffness and low flexural stiffness. This was achieved by cutting a checker board pattern into the syntactic foam. Finally, three constrained layers of damping material were placed on top of the stand-off layer. The first constrained layer (from the bottom) consisted of 0.004 inch of VEM constrained by 0.005 inch of aluminum. The other two constrained layers each consisted of 0.002 inch of VEM constrained by 0.005 inch of aluminum. For all layers the Hueston Industries F-440 VEM was used. The internal damping treatment was applied in the chemically-milled pockets between the integral stiffeners for all 8 spar-rib bays shown in Figure 9. Additionally, there were viscoelastic links (VELs) placed between the caps of the integral stiffeners and the notches in the ribs. The VELs were located in all rib notch locations. The VEL material was slightly tacky at room temperature. A VEL thickness of 0.50 inch was used to provide an interference fit. The purpose of the VEL was to provide a link (having both stiffness and damping) from the stiffener cap to ground (rib notch), thereby reducing stiffener rotation. Figure 42 shows the stand-off damping treatment applied to the internal surface of the wing skin. Figures 43 and 44 shows the VELs located in the rib notches.

C. INSTALLATION

The installation of the damping treatments was simple and straightforward. A description of the external treatment installation follows. First the UOWS was cleaned with solvent to remove all oil and dirt. Next, the external damping treatment was pre-cut to fit between the fastener rows for each spar-rib bay. The treatment was sized to ensure that access to the fasteners was not impaired. Next, a small amount of split peel ply or release paper was removed from the bottom of the damping treatment, exposing the first layer of VEM. The damping treatment was then carefully centered

onto the appropriate spar-rib bay. Figure 45 illustrates this step. Finally, the procedure was to gradually remove the release paper from under the damping treatment while simultaneously adhering the treatment. Special care was necessary to minimize entrapped air bubbles. A small, flat plastic scraper was rubbed over the surface of the external treatment as it was applied to squeeze out as much air as possible. This step is illustrated in Figure 46. A nice feature of the external damping treatment was that small amounts of compound curvature could be accommodated without adversely affecting the quality of the application.

The internal stand-off treatment was applied in a similar manner except additional effort was required to avoid damaging the brittle stand-off layer. The pieces of internal damping treatment were much smaller than the external damping pieces and therefore air entrapment was not a problem. Hand pressure was sufficient to apply the internal treatment so the plastic scraper was not used. The VELs were provided with release paper on the two surfaces which were to adhere to the skin stiffener and the rib notch. During installation, the release paper on the rib notch side was removed and the VEL was positioned in the rib notch. Just before installing the skin, the second release paper was removed. The thickness of the VEL was such that an interference fit resulted; however, the force required to install the UOWS tightly to the substructure was nominal and easily provided by advancing the fasteners.

V. FLIGHT DATA

Flight data were gathered to obtain UOWS response data during high load factor maneuvers and to assess the effectiveness of the damping systems. These tests were conducted by McDonnell Aircraft Corporation, St. Louis MO (MCAIR), at the request and sponsorship of Warner Robins ALC. Numerous other investigations have provided some flight data, along with data reduction and analysis. These investigations showed that obtaining accurate UOWS panel response data was highly dependent on whether the panel had been installed properly and the instrumentation used effectively. Inconsistencies in these two areas, among others, can easily lead the investigator to erroneous results. In one previous investigation, which had been intended to serve as the baseline response, a build-up of sealant (for the purpose of protecting instrumentation) on top of stiffener #4 inadvertently contacted the base of the rib notch of rib 188 and very significantly affected the results. In another case, sealant was placed between the UOWS and all substructure ribs and spars; this reduced response but also made removal of the UOWS extremely difficult. At times the strain gages used were either not located closely enough to the locations where failures were occurring, or were oriented in the wrong directions to adequately measure the damaging strain levels. Therefore, care must be exercised in assessing relevance and interpreting results from other studies.

The flight test data collected for this investigation included the baseline response of the F-15 UOWS as well as the UOWS response with various candidate damping treatment configurations. Strain gages placed on internal and external surfaces of the panel were used to record the bulk of the response data. In some cases internal accelerometers were also used. Figure 47 shows the location of the strain gages mounted adjacent to stiffener #4 at rib 188. One was positioned between the two rows of rib 188 fastener holes and the other was located just inboard of these fastener holes.

The location and orientation of these strain gages were such that the strains inducing the fatigue cracks should be measured. Historically, many cracks have been discovered along stiffener #4. Based on past analyses, it was observed that the response data obtained at the intersection of stiffener #4 and rib 188 could be used to represent the response over the remaining panel. Thus, the analysis performed centered on the UOWS response measurements taken at this location.

A plot of angle-of-attack (AOA) versus dynamic pressure is given in Figure 48 for typical flight conditions for which high load factor maneuver data were gathered. The range of dynamic pressure, q of 350 psf to 500 psf, for the 12° AOA shown in this plot illustrates the difficulty, if not impossibility, of duplicating the service conditions for which damage is induced. The power spectral density (PSD), shown in Figure 49, was typical of the UOWS response at the strain gage locations shown in Figure 47 for an undamped panel. The flight conditions for this PSD were: 11° AOA,

5.9 g load factor, 0.80 Mach, 20,000 feet altitude, and 424 psf dynamic pressure. Figure 49 shows high strain levels occurred in the 300- to 400- hertz (Hz) band. It is obvious that this peak results in the most significant contribution to cumulative high cycle fatigue crack damage.

Several damping treatment configurations were flight tested. The external and internal treatments, which were recommended to W-R ALC for F-15 retrofit, were included in the flight tested damping treatments. Unfortunately detailed data are not available at the time this report was written; thus no specific flight test results can be presented. The preliminary flight test results received from MCAIR are very promising and appear to extend the UOWS service life to the desired 8000 hours.

VI. DISCUSSION

A. LIFE EXTENSION

A comparison between the frequency response of the baseline UOWS and the UOWS with the external damping treatment installed is presented in Figure 50. The acceleration Frequency Response Functions (FRFs) were integrated twice to obtain the compliance (displacement) FRFs; the compliance FRFs were assumed to be proportional to strain. Figure 51 makes a similar comparison for the internal damping configuration. Notice the dramatic, beneficial reduction in response due to the internal treatment. The comparisons in this report were made on the basis of RMS stress rather than by considering peak values. Figure 52 presents the equation used to calculate the life extension factor. The ratio of the damped to the baseline response was raised to the proper exponent to give the life extension factor (i.e., ratio of lifetimes). The RMS of the compliance FRF between 300 and 400 Hz was the basis of the calculation. The reader is referred to Appendix B for details.

Calculations made in this manner reveal that the UOWS with the "1980 Damping Treatment" (TC1) will last four times as long as the baseline UOWS (bare UOWS); thus the life extension factor is 4. The life of the baseline UOWS is approximately 1,250 hours; therefore, the projected life with the "1980 Damping Treatment" is 5,000 hours. Obviously, this is an estimate; however, it does provide a measure of performance for the damping treatments. Similar estimates gave life extension factors for the new recommended external and internal treatments of 5 and 34, respectively. The internal treatment is considered the primary configuration for resolving the UOWS high cycle fatigue cracking. This is because of the dramatic reduction in response achieved with it installed. Its large life extension factor should offset a variety of uncertainties not accounted for by this investigation, such as precise temperature at which damage accumulates, the fact that RMS stresses were used instead of peak values, and potential changes in future operational usage.

B. COST SAVINGS

The maintenance cost savings from retrofitting the F-15 fleet with the internal damping treatment assume that installation of the damping will preclude only one UOWS rework for all aircraft in the fleet. This assumption should result in a conservative estimate. All costs are in FY91 dollars.

The labor cost to rework UOWS on a single aircraft is approximately \$0.1 M. Multiplying by 650 to account for reworking all 650 aircraft in the fleet results in a labor savings of over \$65 M. The materials to rework a single aircraft cost \$27 K.

For 650 aircraft this figure becomes \$17.5 M. To install the internal damping treatment will require installation and removal of the wing skin at a cost of \$7.7 K per aircraft, or \$5 M for the fleet. The cost of the damping materials themselves will be approximately \$2.5M for all 650 aircraft. Adding the UOWS rework labor and materials savings of \$65 M and \$17.5 M, respectively, and subtracting the cost of labor and materials for installing the damping treatments results in a \$75 M cost savings overall.

VII. CONCLUSIONS

The Fight Dynamics Directorate, at the request and sponsorship of Warner-Robins Air Logistics Center, tested 13 candidate add-on damping treatments for the F-15 UOWS. Of those tested, two damping treatments were recommended for F-15 fleet retrofit. One treatment was an externally applied constrained-layer treatment and the other was an internally applied stand-off treatment with viscoelastic links in the rib notches. The external and internal treatments resulted in life extension factors of 5 and 34, respectively. The damping treatments were thermally aged and corrosion tested; no adverse effects were noted. Three hundred F-15 aircraft have accumulated 10 years of service experience with the "1980 Damping Treatment" and to the authors' knowledge there have been no reports of concern or adverse effects associated with add-on damping treatments. At this time, there is no evidence to indicate that the recommended damping treatments should not be used to alleviate the UOWS fatigue cracking. It is projected that retrofit of the F-15 fleet with UOWS containing the internal treatment will result in a net savings of \$75M in maintenance and repair costs over the next 25 years. The recommended damping treatments are fully qualified for F-15 fleet retrofit and represent a viable, cost effective solution which will substantially improve the F-15 UOWS service life.

VIII. RECOMMENDATIONS

It is recommended that the external damping treatment be retrofitted to the entire F-15 fleet. It can be installed in the field, extending the life of the UOWS and minimizing accumulated damage until the aircraft is scheduled for depot maintenance. It is recommended that the internal damping treatment be installed during depot maintenance to provide the maximum protection to the UOWS and adjoining structure. The adjoining structure (r.os) would experience a small reduction in vibratory loads and would, therefore, also benefit from the application of the damping treatment. The large life extension factor of the internal treatment would also cover a variety of uncertainties, such as the temperature at which damage accumulates and possible changes in future operational usage.

APPENDIX A: DAMPING TREATMENT CONFIGURATIONS

This Appendix provides information on the 13 damping treatment configurations which were tested. The four basic lay-ups used in this investigation are presented in Figure A1. Additional details on the lay-ups are provided in Figure A2. A comparison of the various candidate add-on damping treatment test configurations (TC) along with the recommended internal and external configurations is shown in Figure A3. Figures A4 through A13 give the test configurations considered during this investigation, whether the damping treatments were internally or externally applied, and where on the UOWS the treatments were located (i.e., spar-rib bays to which damping treatments were applied). TC1 is the "1980 Damping Treatment" and was described in Figure 37 of this report. The recommended external and internal treatments were also previously described in Figures 39 through 44. TC7 was the same treatment as TC6 except each bay has only the middle 50% of area covered. TC8 was the same as TC6 with the addition of the VELs in all stiffener-rib notches. Figure A12 describes TC10 which has the appearance of a flow fence. A photograph of these damped flow fences is shown in Figure A14. Figure A13 shows TC11 which has the same lay-up as TC2 with the addition of "damping strips" as shown; bays L1, L2 and L3 are covered with the "damping strips." Figure A15 is a table of test results for the 300 to 400 Hz frequency band. Column 1 is the test configuration number. Column 2 lists the accelerometer number from Figure 24. Column 3 is the ratio of the UOWS RMS response with the damping applied to the baseline UOWS RMS response. Column 4 is the results of the calculations using Figure 52 and Appendix B. Column 5 is the average life extension (LE); this number is considered representative of that expected in service. Figure A16 is a bar graph comparing the life extension factors of the various test configurations. Although the damped laminar flow fence performed well, it was not considered a viable solution because of the potential adverse effects on the wing flow field.

APPENDIX B: METHODOLOGY FOR CALCULATION OF LIFE EXTENSION

The Palmgren-Miner cumulative fatigue damage law is the basis for life extension calculations. It has been observed that an adequate approximation is that all fatigue curves in the region of interest have the same slope regardless of stress concentration factors or average stress. The S-N curves are considered to be straight lines on log-log scales. This situation is presented in Figures B1 and B2. When the alternating (or RMS) stress is reduced from S_H to S_{10H} , the life is extended from N_H to N_{10H} . The normalized equation is presented in Figure B2. The rule of thumb used here is that reducing alternating (or RMS) stress by a factor of 2 results in a factor of 10 for life extension. This is plotted in Figure B1 and the equation is presented in Figure B2. This is a conservative approach. The normalized approach is valid for add-on damping treatment because neither stress concentration nor average stress is changed. It remains to calculate the ratio of damped to undamped (baseline) RMS stress (i.e., normalized).

For a random process of interest, here the governing equation is:

$$S_{\sigma}(f) = |H_{\sigma p}(jf)|^2 S_p(f) \quad \text{Eqn - B 1}$$

where:

$\sigma(t)$ is stress - psi

$p(t)$ is pressure - psi

S_{σ} is PSD - (psi)²/Hz

$H_{\sigma p}$ is FRF - psi/psi

S_p is PSD - (psi)²/Hz

The stress is considered to be representative of a crack location in service. The pressure is from the representative flight condition causing all of the damage. Over the frequency range of interest, the PSD level is a constant:

$$S_p = P_o \quad ; \quad f_1 < f < f_h \quad \text{Eqn - B 2}$$

The area under the PSD curve is the square of the RMS:

$$\sigma_{RMS, f_1-f_h}^2 = \int_{f_1}^{f_h} S_{\sigma}(f) df = P_o \int_{f_1}^{f_h} |H_{\sigma p}(jf)|^2 df \quad \text{Eqn - B 3}$$

and the RMS is proportional to the integral:

$$\sigma_{RMS, f_l - f_h} = \left[\int_{f_l}^{f_h} |H_{gp}(j f)|^2 df \right]^{1/2} \quad \text{Eqn - B 4}$$

If adequate flight data are available, the above equations would be used to calculate a ratio for damped and baseline conditions.

For the laboratory the governing equation is:

$$S_g(f) = |H_{gF}(j f)|^2 S_F(f) \quad \text{Eqn - B 5}$$

where:

$g(t)$ is acceleration - g

$F(t)$ is shaker force - lb

S_g is PSD - g^2/Hz

H_{gF} is FRF - g/lb

S_F is PSD - lb^2/Hz

For the present purposes, conceptually there is no difference between flight pressure and laboratory shaker force:

$$F(t) = A p(t) \quad \text{Eqn - B 6}$$

The units may be changed:

$$H_{gF} = 386 H_{gP} \quad (\text{in}/\text{sec}^2/\text{lb}) \quad \text{Eqn - B 7}$$

Again conceptually, the stress is a linear function of displacement:

$$S_\sigma(f) = K_{\sigma d} S_d(f) \quad \text{Eqn - B 8}$$

where:

$d(t)$ is displacement - inch

S_d is PSD - $(\text{in}^2)/\text{Hz}$

The displacement and acceleration FRFs are related by:

$$H_{dF} = \frac{1}{(2\pi)^2} \frac{H_{aF}}{f^2} \quad \text{Eqn - B 9}$$

The following equation is useful:

$$S_d(f) = |H_{dF}(jf)|^2 S_F(f) \quad \text{Eqn - B 10}$$

where:

H_{dF} is a FRF. (in/lb)

Substituting Eqn B9 into B10 yields:

$$S_d(f) = \frac{|H_{aF}(jf)|^2}{(2\pi)^4 f^4} S_F(f) \quad \text{Eqn - B 11}$$

Using Eqn B8 leads to:

$$S_d(f) = \frac{K_{sd} |H_{aF}(jf)|^2}{(2\pi)^4 f^4} S_F(f) \quad \text{Eqn - B 12}$$

Over the frequency range of interest, the force PSD is a constant:

$$S_F = F_o ; f_l < f < f_h \quad \text{Eqn - B 13}$$

The square of the RMS is given by the integral:

$$\sigma_{RMS, f_l-f_h}^2 = \frac{K_{sd} F_o}{(2\pi)^4} \int_{f_l}^{f_h} \frac{|H_{aF}(jf)|^2}{f^4} df \quad \text{Eqn - B 14}$$

The RMS is proportional to the integral:

$$\sigma_{RMS, f_l-f_h} = \left[\int_{f_l}^{f_h} \frac{|H_{aF}(jf)|^2}{f^4} df \right]^{1/2} \quad \text{Eqn - B 15}$$

which is used for calculating the ratios. The complex-valued FRF is calculated from a numerical approximation of:

$$H_{gF}(j f) = \frac{S_{gF}(j F)}{S_F(f)} \quad \text{Eqn - B 16}$$

where S_{gF} is cross-PSD: (g-lb/Hz)

APPENDIX C: CORROSION TESTS

This Appendix presents the results of the corrosion tests performed during this investigation. Figure C1 presents sketches of the lay-ups 112 and S/3. The edge sealant of the "1980 Damping Treatment" is also indicated. Any polymer will absorb moisture. The VEM used will absorb a maximum of 5%, and the syntactic foam a maximum of 0.5%. In all cases, the paint which provides the basic corrosion protection to the metal is not disturbed. Good adhesion of the damping treatment requires a chemically clean, active surface. An approved solvent for grease and dirt should be used. Also, extremely light mechanical abrading may be performed. In any event, the basic integrity of the paint should not be disturbed. Note that the predominant mode for moisture entry is the edge, because the aluminum is impermeable to moisture. Other possibilities are moisture entering the grooves of the stand-off foam or through punctures in the aluminum. For moisture to be present at the paint surface, it must be absorbed through the sealant and pressure sensitive adhesive (VEM) for lay-up 112 and 112/113 and through the pressure sensitive adhesive (VEM) only for lay-up S/3 (cracks may occur in the stand-off foam). Thus, the protection of the VEM in all cases is added to that of the paint. Several test panels were exposed to a standard 30-day humidity corrosion environment in the laboratory consisting of 120° F, 98% relative humidity (RH), and salt spray. Figure C2 is a photo of a bare (painted but without damping treatment) test panel after exposure; no corrosion is evident. Figures C3 and C4 show the "1980 Damping Treatment" (TC1/lay-up 112) with the edge sealant. Some corrosion is evident in Figures C3 and C4 along one edge of the unprotected aluminum constraining layer next to the edge sealant; none is evident on the basic painted panel. Figure C5 is the "1980 Damping Treatment" without edge sealant. The same panel with one-half of the damping treatment removed is shown in Figure C6. No corrosion is evident in either photograph. Figures C7 and C8 are the external damping treatment lay-up 112/113 without edge sealant. Lay-up 112/113 with edge sealant is presented in Figures C9 and C10. A small amount of corrosion is evident on the top, unprotected constraining-layer. The stand-off damping treatment (lay-up S3) is shown in Figures C11 and C12 without edge sealant and in Figures C13 through C15 with edge sealant; again only small amounts of corrosion are evident on the unprotected constraining-layer. Figures C16 and C17 show the test panel with the viscoelastic link (VEL) applied. No corrosion was observed. No test panels (Figures C2 through C17) showed any evidence whatsoever of corrosion of the painted parent panel due to the application of one of the candidate damping treatments. There was some corrosion of the bare (unpainted) outermost aluminum constraining layer; however, no corrosion of the parent panel was encountered under laboratory testing. This fact strongly suggests that no corrosion problems will be present with the painted UOWS or ribs. It should be noted that there has not been any reported corrosion problems during the "1980 Damping Treatment's" 10 years of service on 300 F-15 aircraft. In view of the fact

that the external damping treatment would be painted, and the internal damping treatment would not be exposed directly to the environment, it is unlikely that there will be corrosion problems with the aluminum constraining layers. Service experience with the very similar "1980 Damping Treatment" system has been completely satisfactory. Simply stated, corrosion will not be a problem.

APPENDIX D: THERMAL AGING TESTS

This Appendix presents the results of the thermal aging tests performed on the candidate damping treatments. Figure D1 is a photo of a "1980 Damping Treatment" (lay-up 112) which was removed from an actual wing previously in service. The damping treatment was peeled back (failing cohesively) to reveal the original painted surface of the UOWS. The environment was normal service only. There was no evidence of discoloration or embrittlement whatsoever. A specimen containing the "1980 Damping Treatment" and exposed to 340° F in air for 8 hours is shown in Figure D2. When the aluminum constraining layer was peeled back, VEM remained on both the aluminum constraining layer and on the base panel. This is indicative of a cohesive failure which is the desired failure mode. Cohesive failure indicates that thermal aging has not caused debonding of the damping treatment from the parent material. In Figure D2, there are regions where discoloration of the VEM is evident, along with regions (approximately 50% of the area) which experienced no noticeable discoloration. This pattern suggested that air had reached the discolored areas and had not reached the unaffected areas. Possibly the air was entrapped when the foil was laid down, or perhaps a slight ridge or buckle of foil was present.

To determine the degradation of the VEM due to thermal aging, cantilever beam test were performed. Figure D3 is a sketch of the cantilever beam modal damping test arrangement. The test approach used to measure the damping system properties followed the standard ASTM E-756-83 procedures. The tests measured damping properties for the second, third, and fourth modes. Comparisons were made between the similar test performed between baseline damping treatments and thermally aged damping treatments. Figure D4 is a plot of modal damping versus temperature for the "1980 Damping Treatment" before and after exposure of the specimen to 340° F for 7 hours and 270° F for 48 hours all in air. Modal damping is seen to decrease by only a small amount over the 50° F to 75° F temperature range of interest. A plot of modal damping versus temperature for the stand-off damping treatment (lay-up S/3) before and after similar thermal exposure is given in Figure D5. Again, modal damping is seen to decrease by only a small amount over the temperature range of interest. The effects of thermal aging on the viscoelastic links (VEL) was determined by measuring changes in the materials dynamic shear modulus. Plots of dynamic shear modulus and material loss factor versus temperature for the VEL material before and after thermal exposure are given in Figure D6. From the plots it can be seen that peak loss factor retains the same value but is shifted to a higher temperature due to thermal aging; dynamic shear modulus is increased approximately 20%. The effect of these changes is judged to be insignificant. Percent elongation to failure of the VELs was recorded using an over-lap shear test. Percent elongation to failure was 1000% before and 150% after thermal aging, respectively. Although the percent elongation to failure decreased significantly after thermal aging, the resulting value allowed more than

adequate extension to withstand the environment. During these tests strength of the VEL material was observed to increase, and failures were cohesive, indicating good bond strength.



F-15 WING STRUCTURE

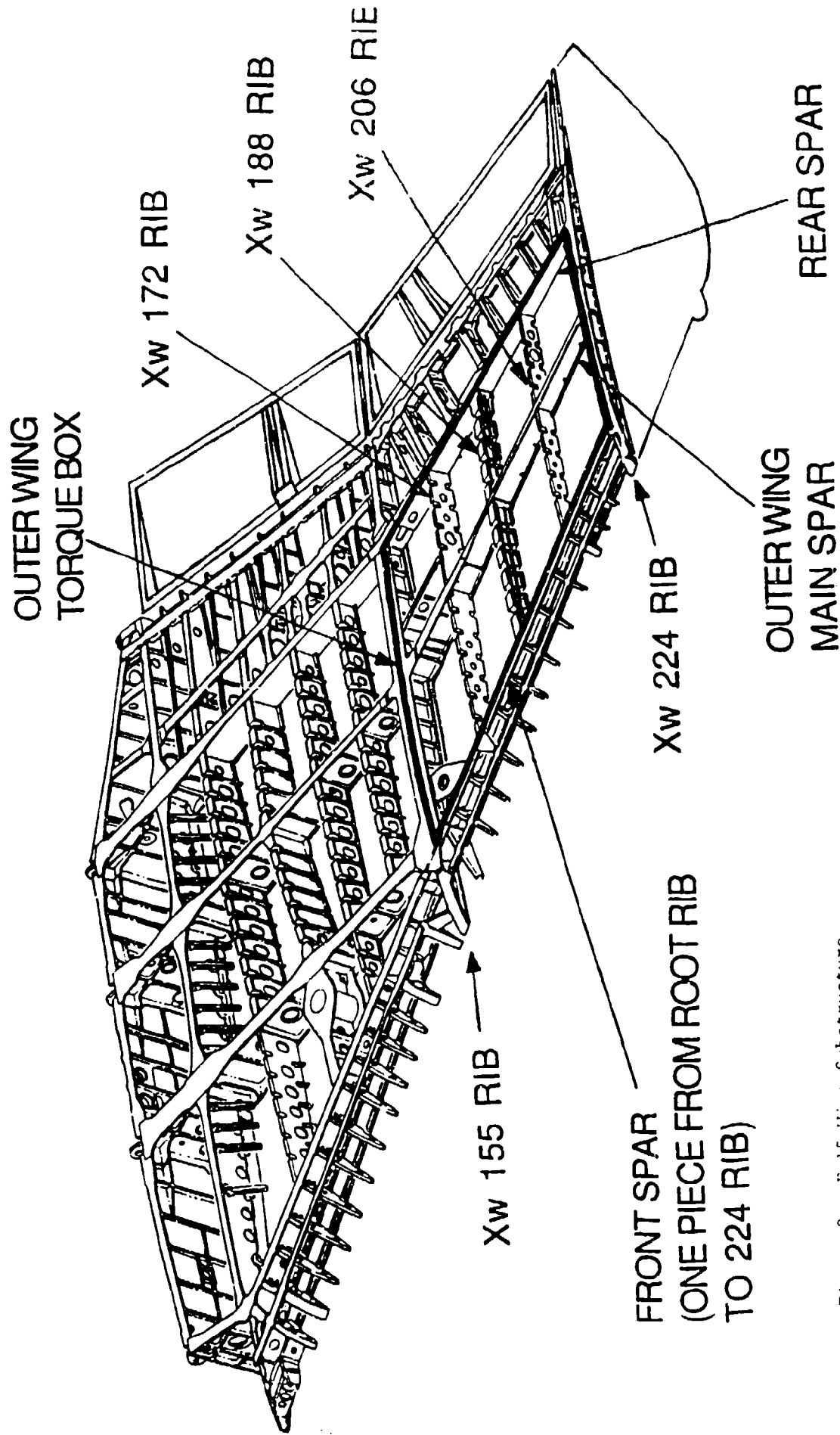
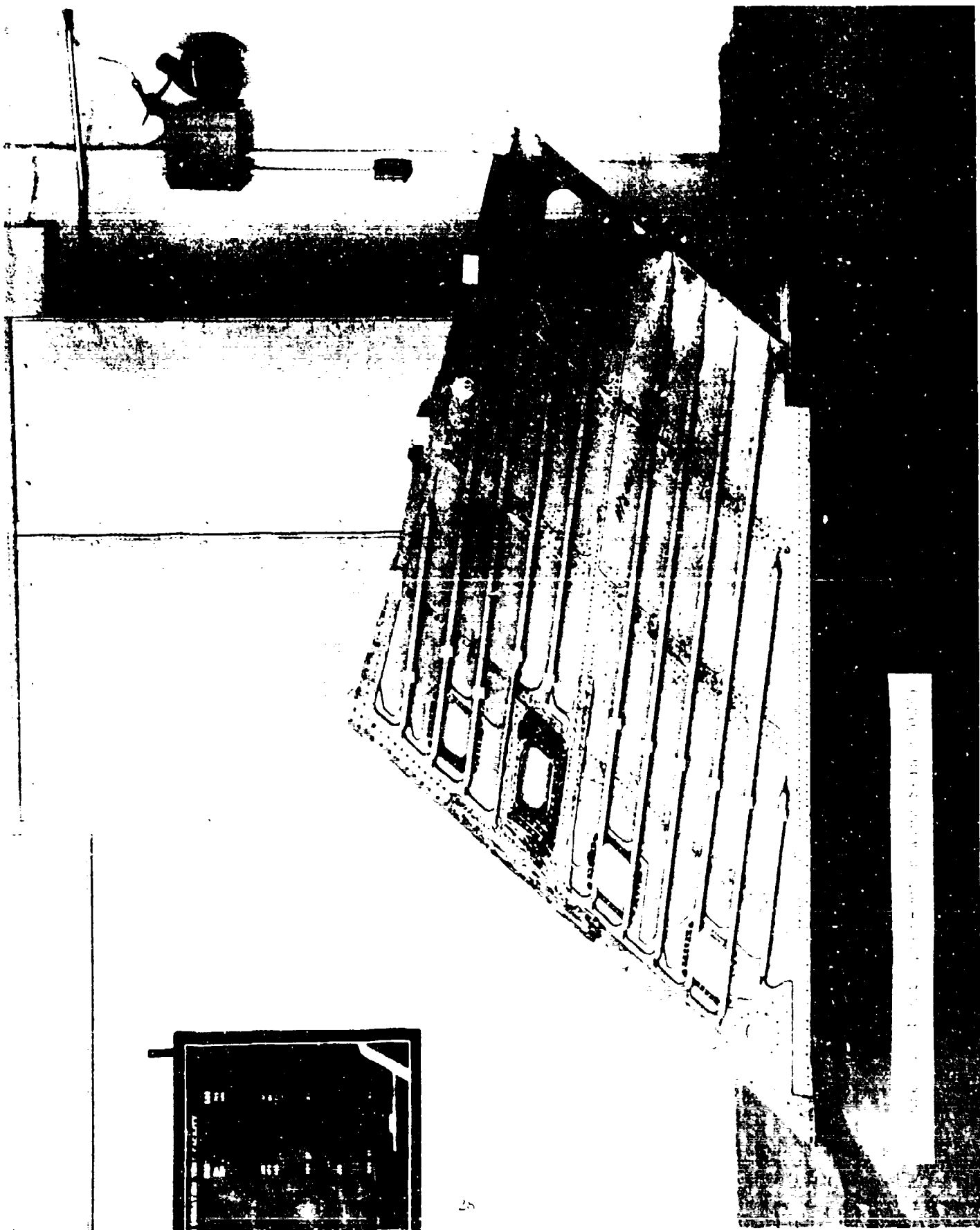
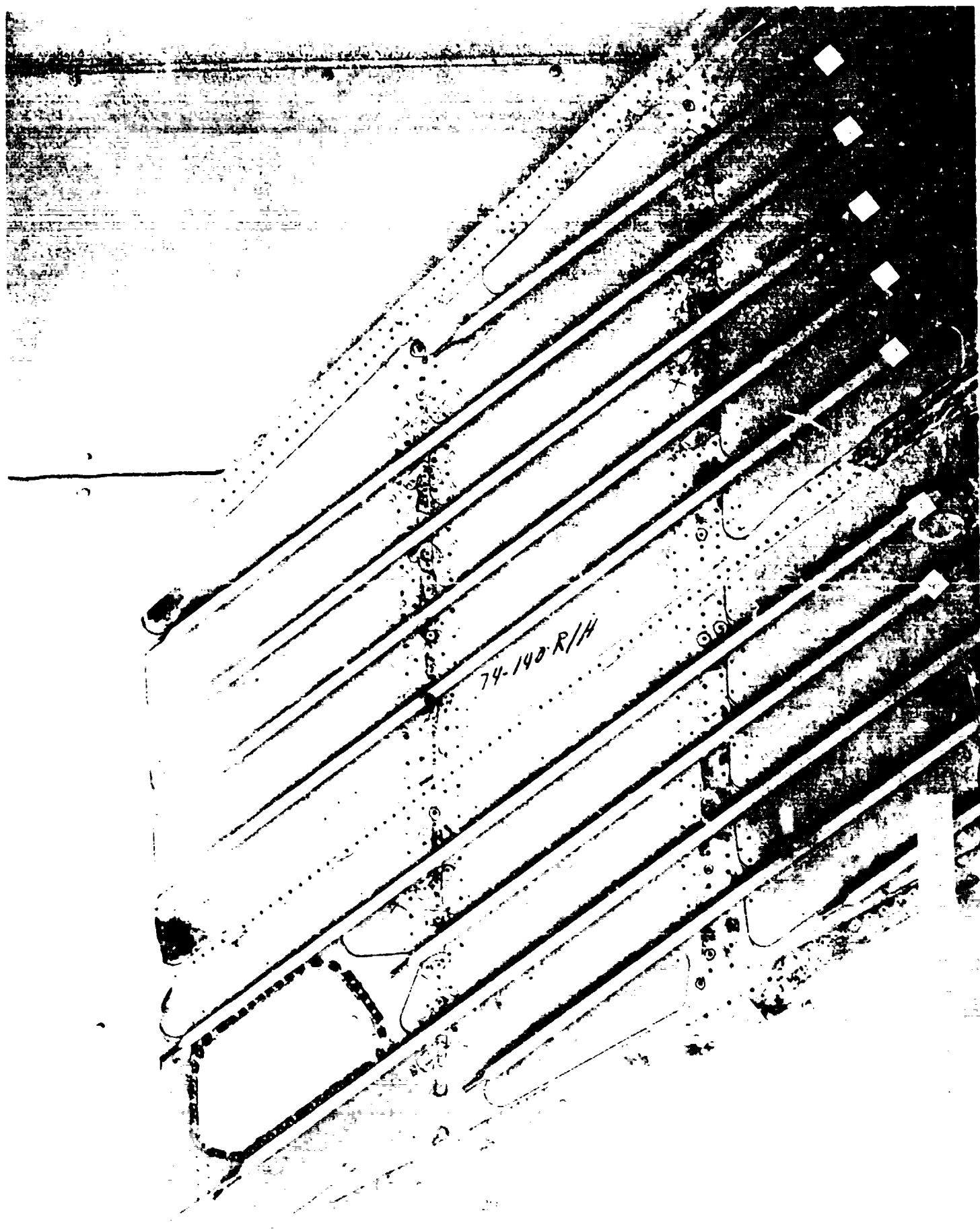


Figure 2. F-15 Wing Substructure





F-15 UPPER OUTER WING SKIN

FIELD INSTALLED STAINLESS STEEL
STRAPS TO EXTEND SERVICE LIFE

5 INCH WIDE BY 1/8 INCH THICK STRAPS
BONDED/RIVITED OVER 206, 188, & 172 RIBS

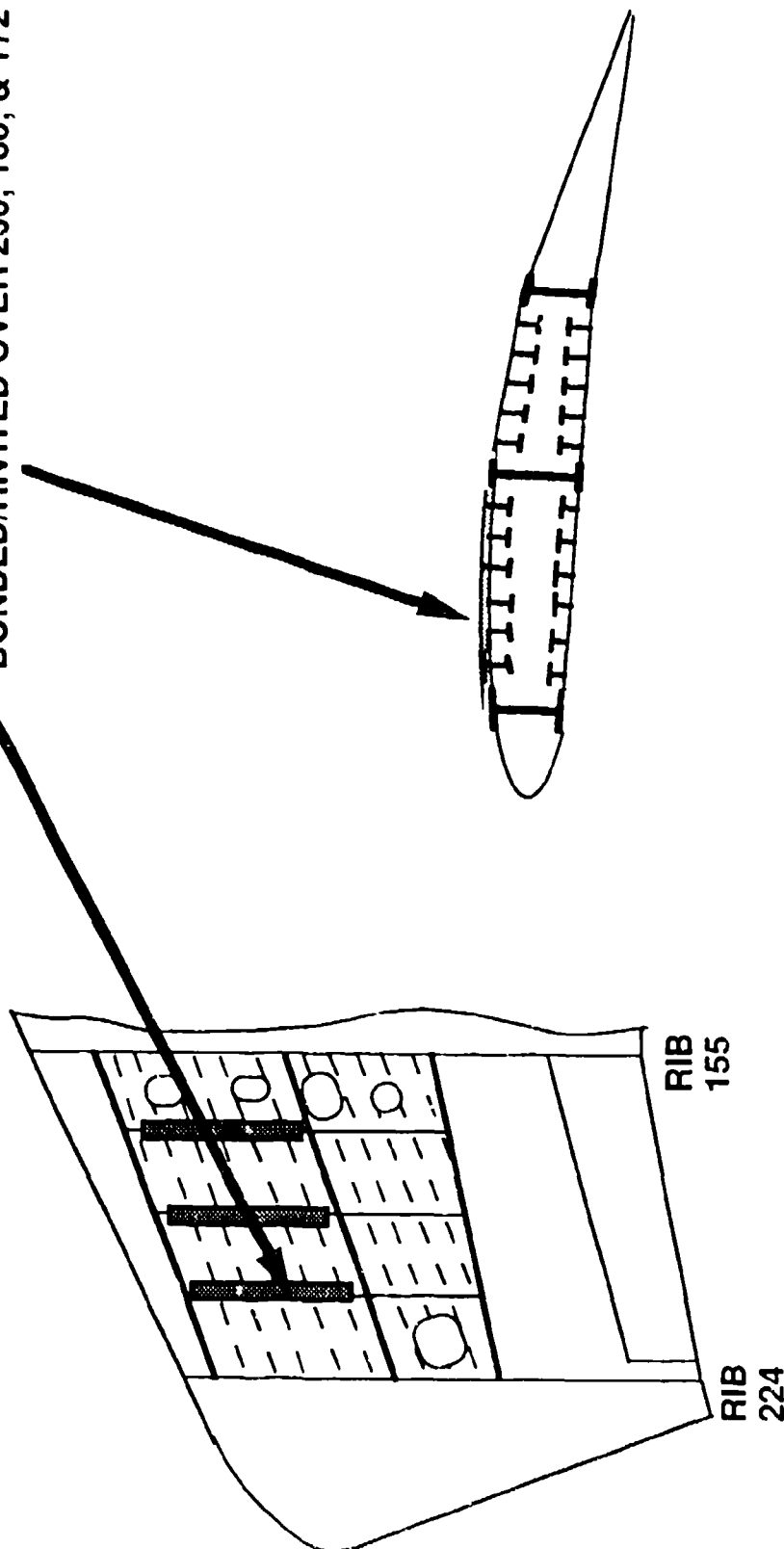


Figure 5. Detail of External Straps



Figure 1. Cracks in Rib Due Fastener Bolts
Between Stiffeners 4 and 5



Figure 7. Cracks in Rib 206 Fastener Holes
Between Stiffeners 7 and 8

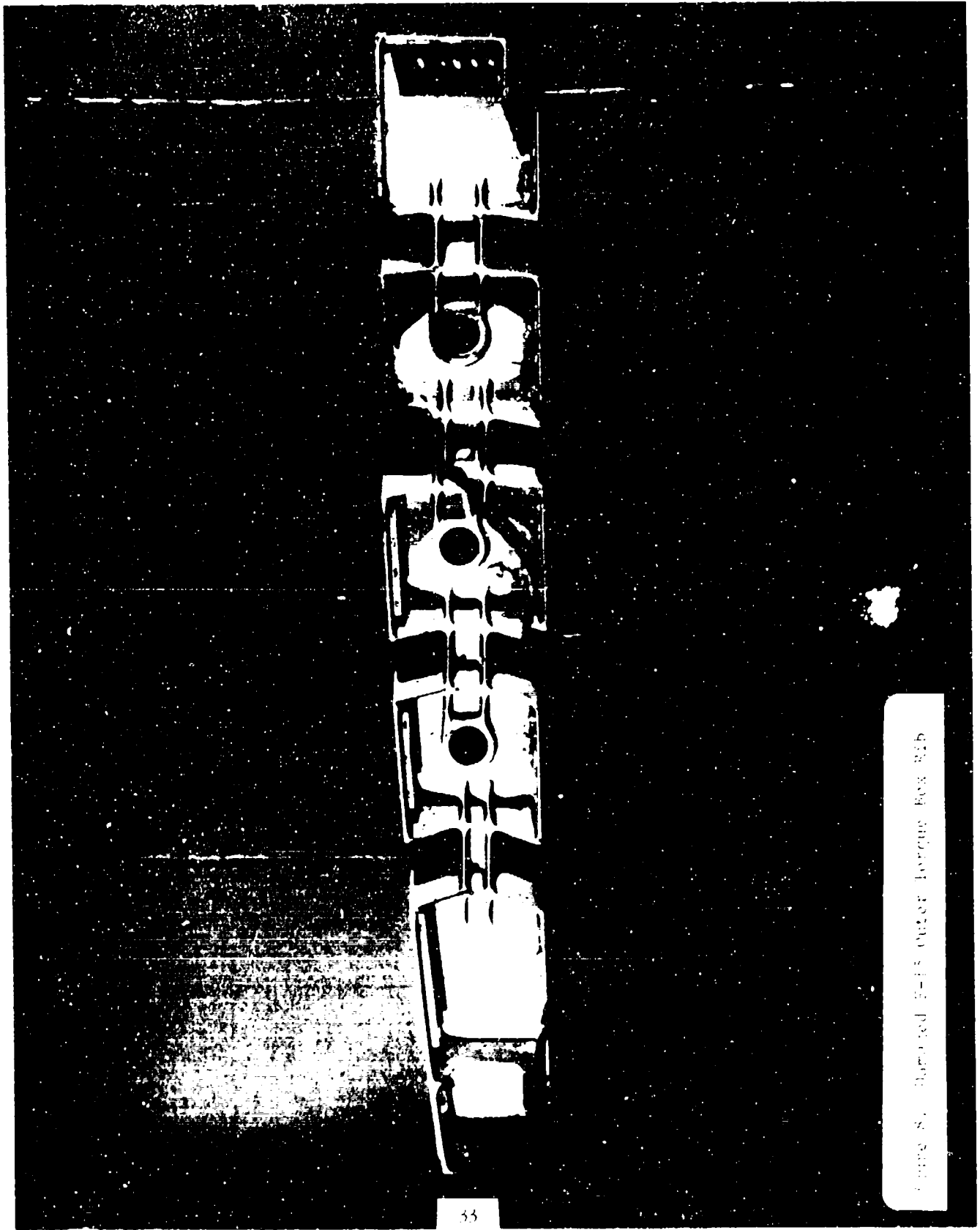


Figure 8. Torque Box 216

SPAR-RIB BAY DESIGNATION

TOP VIEW OF LEFT WING

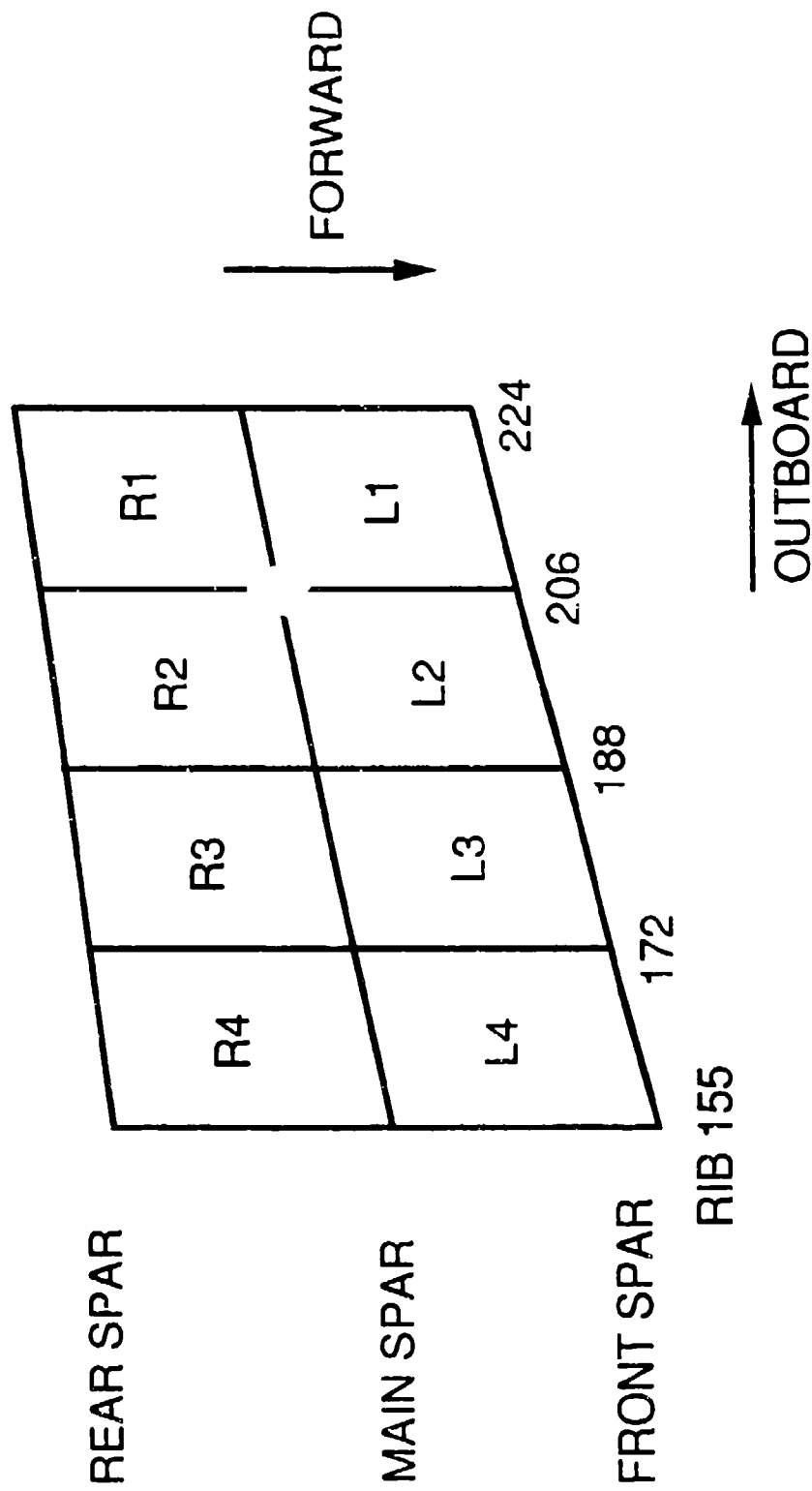


Figure 9. Spar-Rib Bay Designation

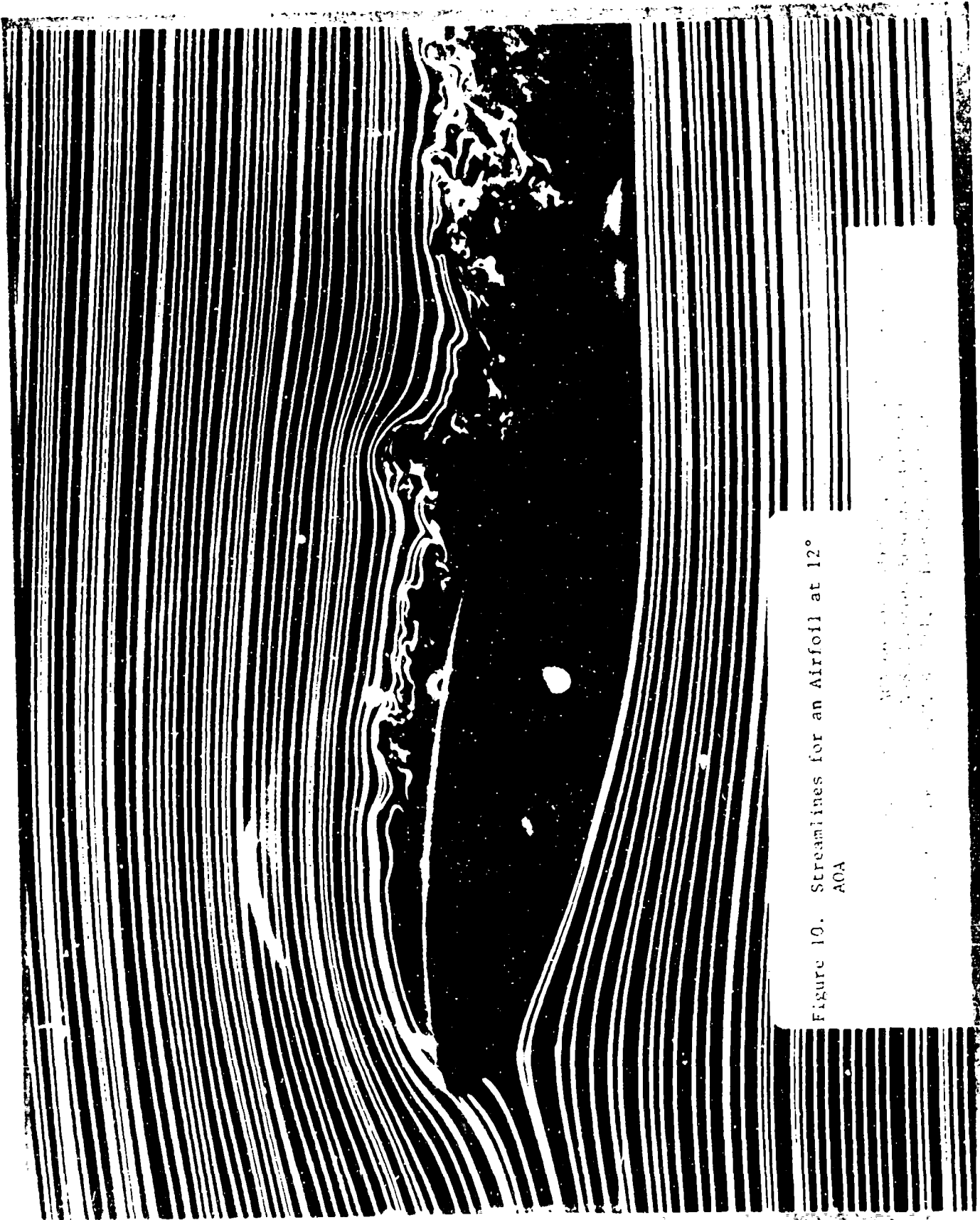


Figure 10. Streamlines for an Airfoil at 12°
AOA

When the airfoil is at an angle of attack of 12 degrees, the flow is separated from the upper surface of the airfoil, resulting in a stall condition. The streamlines are shown as white lines on a black background.

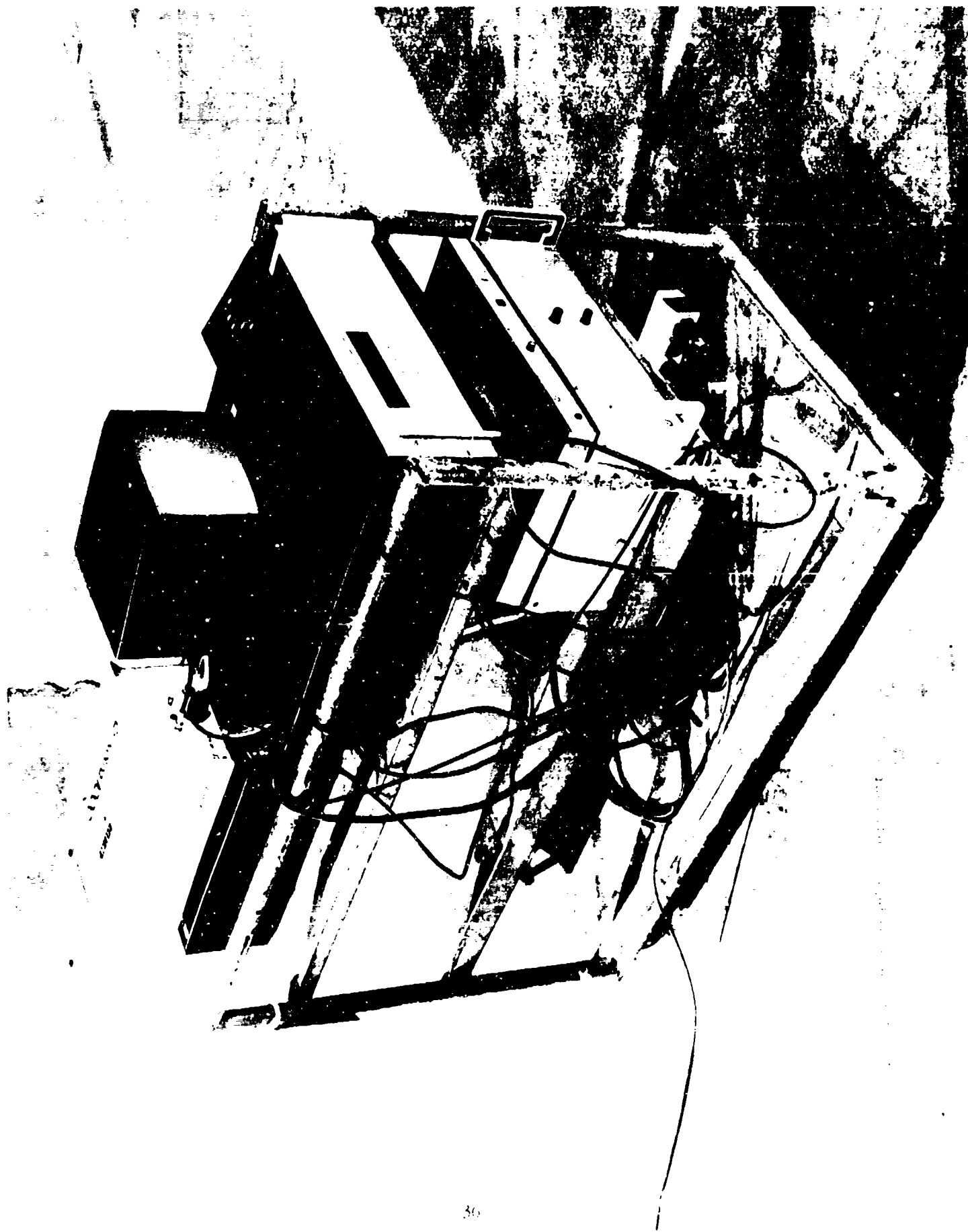
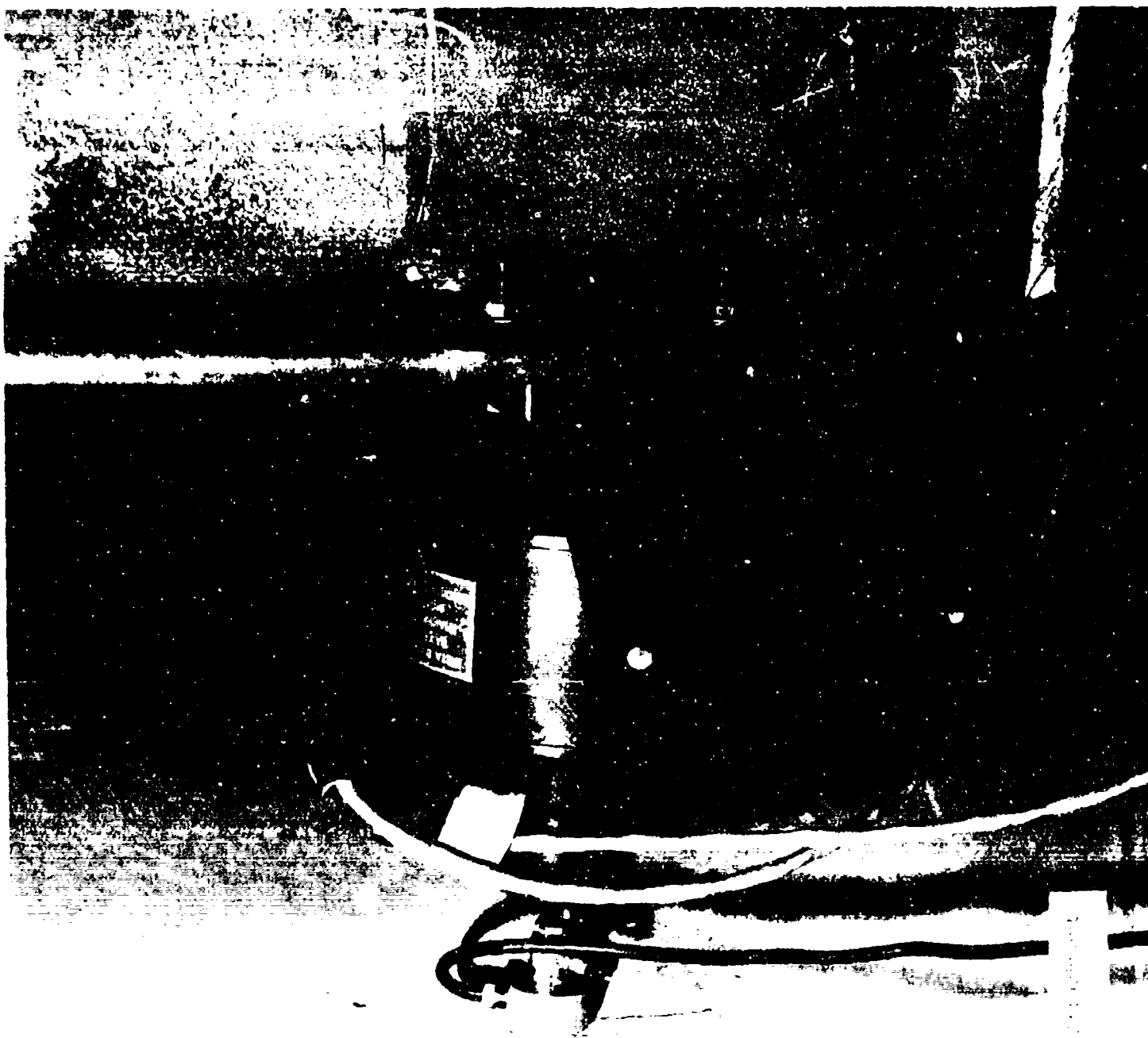




Figure 12. F-15 King With Reflective Tape



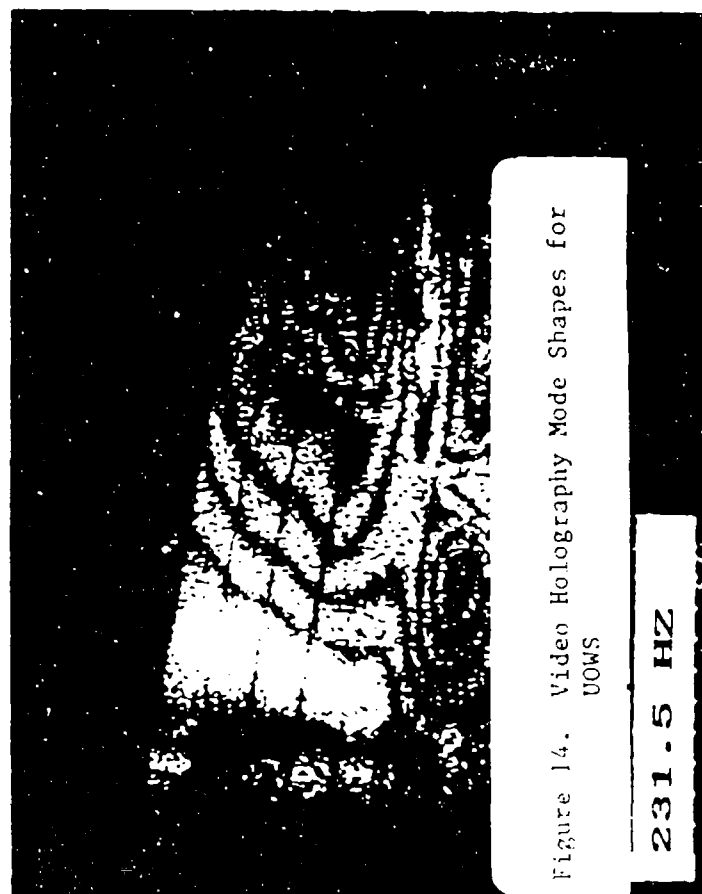
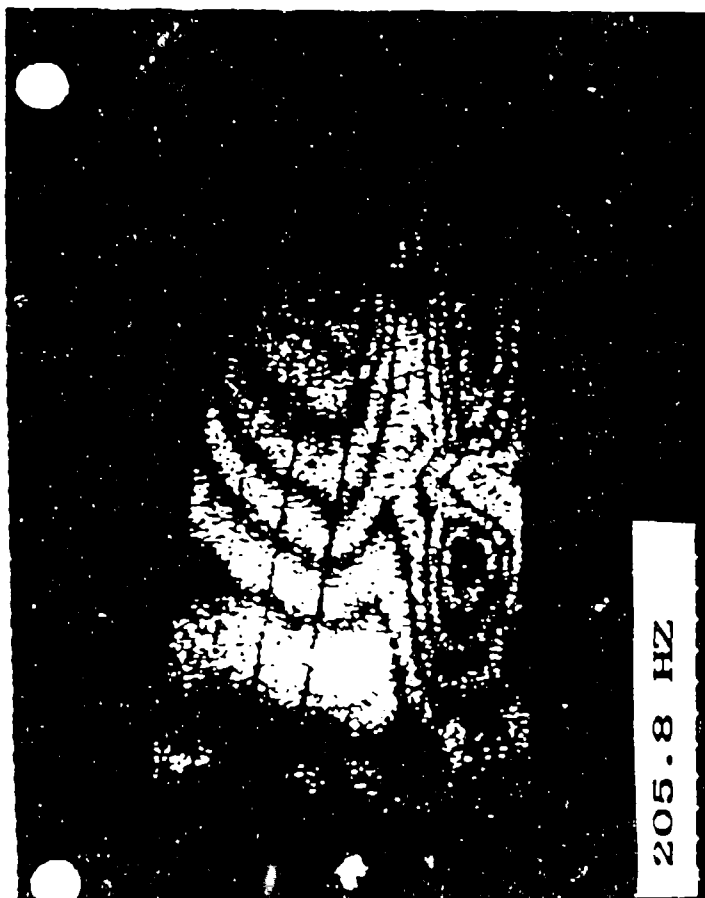
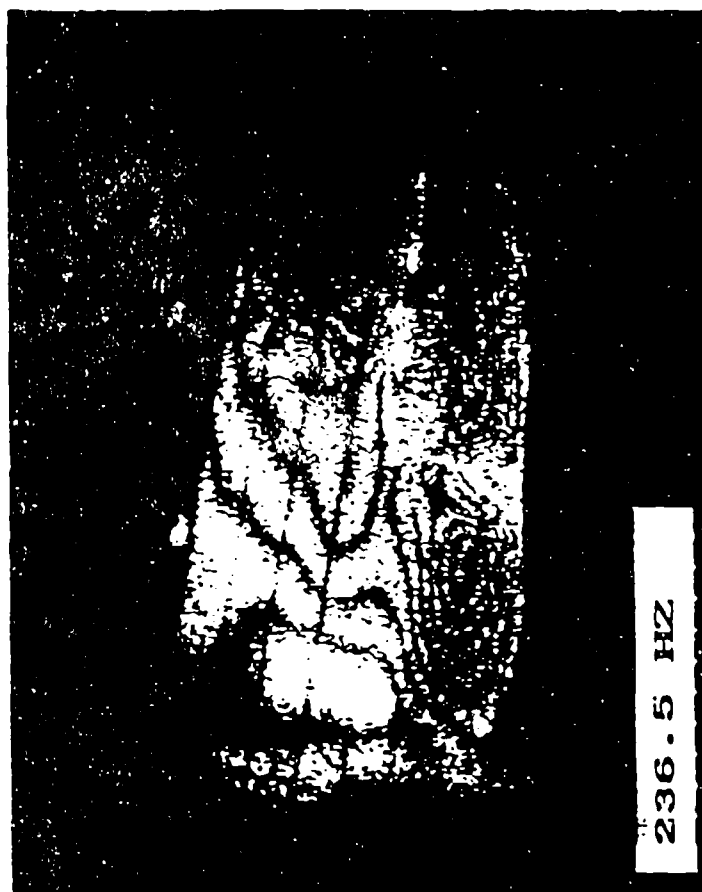
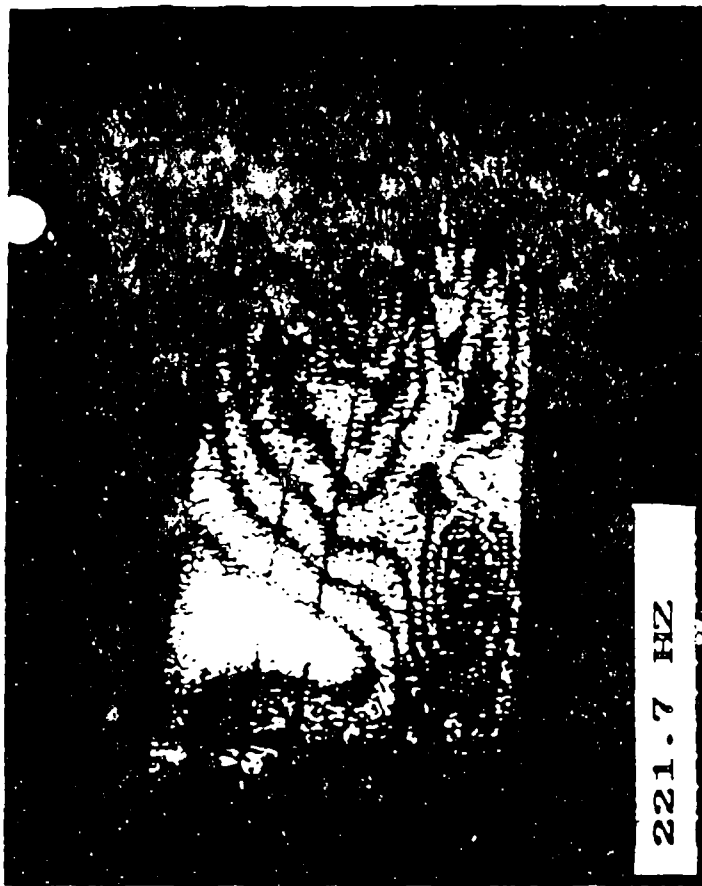
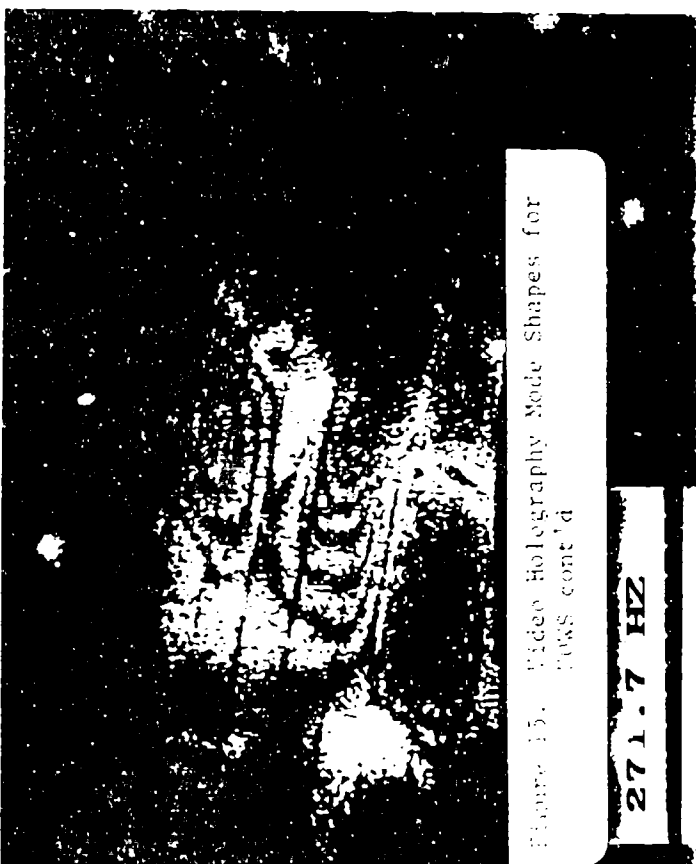
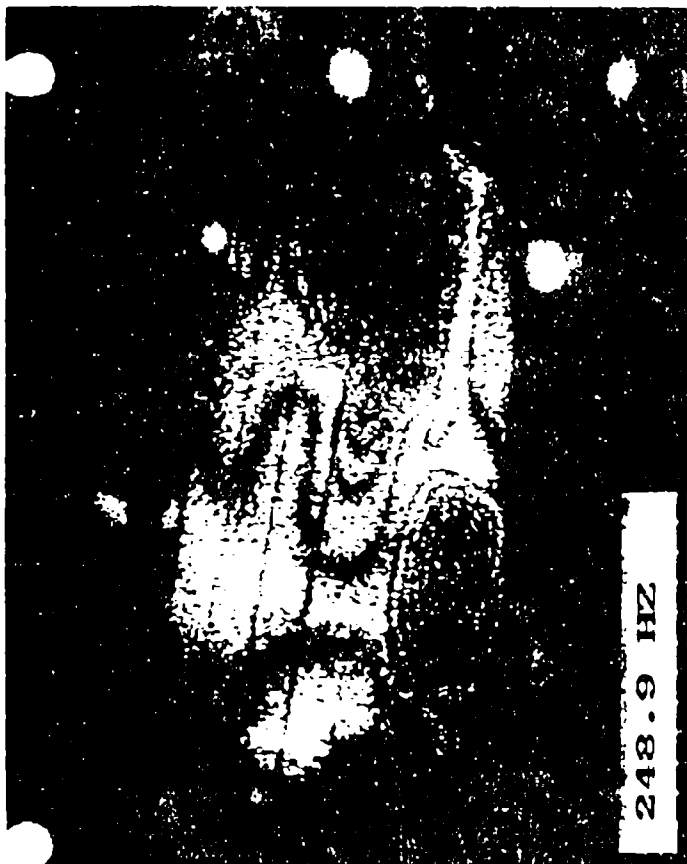
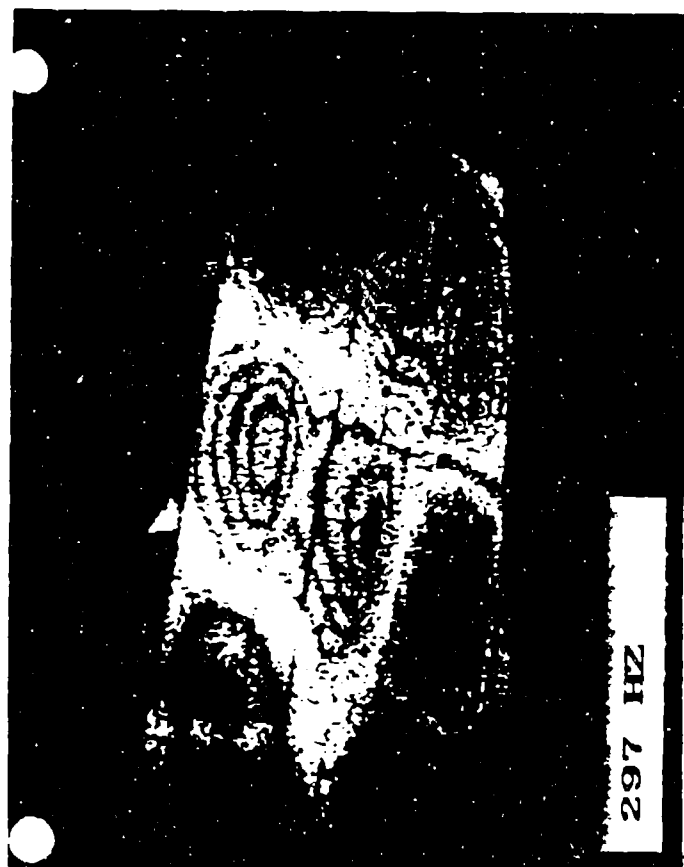


Figure 14. Video Holography Mode Shapes for
UOWS





297 HZ



322 HZ

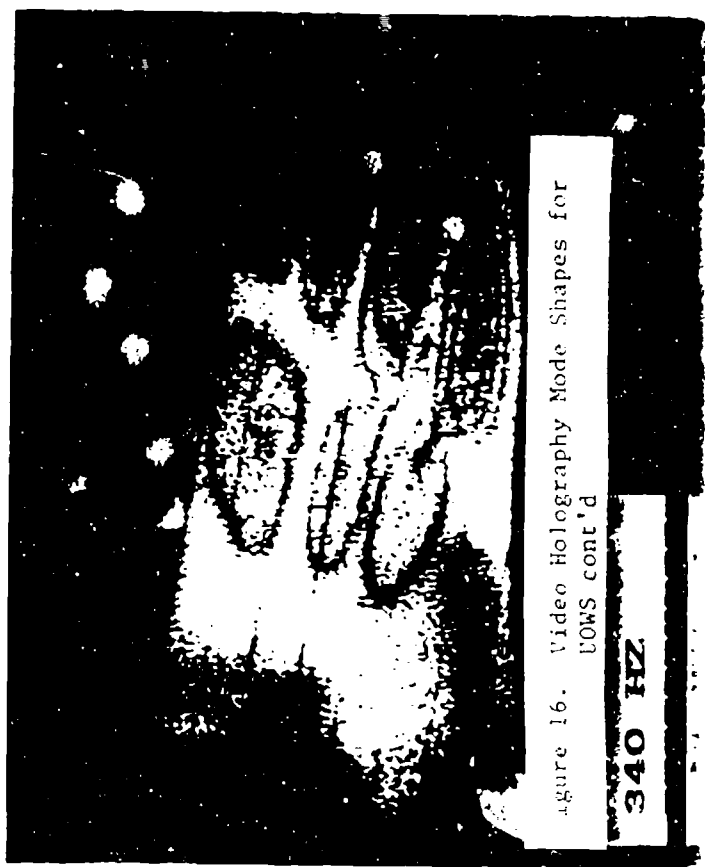
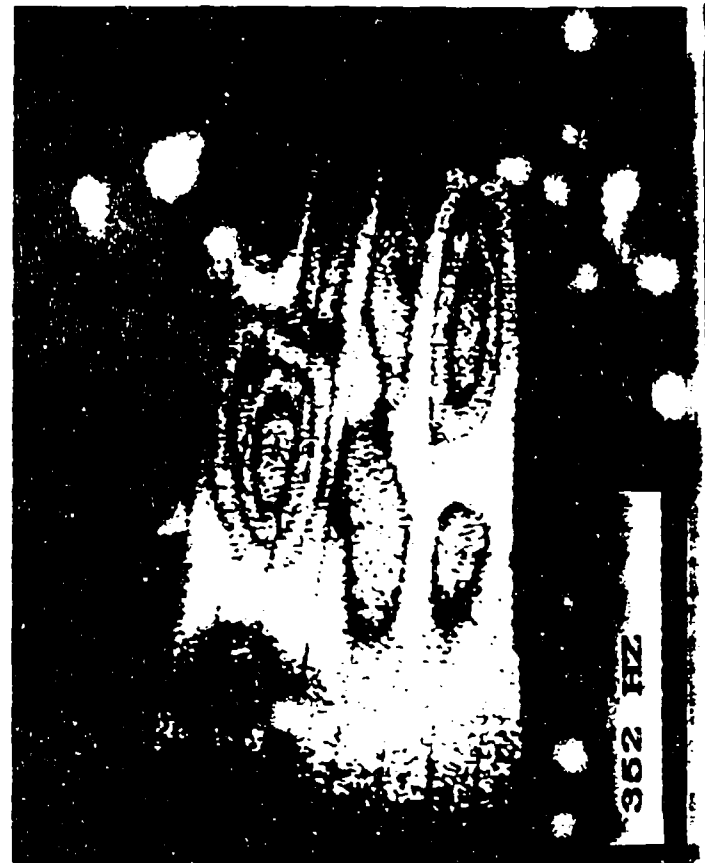
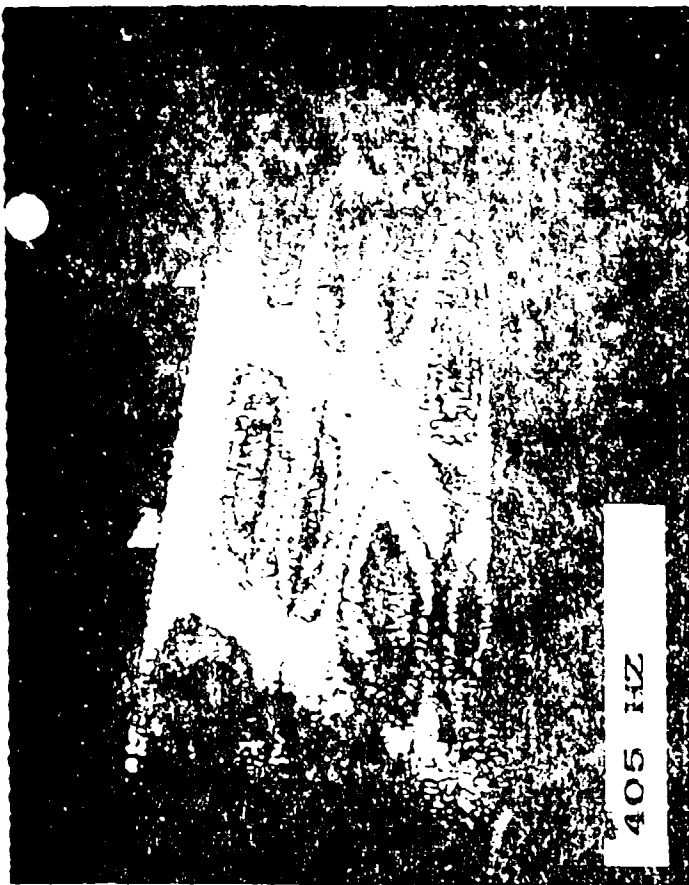


Figure 16. Video Holography Mode Shapes for
UOWS cont'd

340 HZ



362 HZ



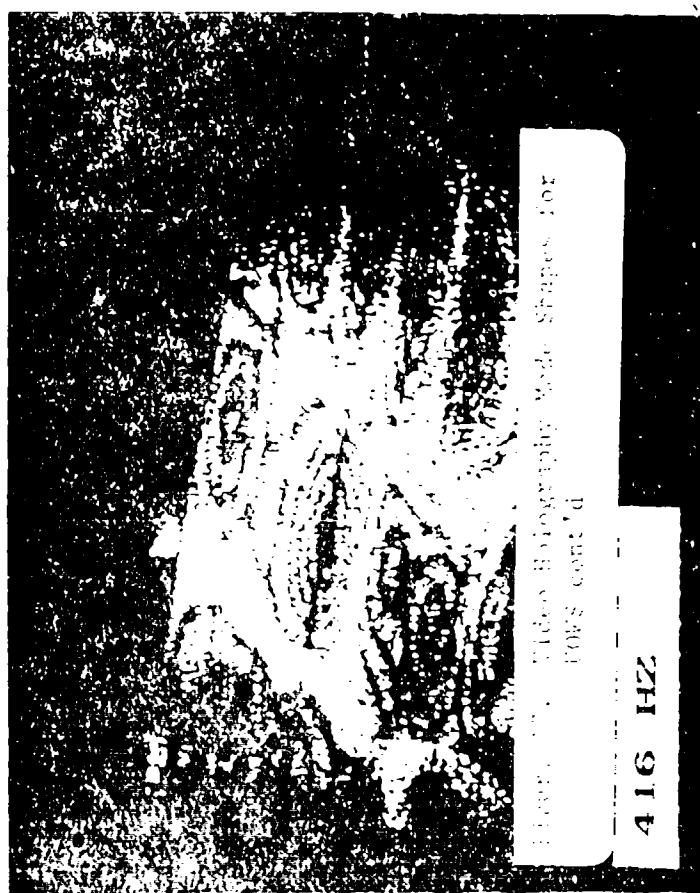
405 HZ



420.5 HZ

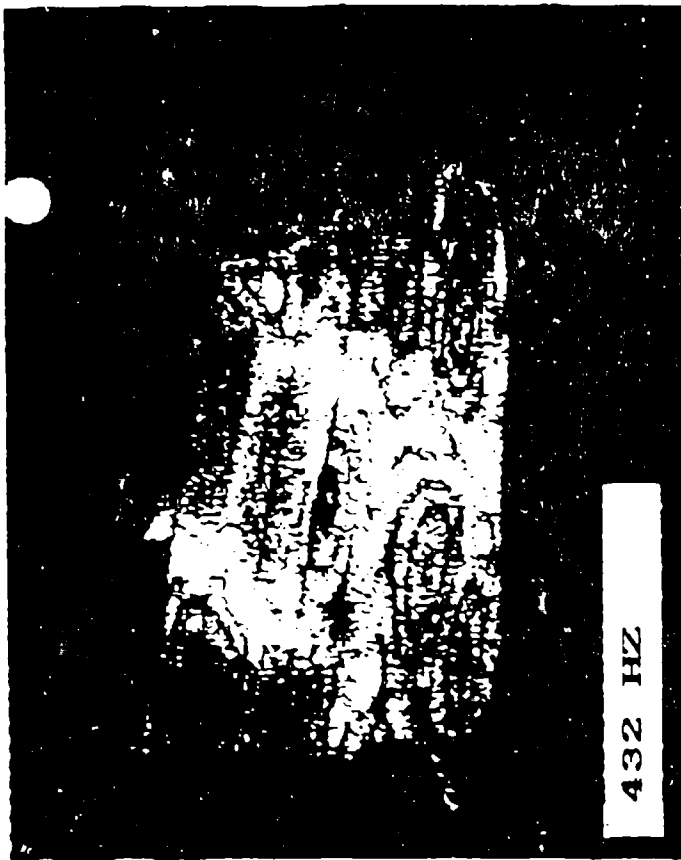


386 HZ



416 HZ

Fluorescence, Video Photography Mode, Stages for
100% cont'd



432 HZ

This image shows a video holography mode shape at 432 HZ. It displays a complex, high-contrast pattern of bright and dark regions, likely representing the vibration mode of a structure. The pattern is somewhat irregular and noisy.



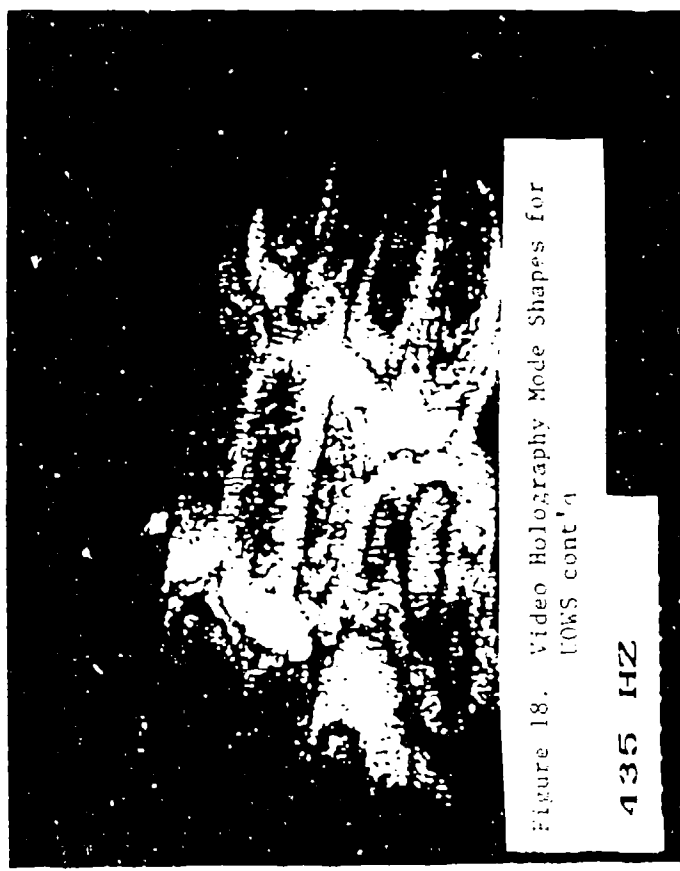
456 HZ

This image shows a video holography mode shape at 456 HZ. It displays a complex, high-contrast pattern of bright and dark regions, likely representing the vibration mode of a structure. The pattern is somewhat irregular and noisy.



422 HZ

This image shows a video holography mode shape at 422 HZ. It displays a complex, high-contrast pattern of bright and dark regions, likely representing the vibration mode of a structure. The pattern is somewhat irregular and noisy.



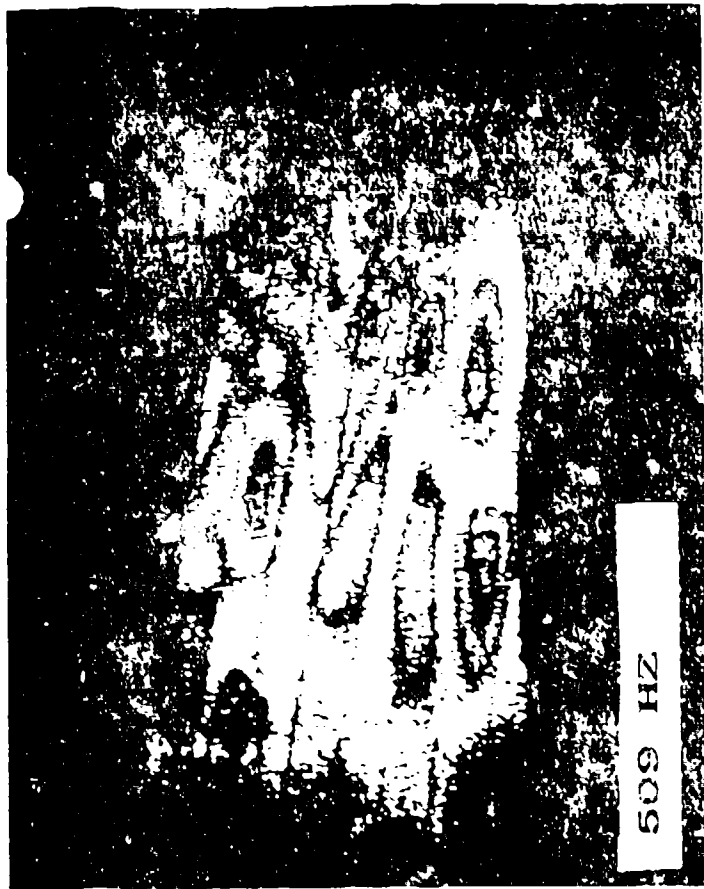
435 HZ

This image shows a video holography mode shape at 435 HZ. It displays a complex, high-contrast pattern of bright and dark regions, likely representing the vibration mode of a structure. The pattern is somewhat irregular and noisy.

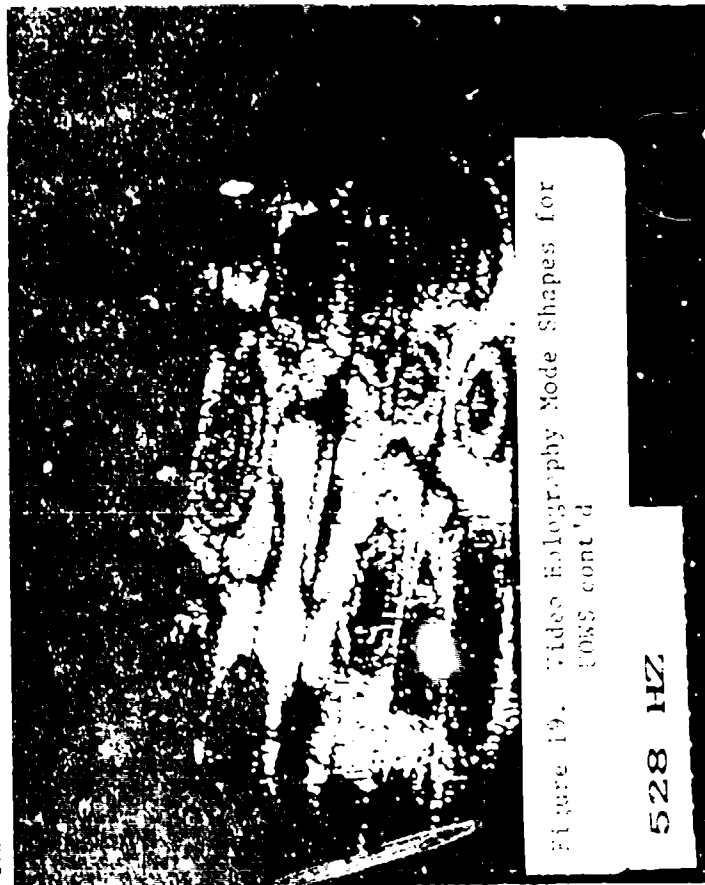
Figure 18. Video Holography Mode Shapes for
TOWS cont'd



486 HZ



509 HZ

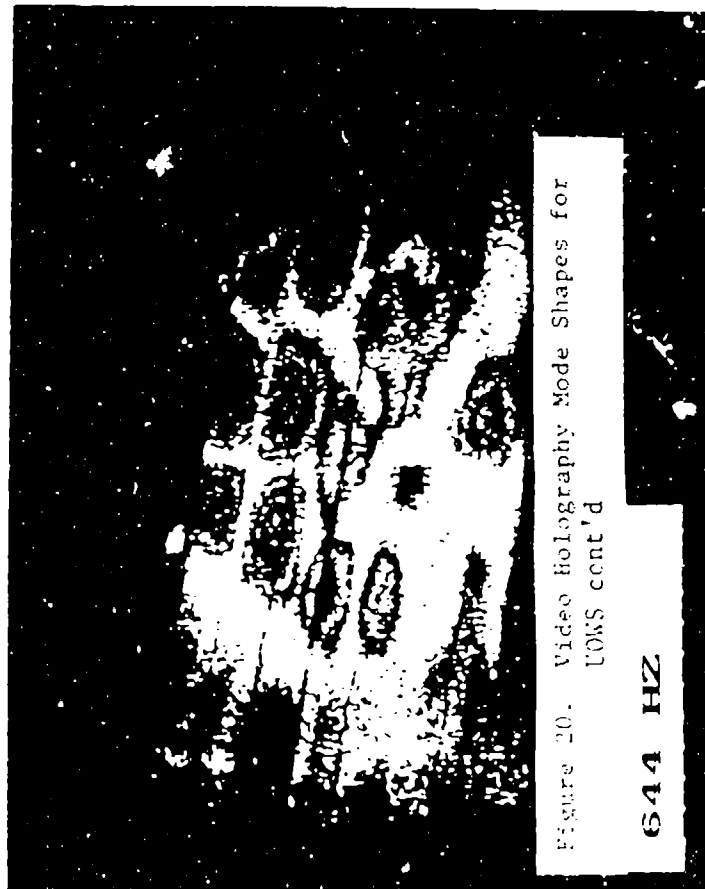


528 HZ

Figure 19. Video Holography Mode Shapes for
E085 cont'd



541 HZ





835 HZ



740 HZ

Figure 21. Video Holography Mode Shapes for
TOWS cent'd



F-15 UPPER OUTER WING SKIN PANEL

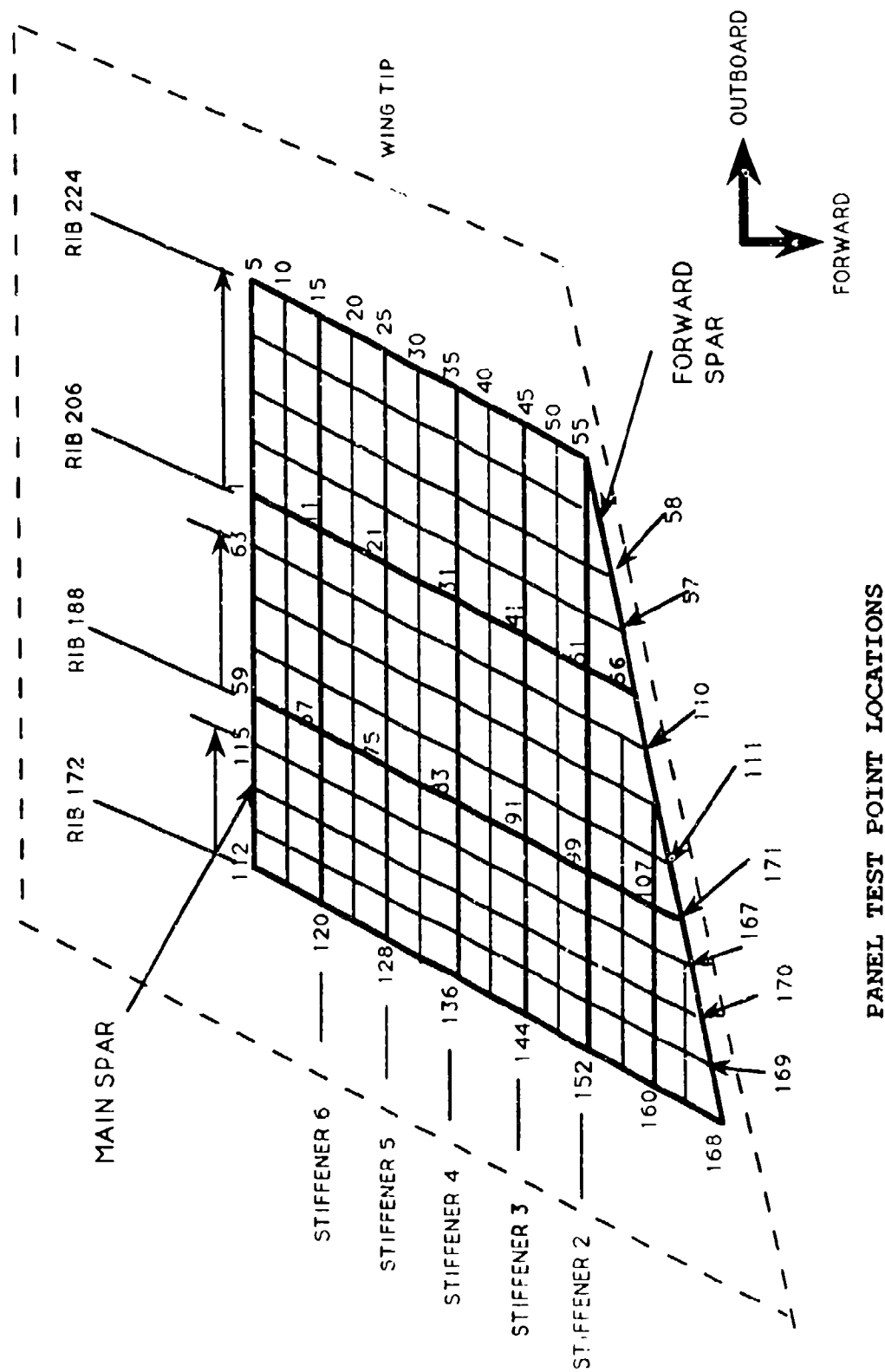


Figure 23. Accelerometer Grid Point Locations on Wing Skin

F-15 UPPER OUTER WING SKIN PANEL

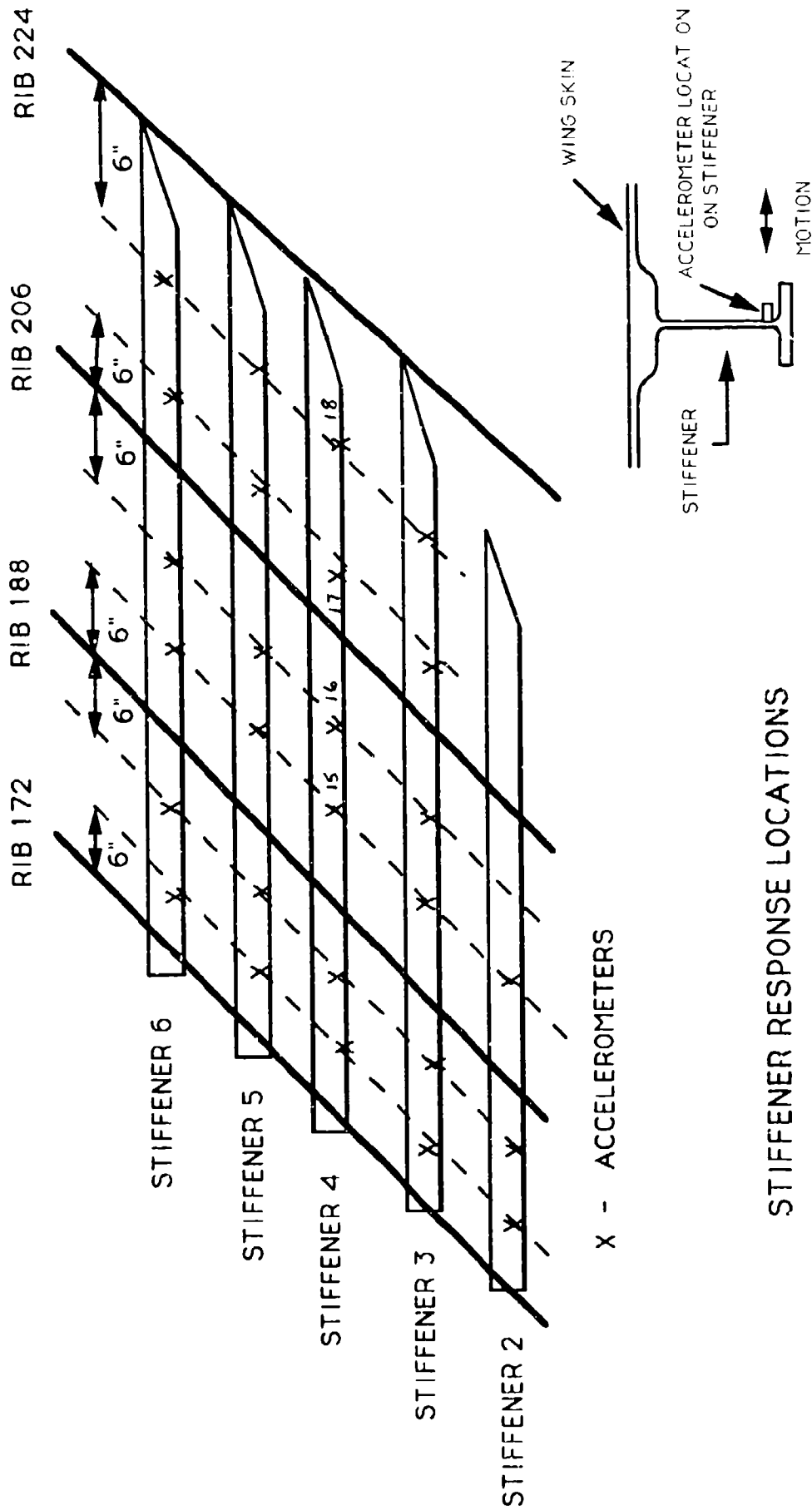


Figure 24. Accelerometer Grid Point Locations on Stiffeners



SUPP J-ELAS 4.1: Test Data Analysis

18-JAN-90

14:31:25

DATABASE: F15

UNITS : IN

VIEW : No stored VIEW

DISPLAY : No stored OPTION

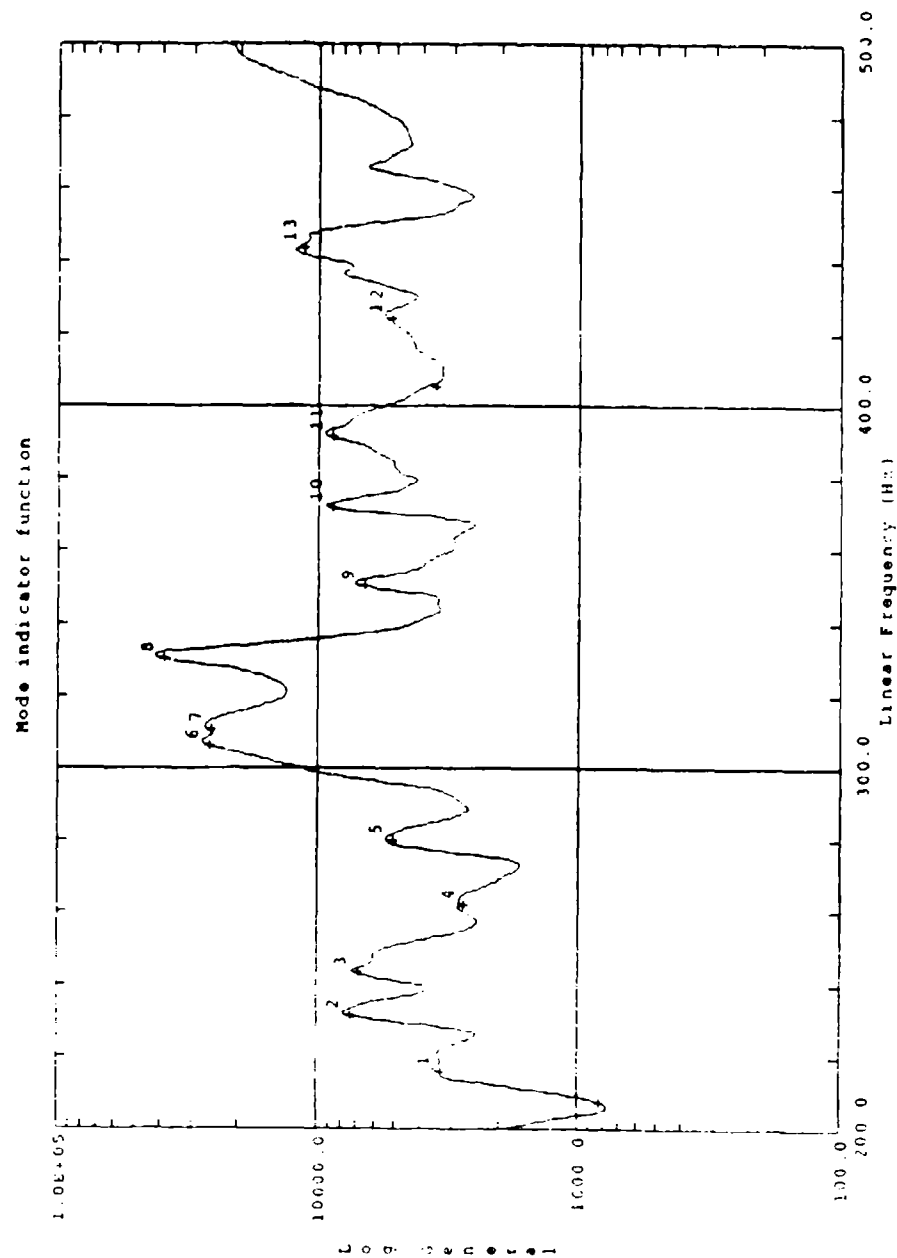


Figure 26. Modal Indicator Function for Skin Response

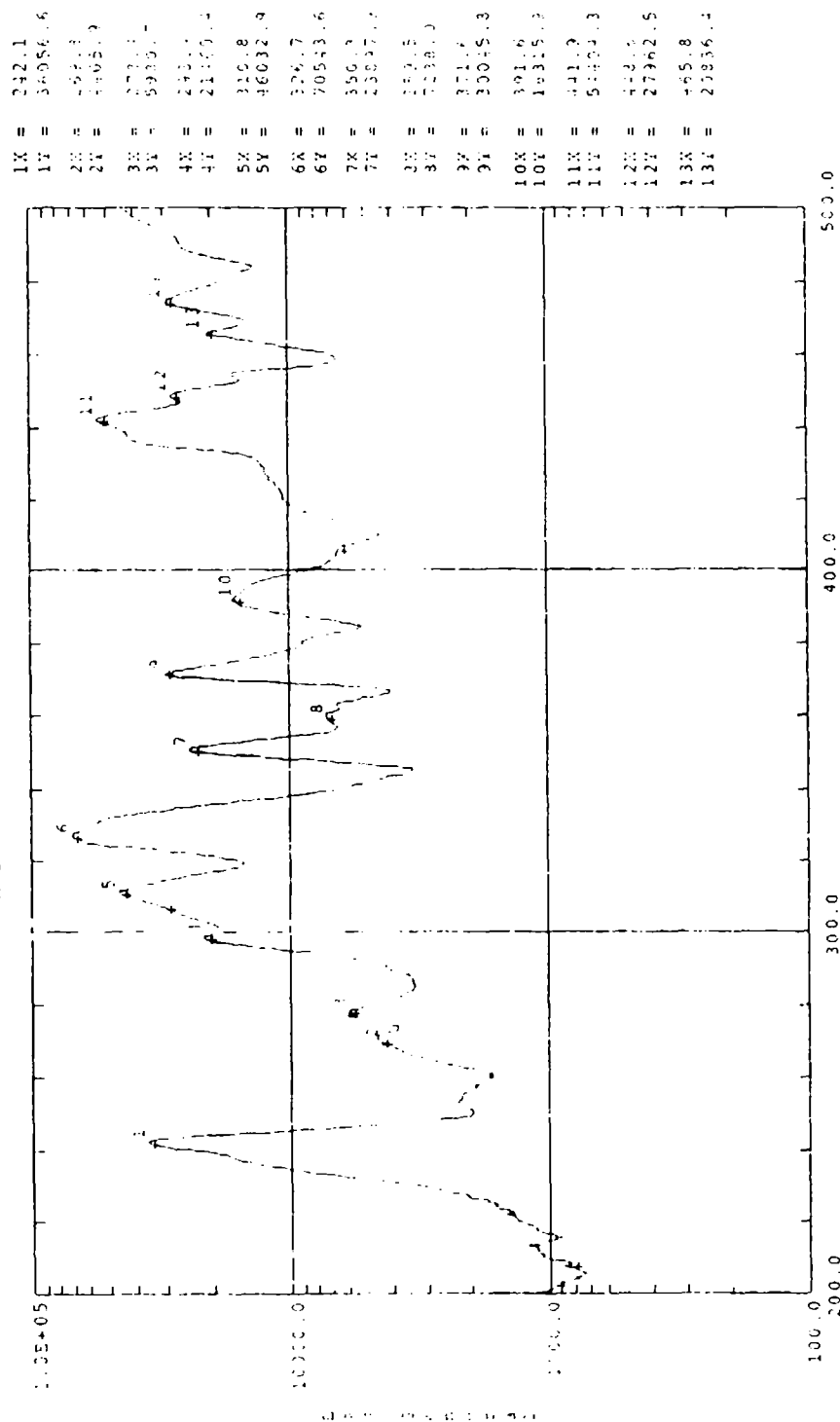
LABORATORY PDS

UNITS IN

VIEW 1 No Rotated VIEW

DISPLAY 1 No stored OPTION

Modal indicator function



5 : 212+ 212+ 1

18-JAN-90 13:19:19

Figure 27. Modal Indicator Function for Stiffener Response

1-OCT-89 11:46:29
 DISPLAY : No stored OPTION

SPIC INCAS 4.11 Test Data Analysis
 DATABASE: 115
 VIEW : No stored VIEW

MODEL / FREQ(HZ): 299.10062 DAMPING(R): 0.9327321
 ACCEL / EXCI FORCE MAG MIN: 7.93E-03 MAX: 7.47E+02

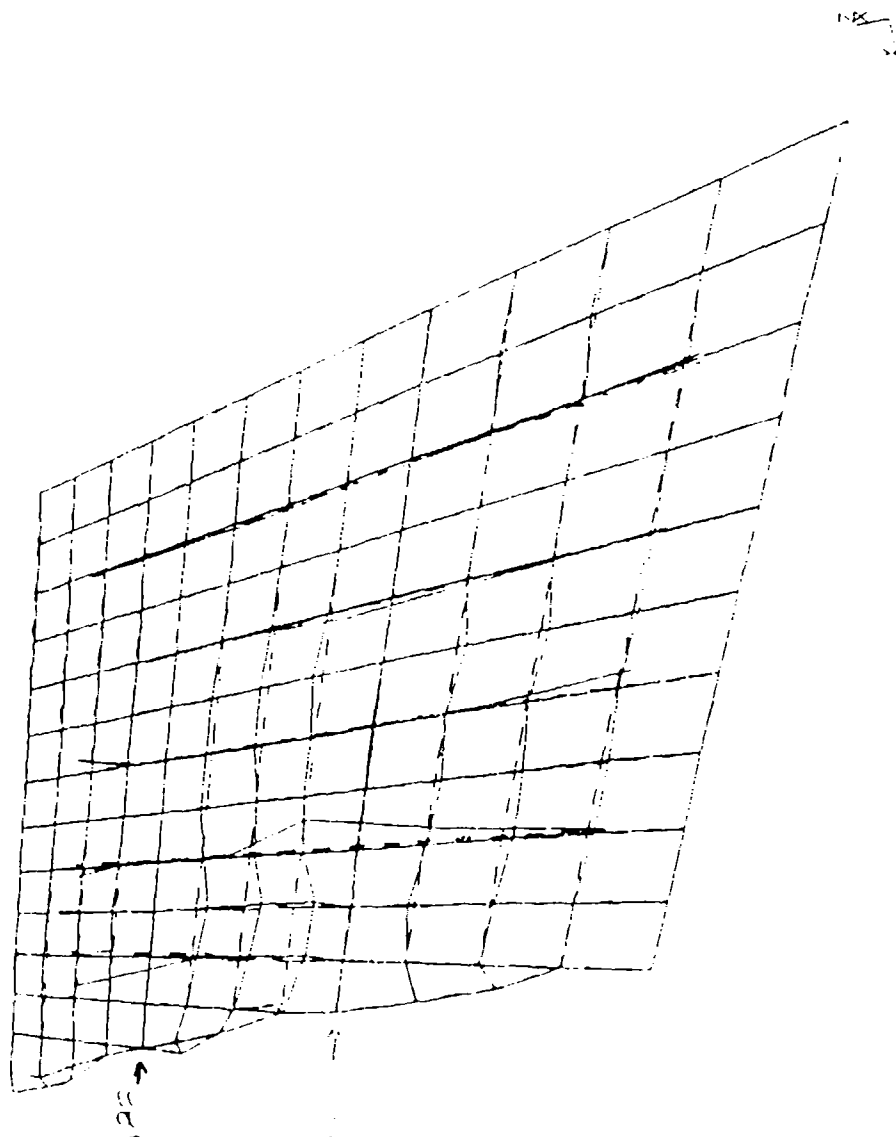


Figure 28. Combined Skin and Stiffener
 Mode Shape at 299.1 Hz

11:47:32
UNIT: IN
DISPLAY: NO STORED OPTION

SUBJECT: 89

TEST DATA ANALYSIS

DATA BASE: P15
VIEW: NO STORED VIEW

MODE: 12 FREQUENCY: 316.225892 DAMPING RATIO: 1.1954002
ACCEL / EXCI FORCE MAG MIN: 2.335E-02 MAX: 5.145E+02

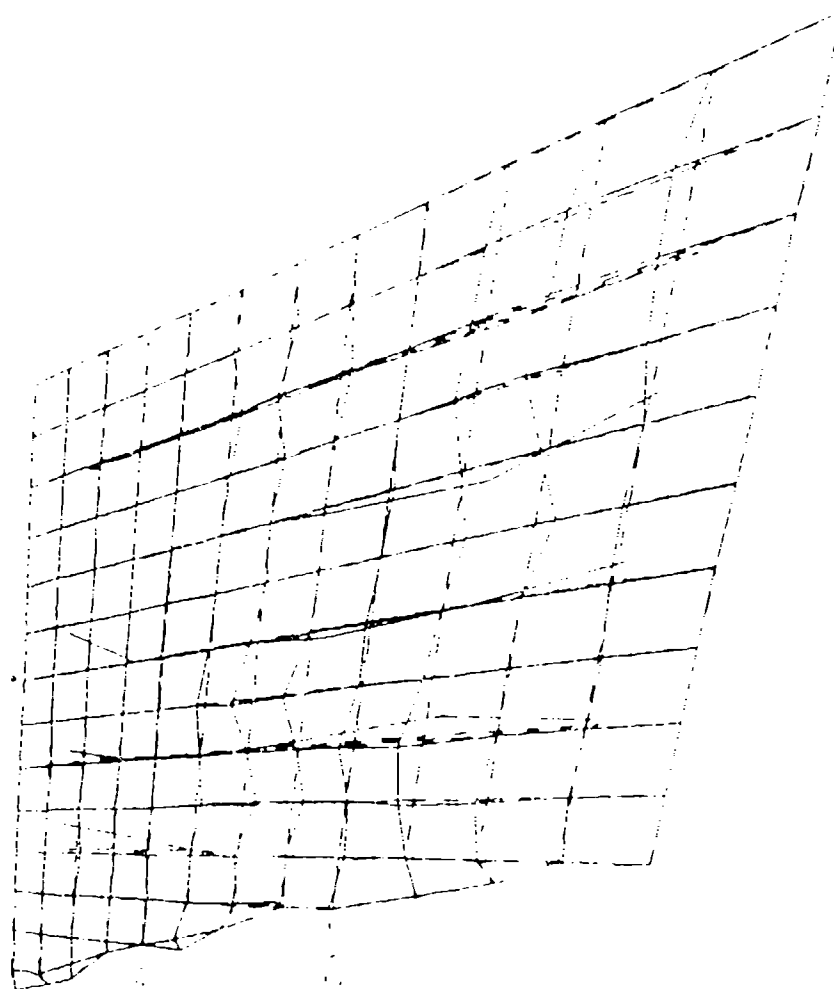


Figure 29. Combined Skin and Stiffener
Mode Shape at 306.3 Hz

SDRC I-DEAS 4.11 Test Data Analysis
 DATABASE: F15
 VIEW : No stored view

3-OCT-89

11:49:06

UNITS : IN
 DISPLAY : No stored OPTION

MODEL: FREQUENCY: 114.30112 DAMPING(V): 1.2925593
 ACCEL / EXCI FORCE MAG MIN: 2.76E-01 MAX: 6.64E+02

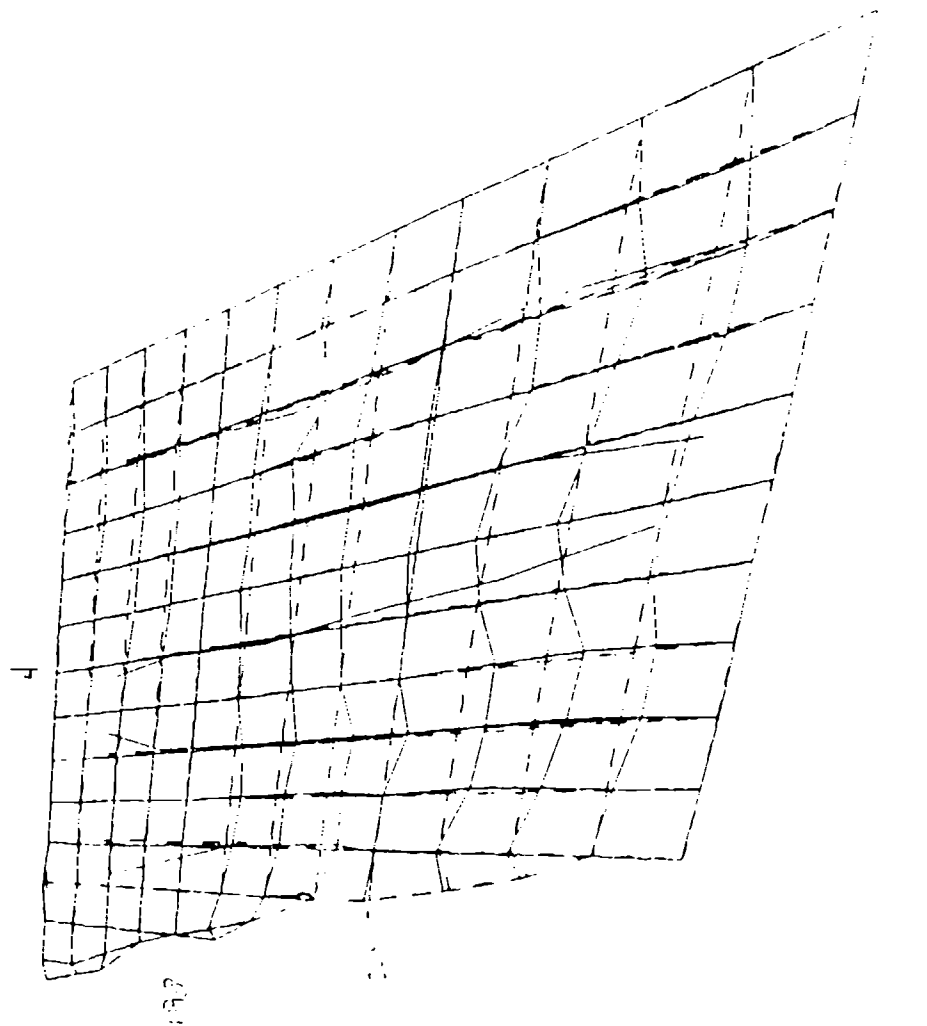


Figure 30. Combined Skin and Stiffener
 Mode Shape at 314.3 Hz

SRC I-DEAS 4.10 Test Data Analysis 3-OCT-89 11:46:49
 DATABASE: P15 UNITS: IN
 VIEW: No stored VIEW DISPLAY: No stored OPTION

MODE: 4 FREQUENCY: 333.6554 DAMPING(R): 0.61655554
 ACCEL / EXCI FORCE MAG MIN: 5.06E-01 MAX: 7.91E+02

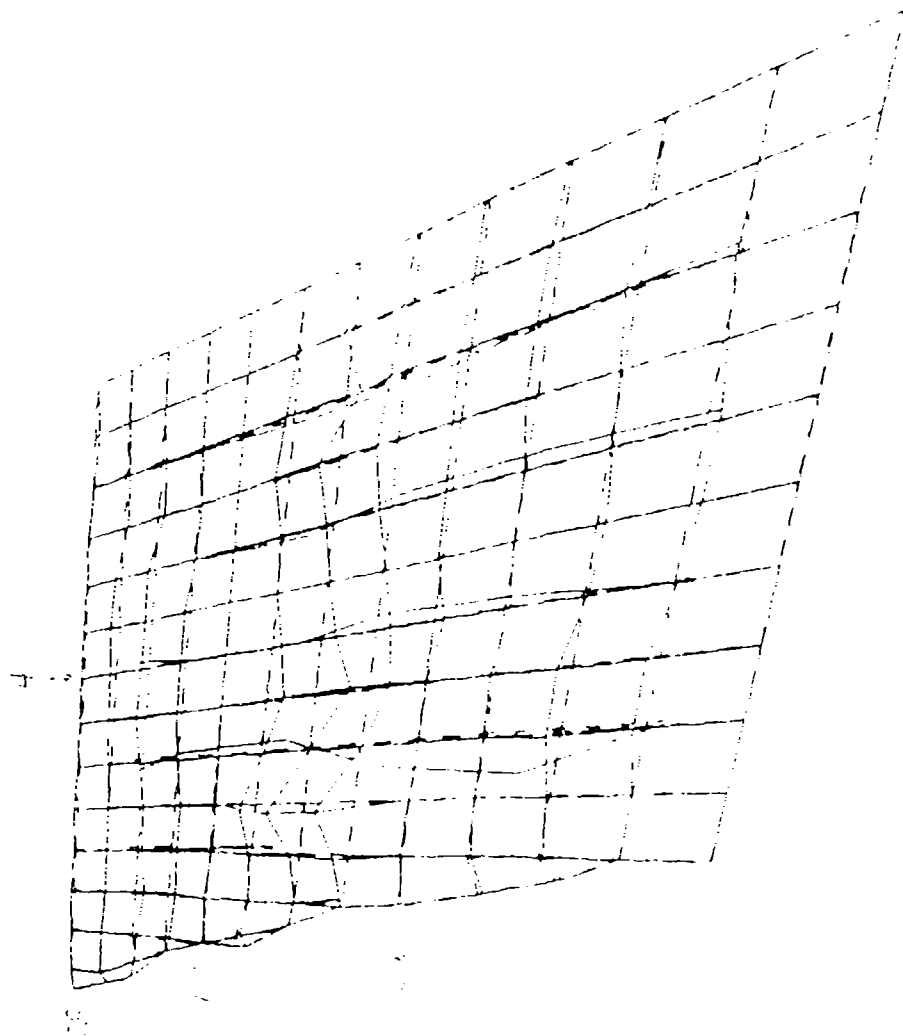


Figure 31. Combined Skin and Stiffener
 Mode Shape at 333.6 Hz

SDPC 2-DEAS 4.1. Test Data Analysis
 DATABASE: F15
 VIEW: No stored VIEW
 3-OCT-89 11:49:23
 DISPLAY: No stored OPTION

MODE: 5 FREQ(Hz): 345.974 DAMPING(%): 0.7867343
 ACCEL / EXCI FORCE MAG MIN: 1.36E-01 MAX: 3.81E+02

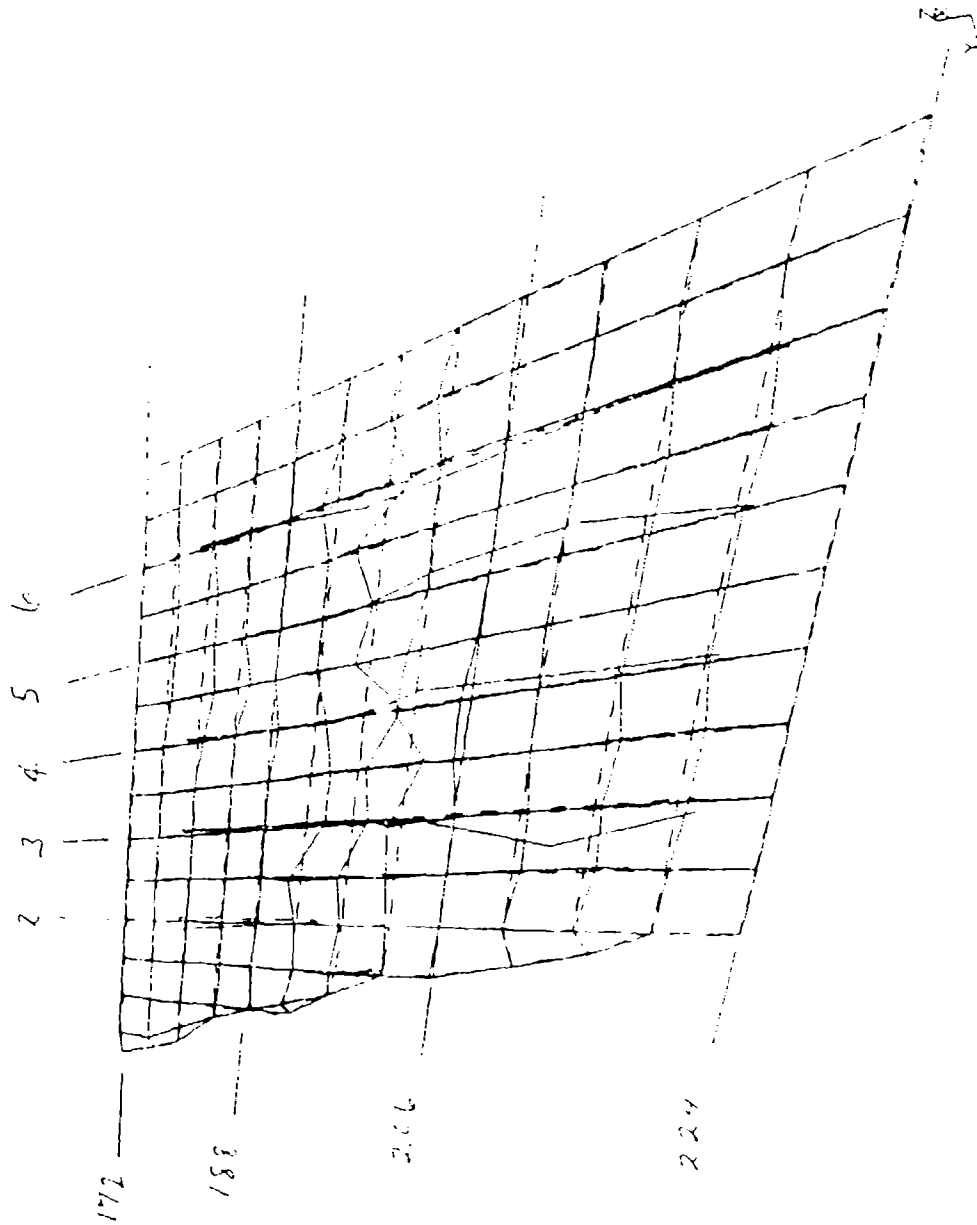


Figure 32. Combined Skin and Stiffener
 Mode Shape at 346.0 Hz

SDP: 1-DEAS 4.1: Test Data Analysis
 DISPLAY: NO STORED VIEW

3-OCT-69 11:49:56
 DISPLAY: NO STORED OPTION

MODE: 6 FREQ(HZ): 371.18332 DAMPING(R): 0.685933
 ACCEL / EXCI FORCE MAG MIN: 1.34E-01 MAX: 4.31E+02

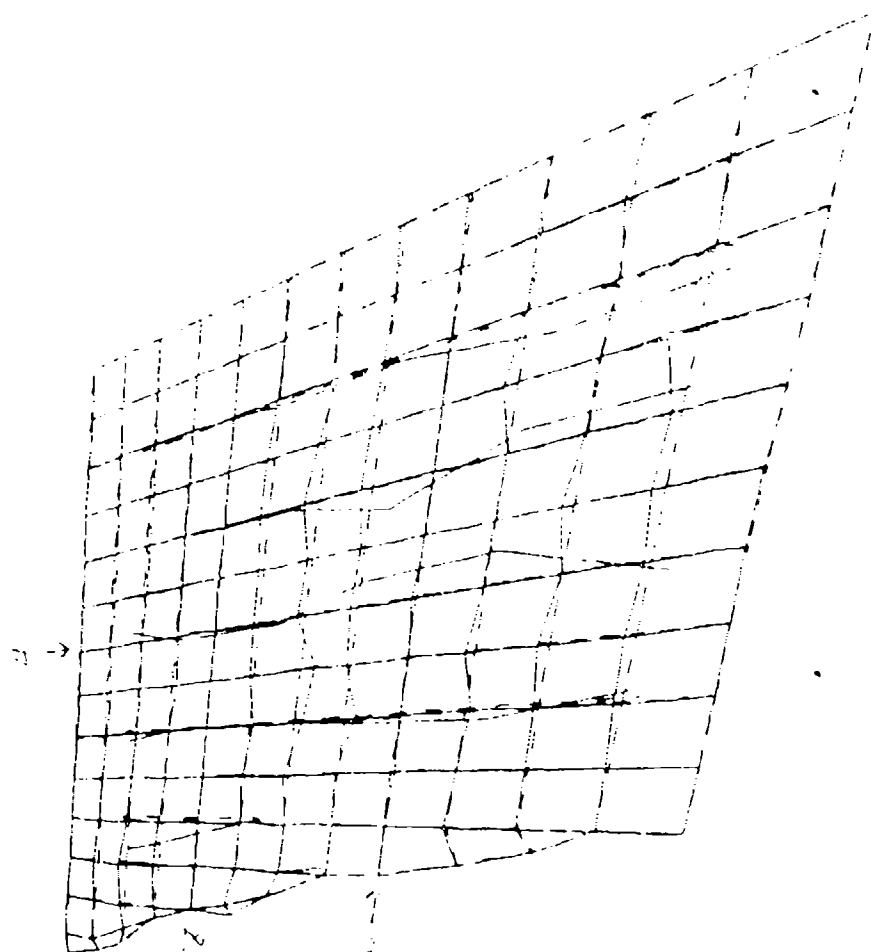


Figure 23. Combined Skin and Stiffener
 Mode Shape at 371.2 Hz

SCPC I-DEAL v.1.1 Test Data Analysis
 CASEBASE: P15
 VIEW: 1 No stored view
 3-OCT-84 11:50:29
 UNITS IN
 DISPLAY: No stored option

MODE17 FREQ(Hz): 395.5129 DAMPING(R): 1.0944693
 ACCEL / EXCI FORCE MAX MIN: 2.31E-02 MAX: 3.95E+02

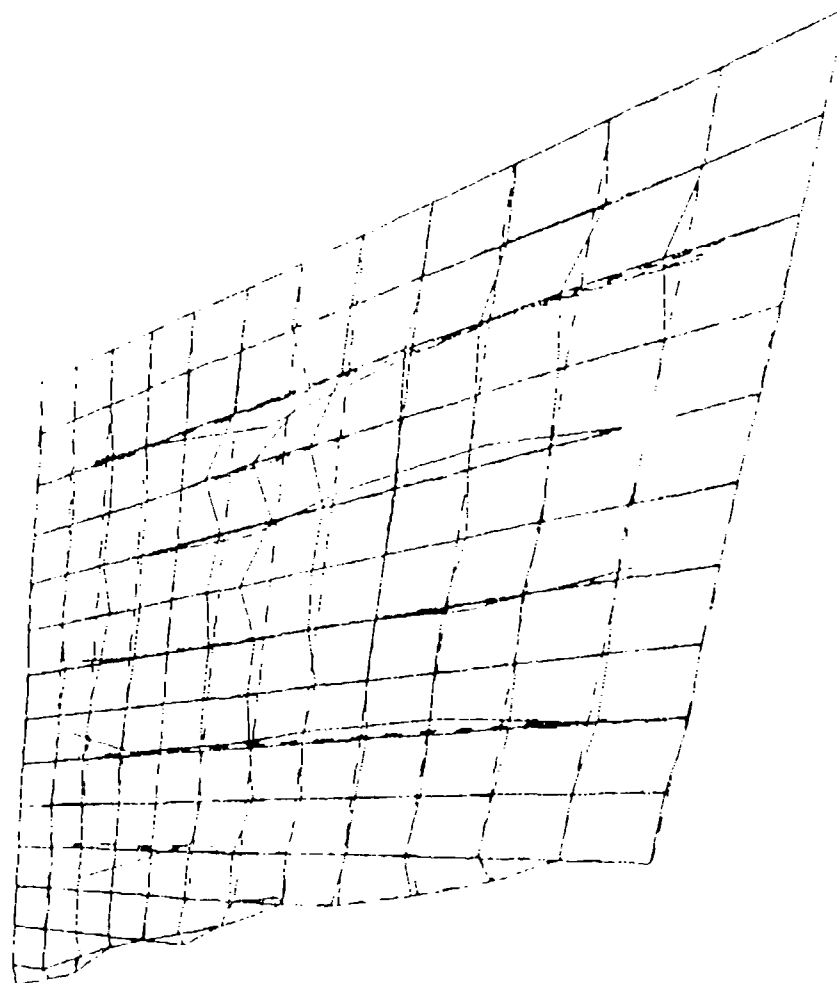


Figure 34. Combined Skin and Stiffener
 Mode Shape at 395.5 Hz

F-15 AIRCRAFT

GROSS WEIGHT = 42000 lbs

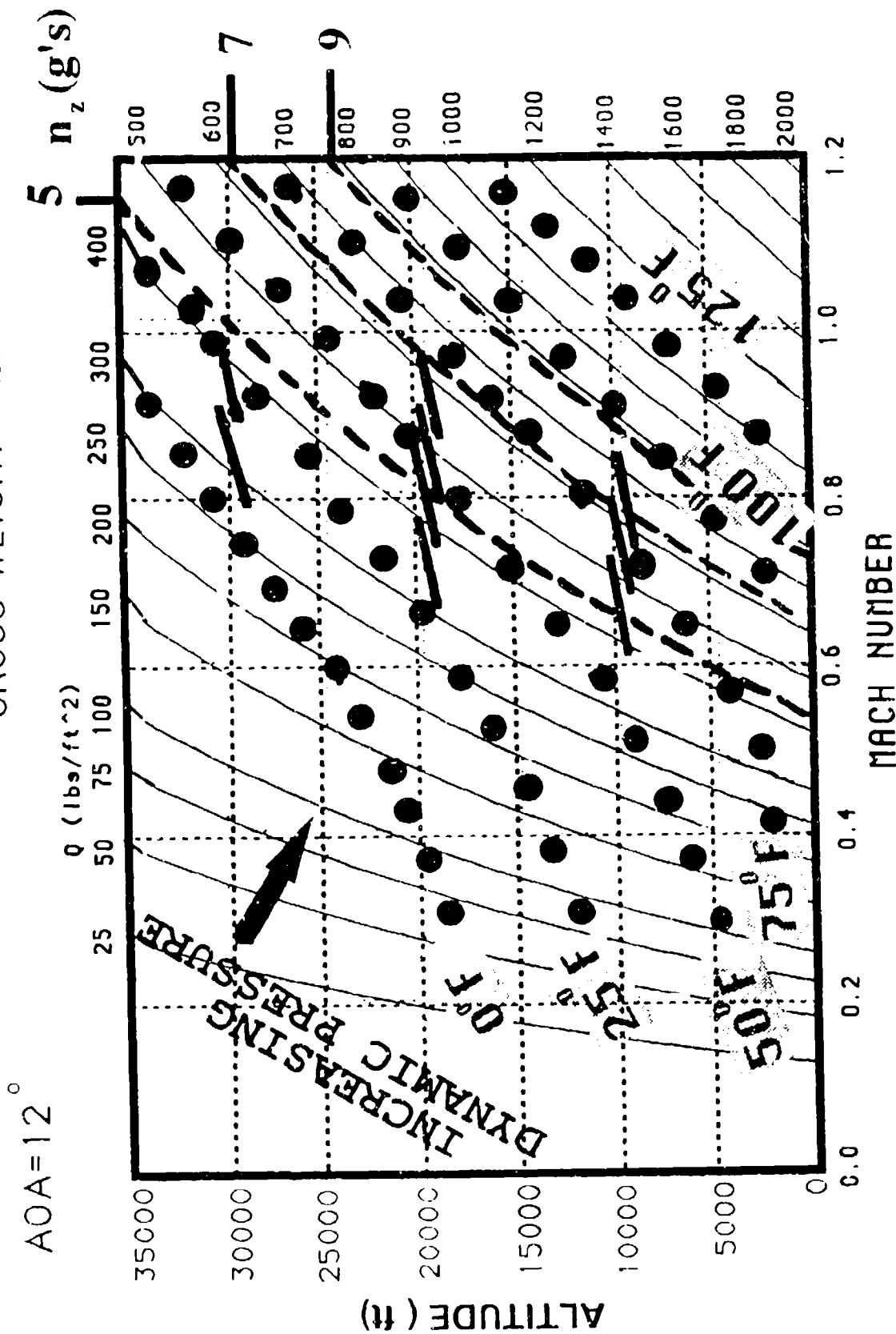


Figure 15. F-15 Aircraft Performance Data

SUSTAINED LEVEL TURNS **GROSS WEIGHT - 42,000 POUNDS** **MAXIMUM THRUST**

AIRPLANE CONFIGURATION
 F-15A/C
 CFT

REMARKS
 ENGINE(1) (2) F100-PW-100
 ENGINE TRIM 97.7%
 U.S. STANDARD DAY, 1966

DATE: 1 OCTOBER 1985
 DATA BASIS: FLIGHT TEST

GUIDE

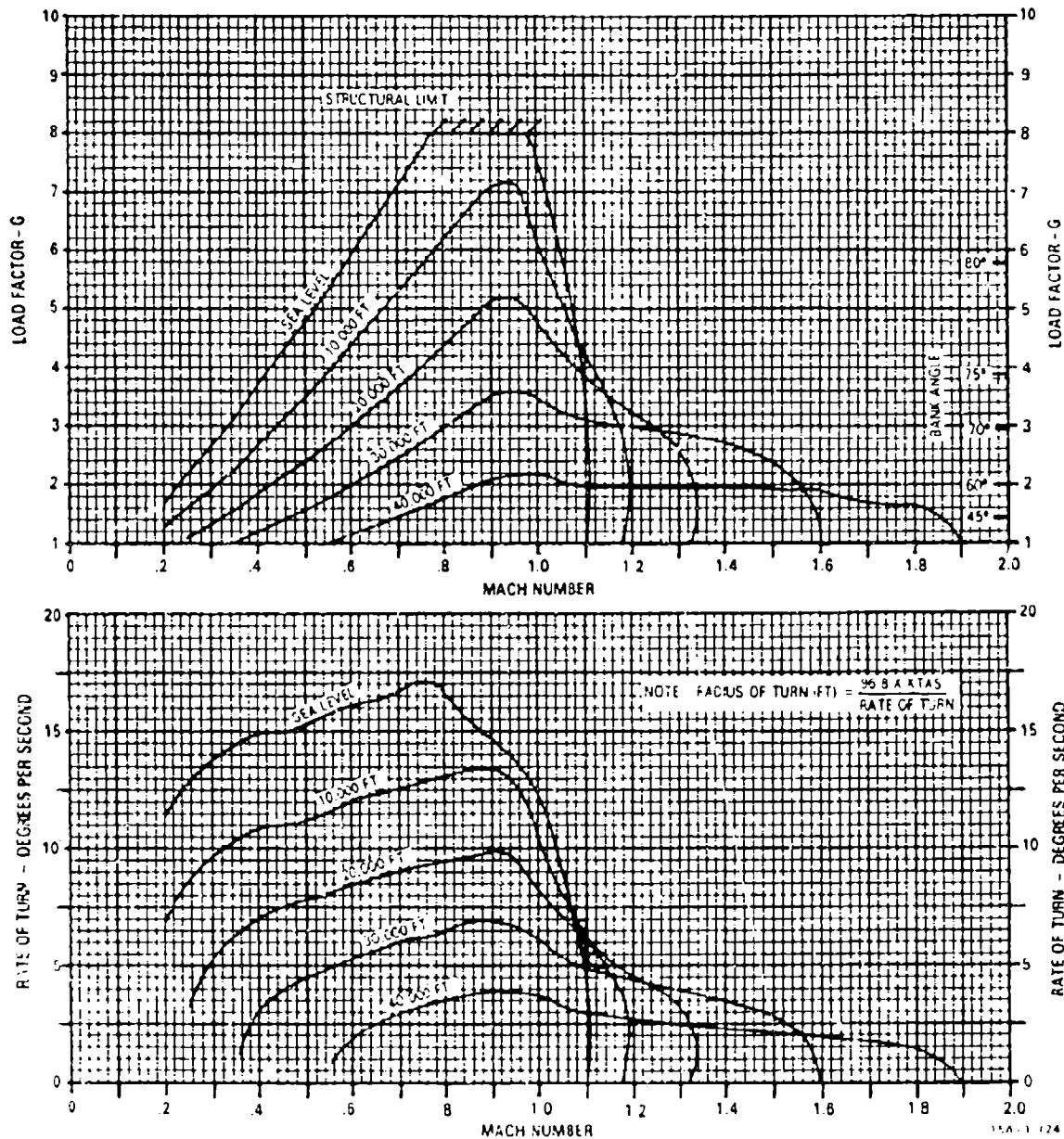
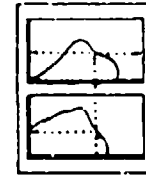


Figure A9-44

A9-52

F-15 UPPER OUTER WING SKIN

TEST CONFIGURATION 1

1980 DAMPING TREATMENT

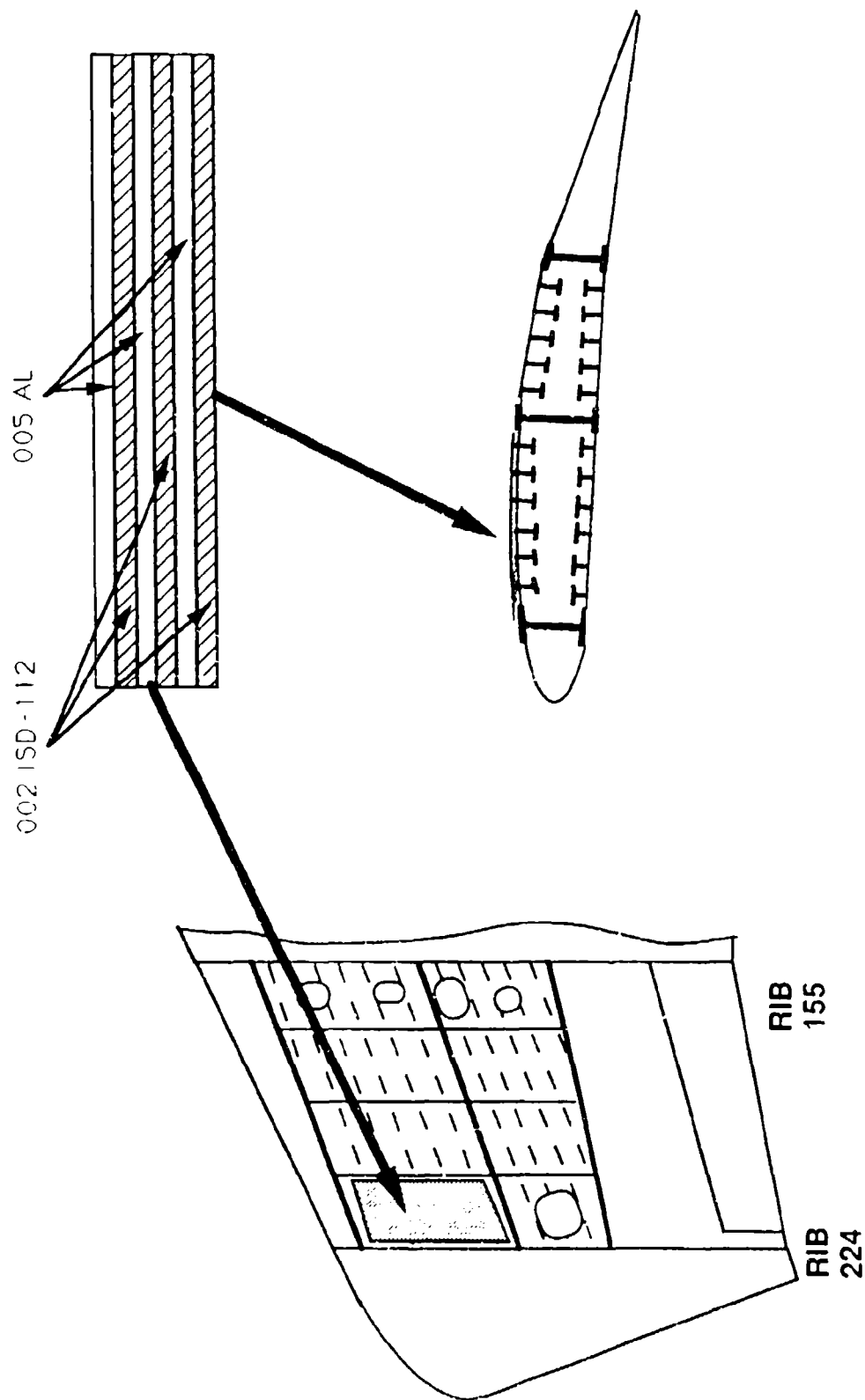


Figure 37. "1980 Damping Treatment"



F-15 UPPER OUTER WING SKIN

RECOMMENDED EXTERNAL DAMPING TREATMENT

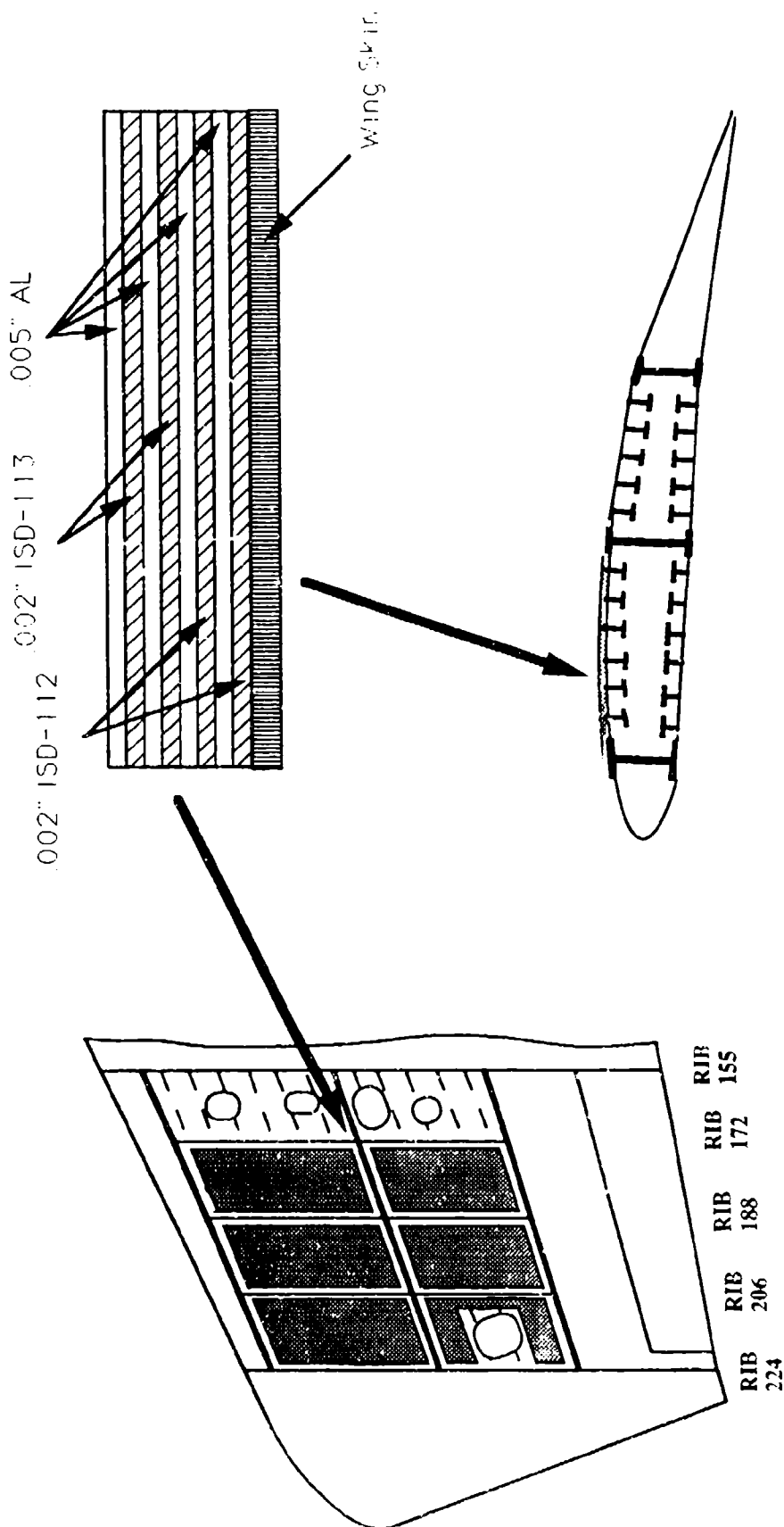


Figure 39. External Damping Treatment Design



Figure 40. External Pumping Treatment

F-15 UPPER OUTER WING SKIN

RECOMMENDED INTERNAL DAMPING TREATMENT

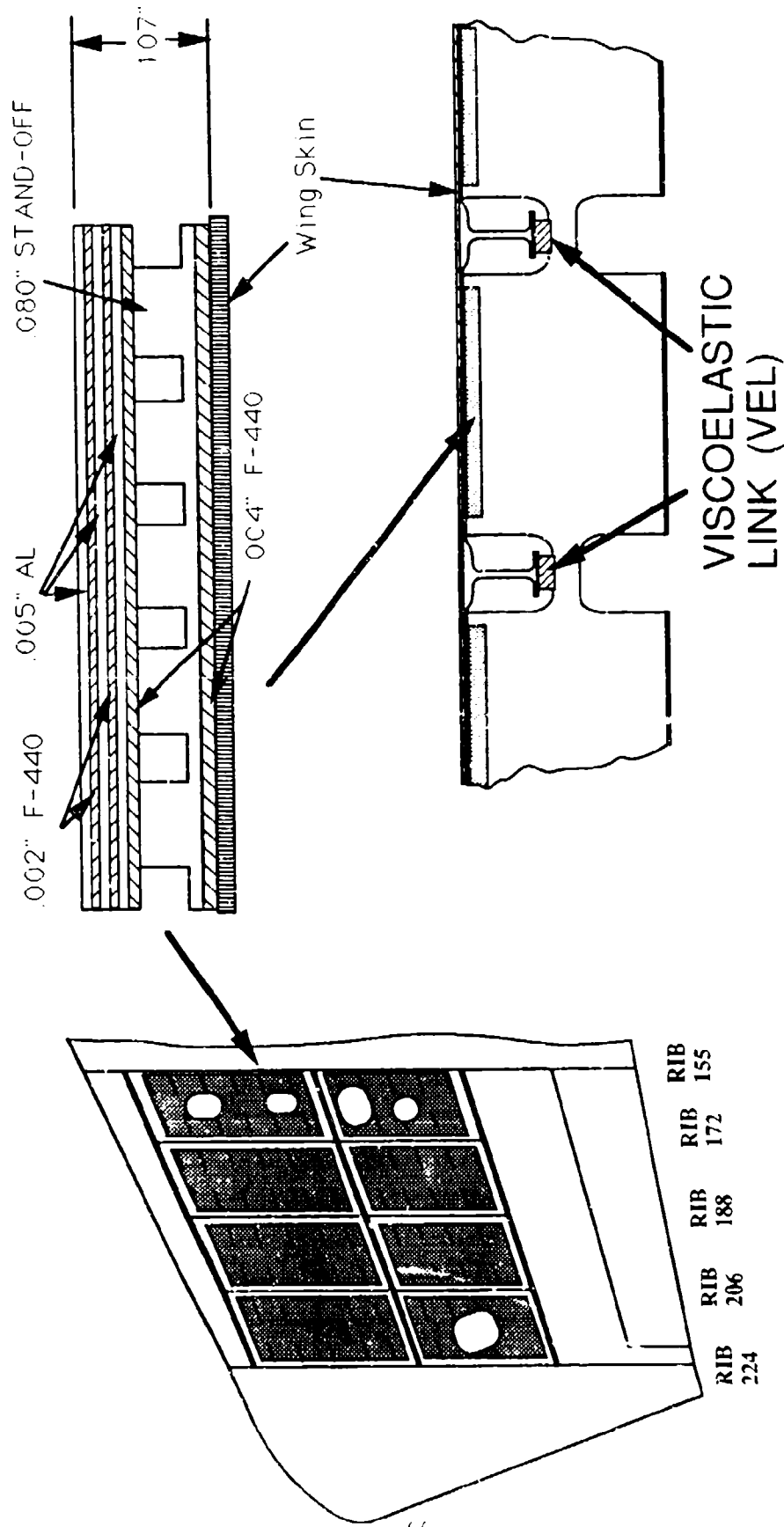


Figure 41. Internal Damping Treatment Design





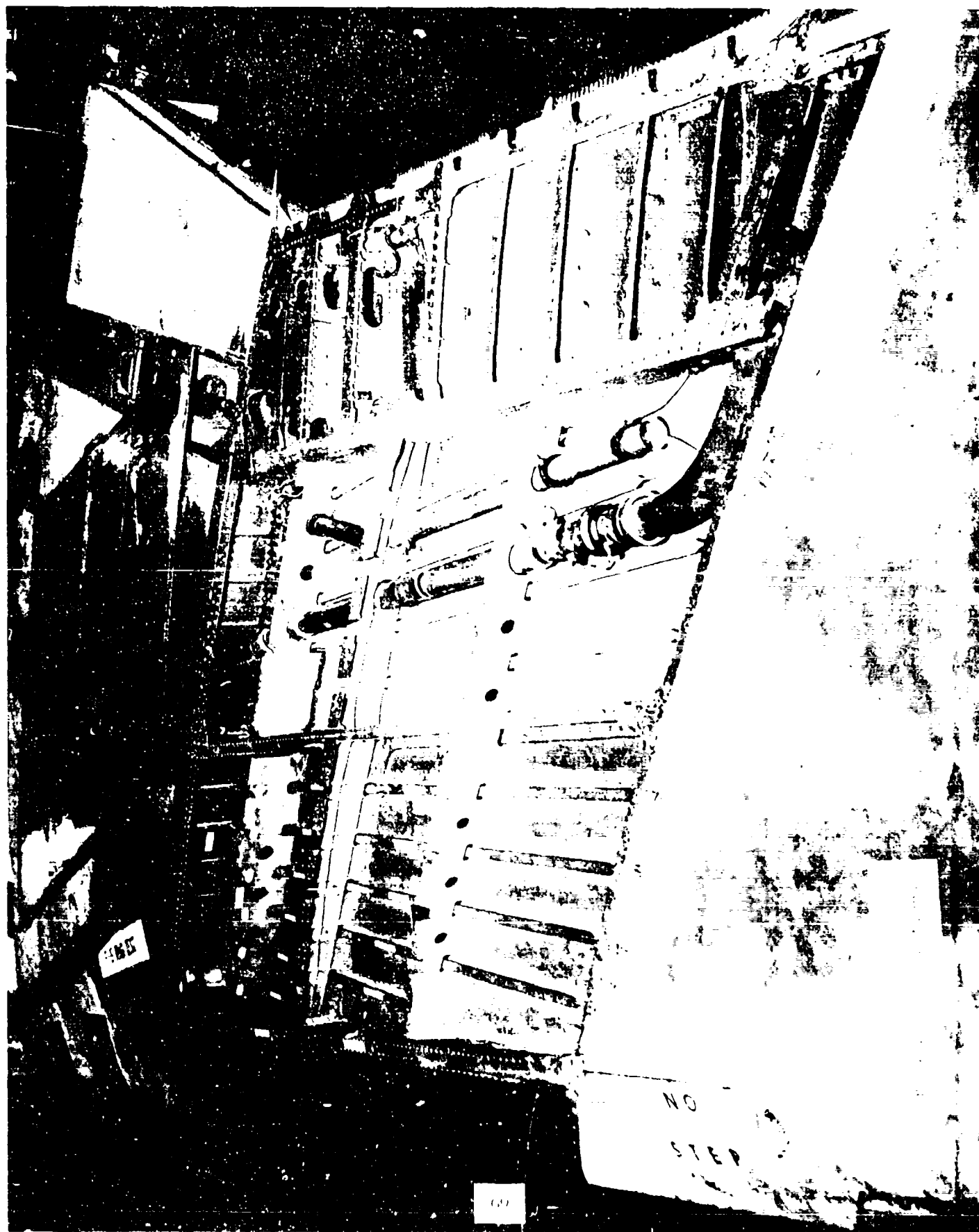


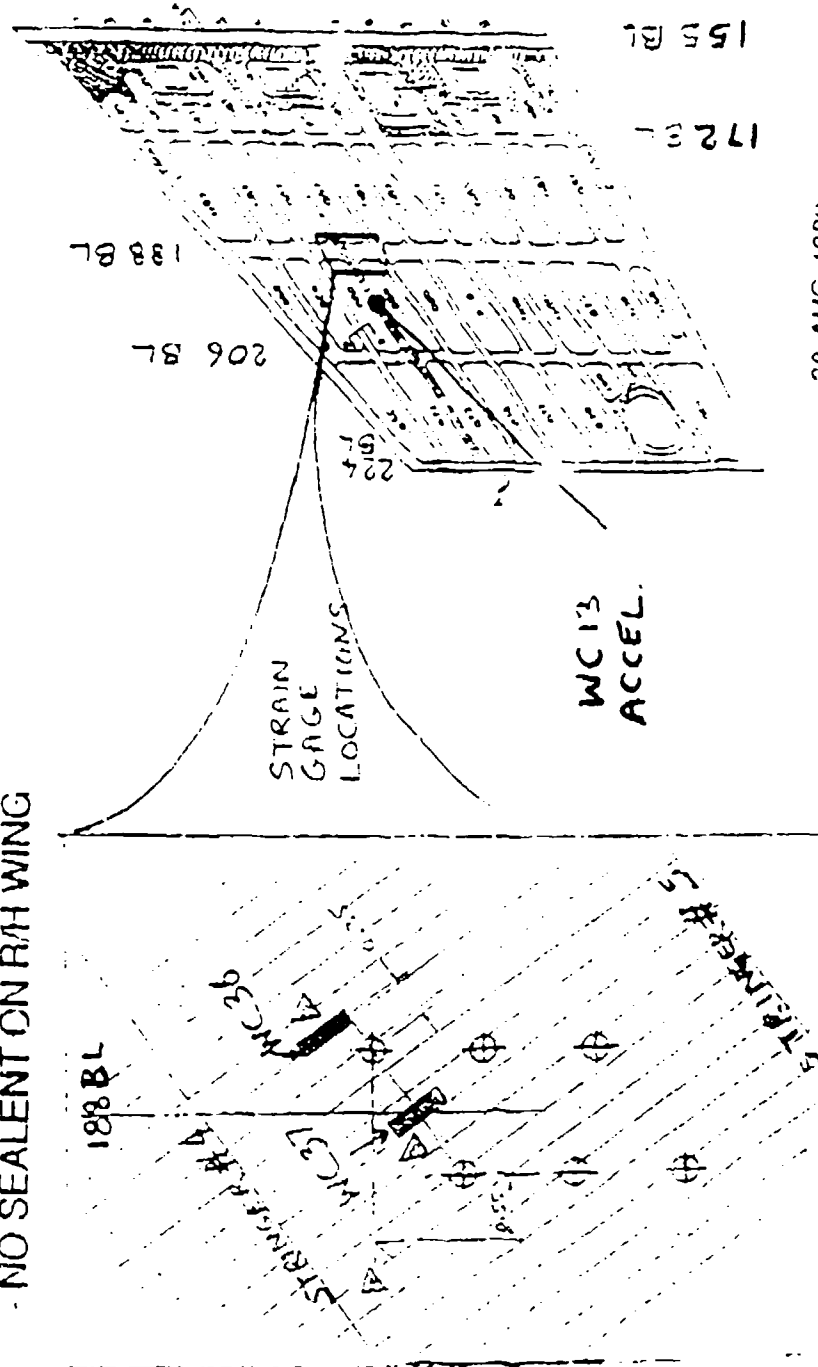




Figure 46. External Treatment Installation

FLIGHT TEST INSTRUMENTATION FOR SEALENT EVALUATION

- L/H AND R/H WINGS INSTRUMENTED
- SEALENT BETWEEN SKIN AND RIBS & SPARS ON L/H OUTER WING
- NO SEALENT ON R/H WING



30 AUG 1989

MCDONNELL AIRCRAFT

Figure 47. Strain Gage Locations for Flight Test

FLIGHT 994 WB21 AOA VS Q

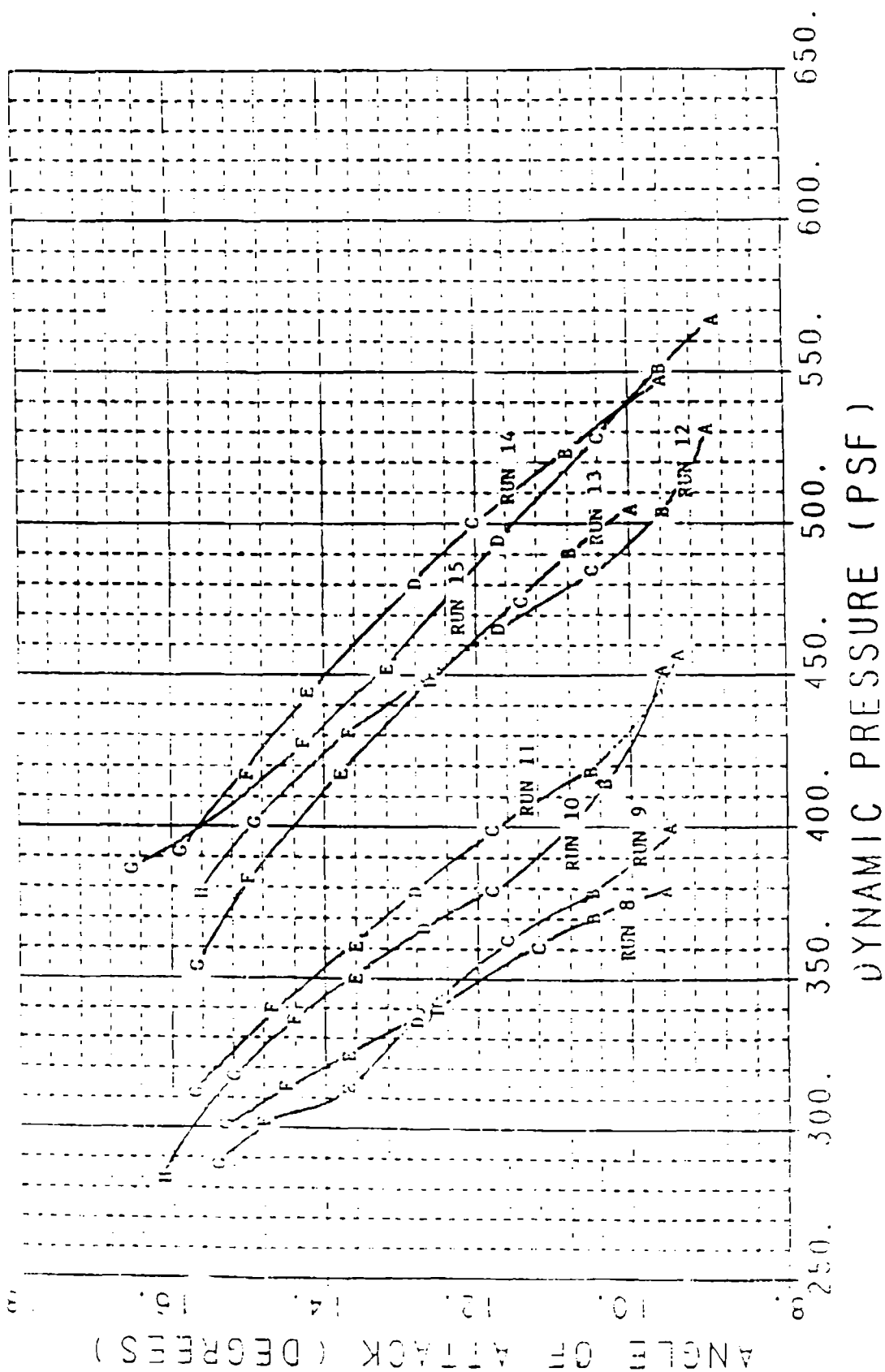


Figure 48. Typical Flight Conditions

F-15 UPPER OUTER WING SKIN LIFE EXTENSION

FLIGHT DATA PSD OF STRAIN GAGE

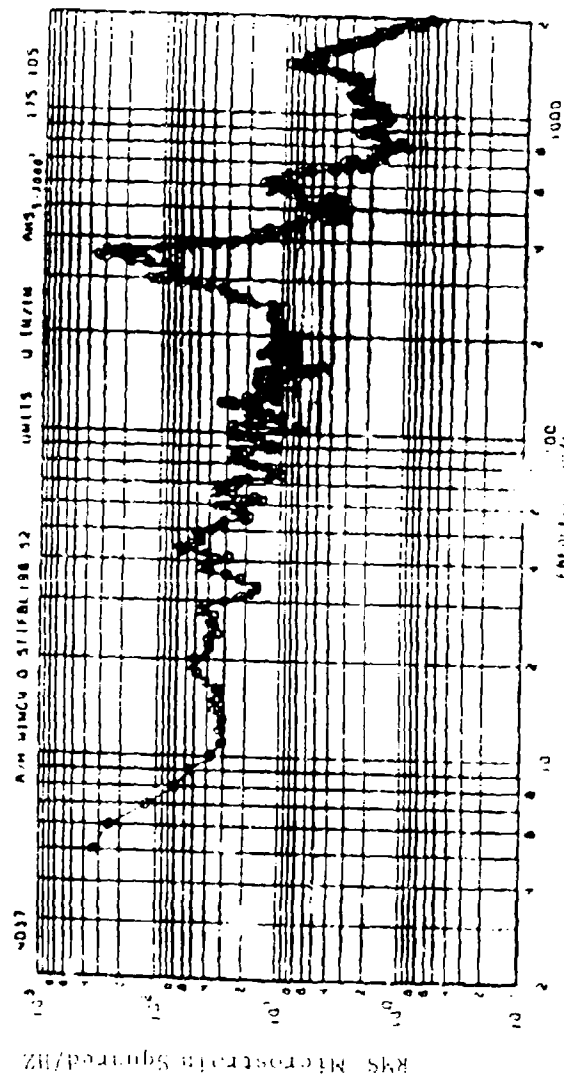


Figure 49. PSD of Strain Gage Flight Data

F-15 WING DAMPING TREATMENT TEST

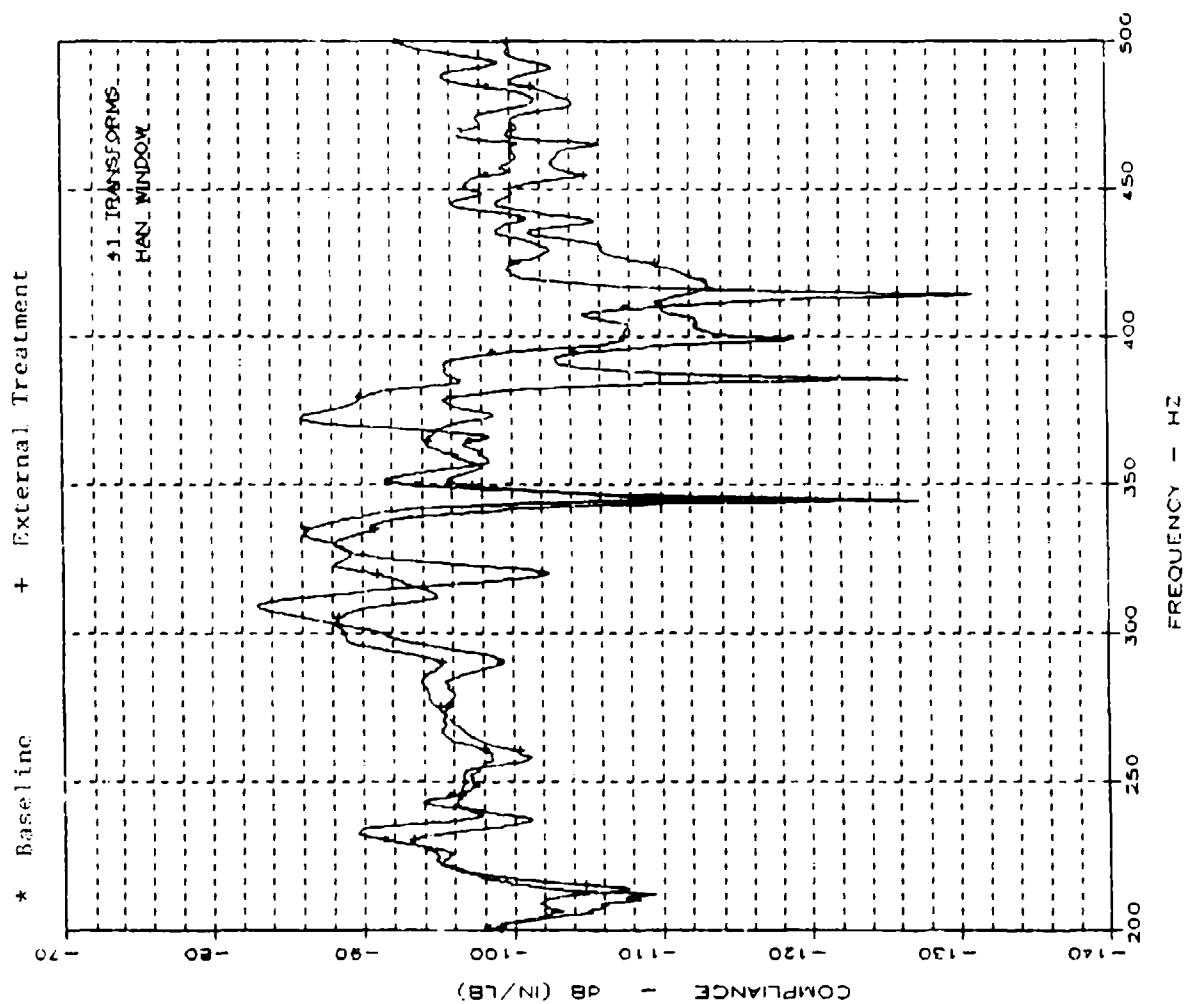


Figure 50. Comparison of the Baseline UOWS and the UOWS with External Damping Treatment

F-15 WING DAMPING TREATMENT TEST

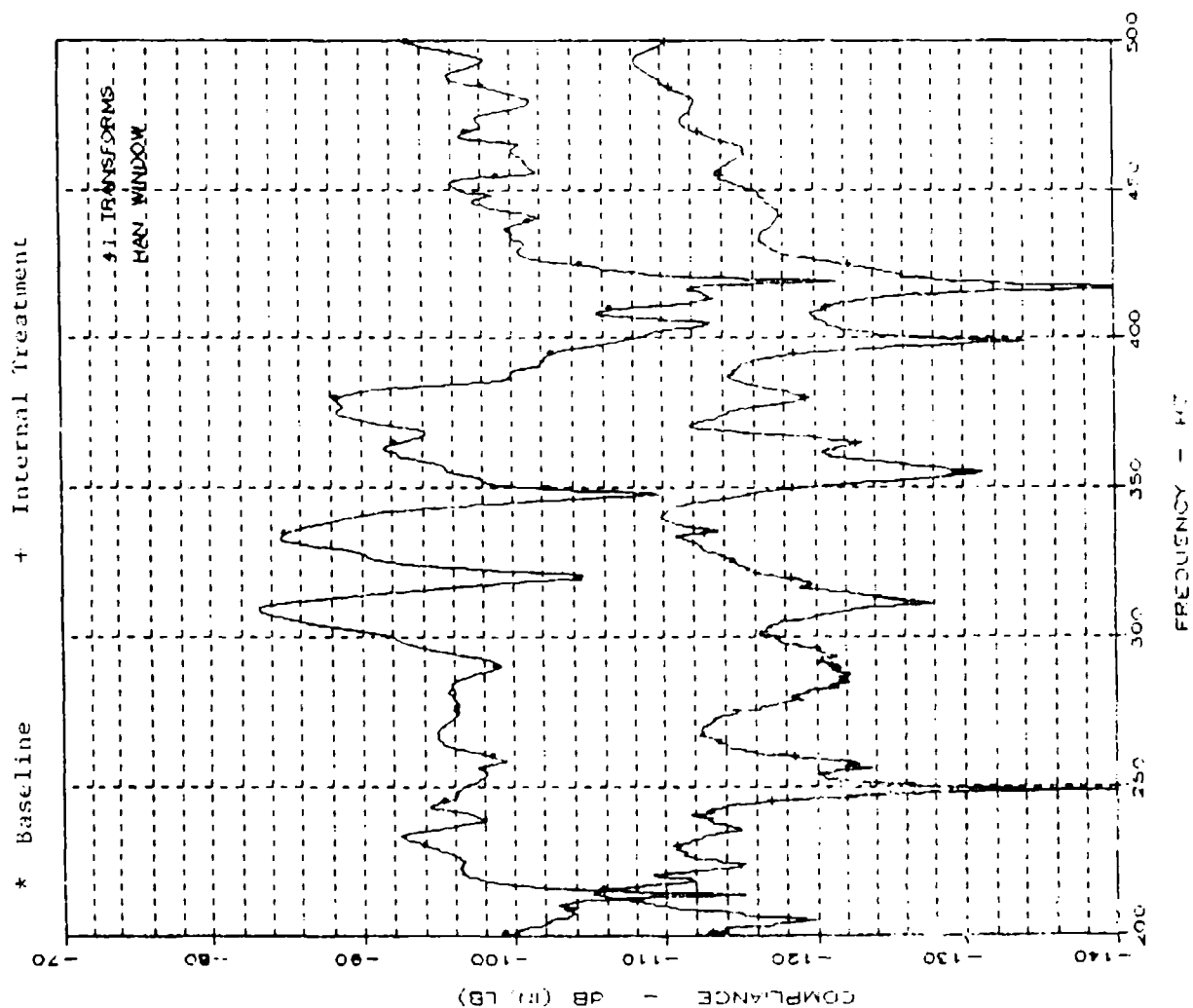


Figure 51. Comparison of the Baseline UOWS and the UOWS With Internal Damping Treatment .

F-15 UPPER OUTER WING SKIN LIFE EXTENSION

LIFE EXTENSION FACTOR CALCULATION

$$\frac{N_d}{N_u} = (S_d / S_u)^{-3.323}$$

WHERE

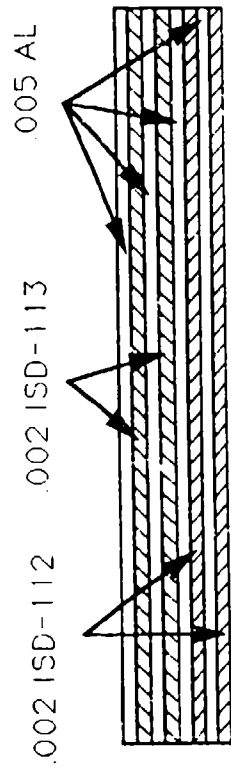
N_d = DAMPED LIFE

N_u = UNDAMPED LIFE

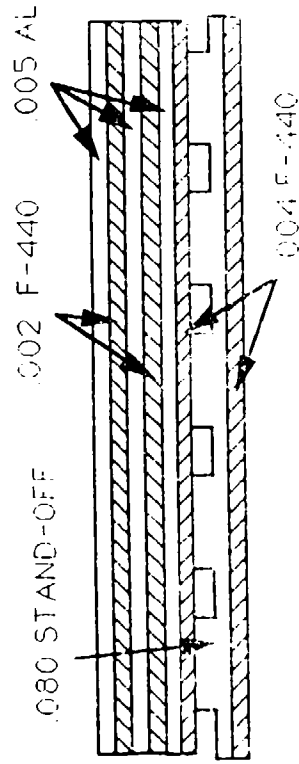
S_d = DAMPED STRESS

S_u = UNDAMPED STRESS

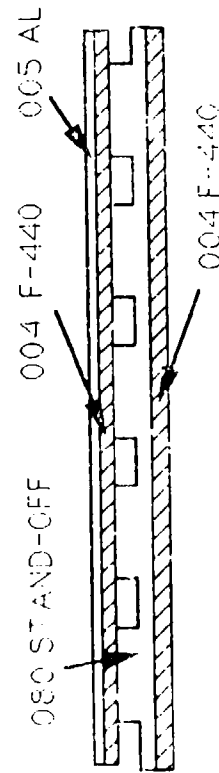
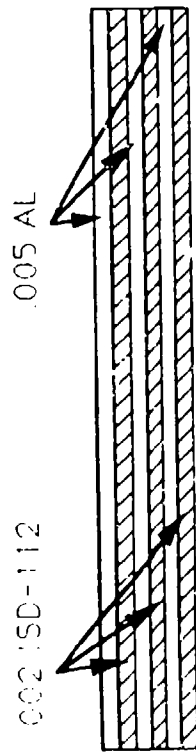
F-15 UPPER OUTER WING SKIN LIFE EXTENSION



1980 DAMPING TREATMENT



S.O.D. CONF 2



S.O.D. CONF 1

Figure A1. Four Basic Damping Treatment Lay-ups

DAMPING TREATMENT LAY-UPS

THICKNESS - IN	112 (1980 DT)	112/113	S/1	S/3
WT - LB/SQ FT				
0.021	5 AL	5 AL	5 AL	5 AL
0.25	2 ISD112	2 ISD113	2 F440	2 F440
	5 AL	5 AL	80 SO	5 AL
	2 ISD112	2 ISD113	4 F440	2 F440
	5 AL	5 AL		5 AL
	2 ISD112	2 ISD112		4 F440
		5 AL		80 SO
		2 ISD112		4 F440
			0.091	0.107
		0.028	0.19	0.37
		0.33		

Figure A2. Details on Damping Treatment Lay-ups

DAMPING TREATMENT CONFIGURATIONS

TEST CONFIG	LAY-UP	SPAR-RIB BAYS	INT OR EXT	VEL	COM	LE
1	112	L1	E		1980	4
2	112/113	L1	E		1989	4
3	112/113	L1,L2	E			5
4	112/113	L2	E			2
5	S/1	L1,L2	E			7
6	S/3	L1,L2,L3	E			26
7	S/3	L1,L2,L3*	E			13
8	S/3	L1,L2,L3	I	VEL		34
9	S/3	L1,L2,L3	I			21
10	"FENCE"	L1,L2,L3	E			75
11	112/113 +	Lam Straps	E			
EXT	112/113	L1,L2,L3,R1,R2,R3	E			5
INT	S/3	L1,L2,L3,R1,R2,R3	I	VEL		34

Figure A3. Tested Damping Treatment Configurations

F-15 UPPER OUTER WING SKIN TEST CONFIGURATION 2

1989 DAMPING TREATMENT

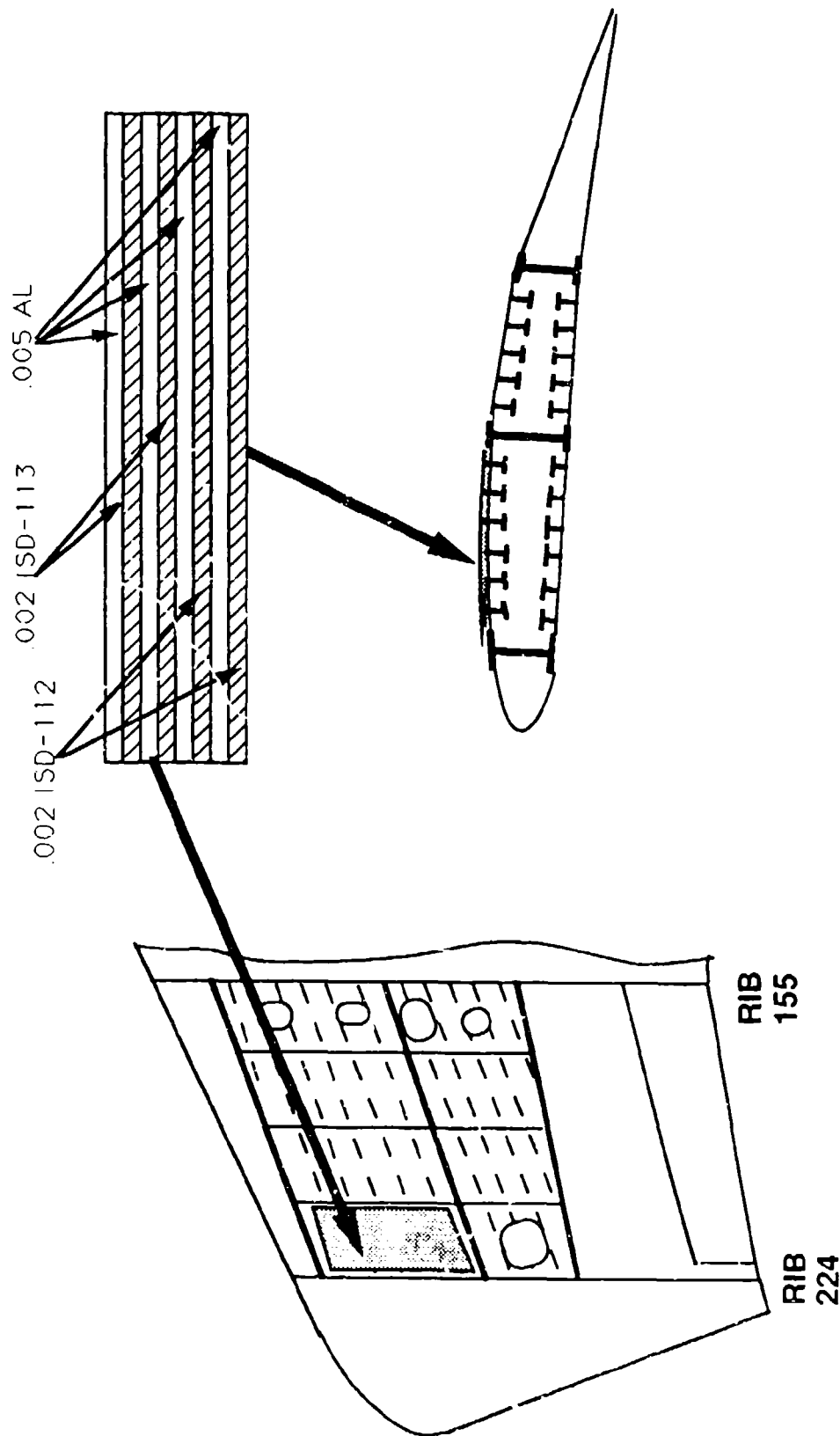


Figure A4. Test Configuration 2

F-15 UPPER OUTER WING SKIN TEST CONFIGURATION 3

1989 DAMPING TREATMENT

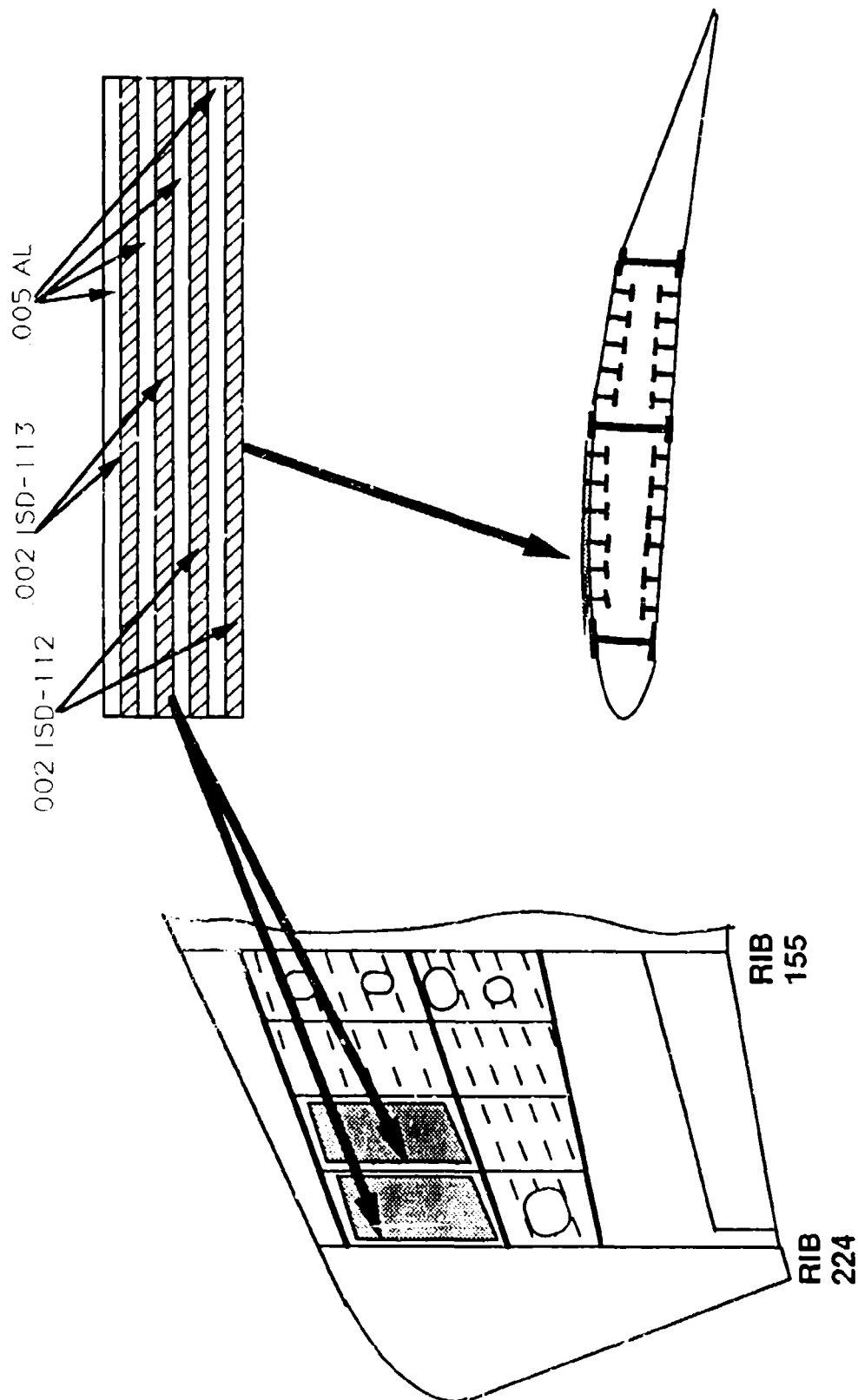


Figure A5. Test Configuration 3

F-15 UPPER OUTER WING SKIN TEST CONFIGURATION 4

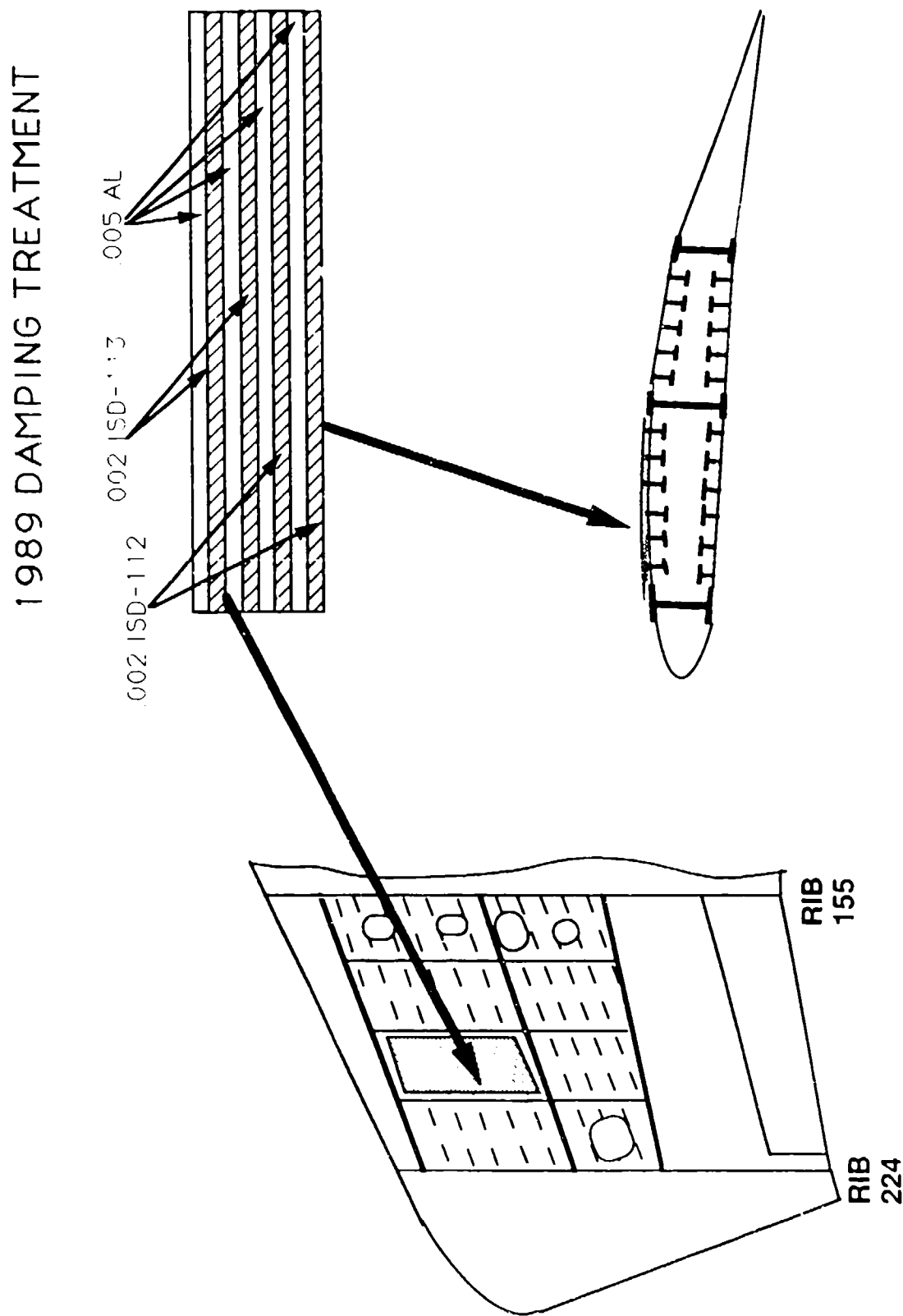


Figure A6. Test Configuration 4

F-15 UPPER OUTER WING SKIN

TEST CONFIGURATION 5

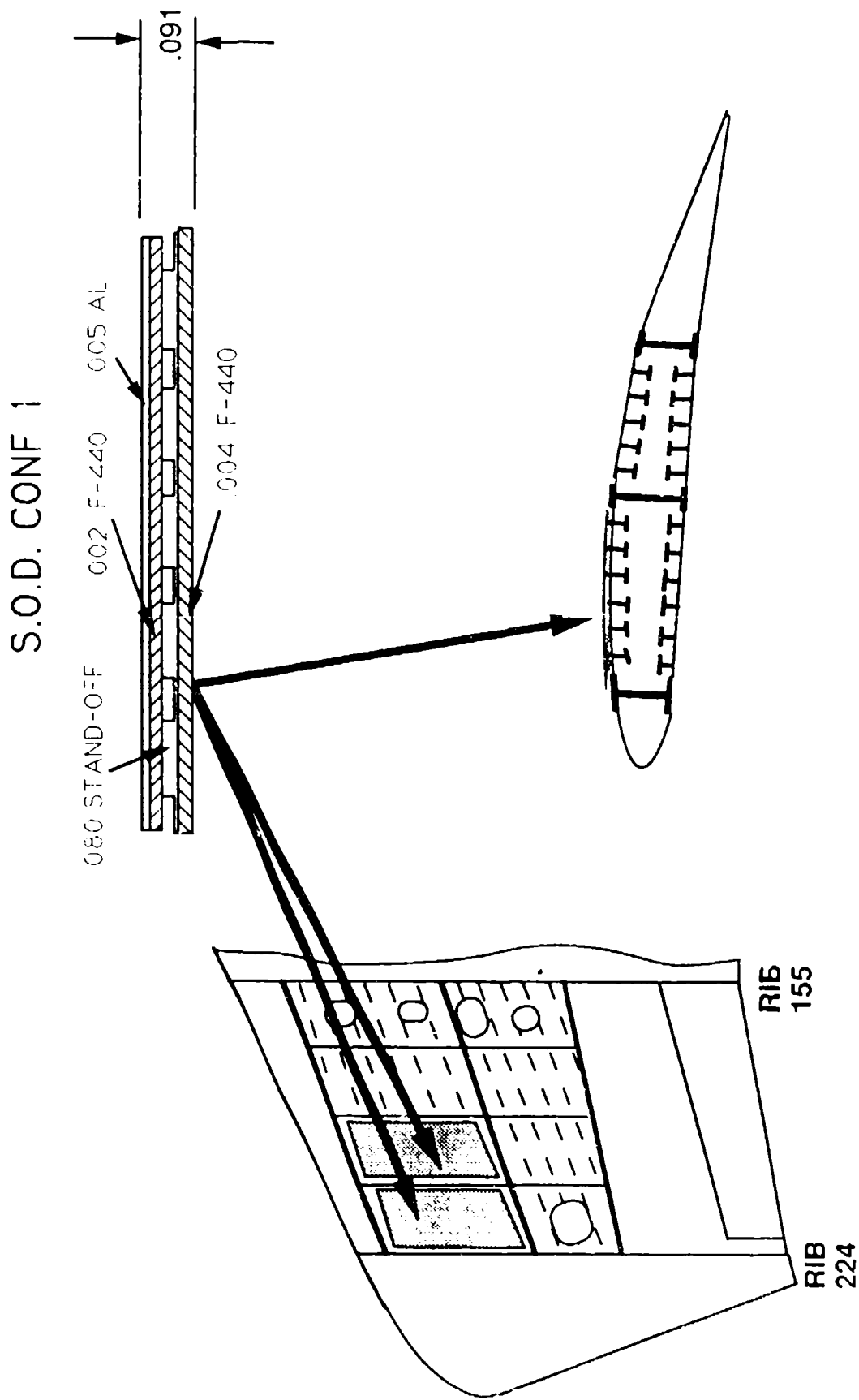


Figure A7. Test Configuration 5

F-15 UPPER OUTER WING SKIN TEST CONFIGURATION 6

S.O.D. CONF 2

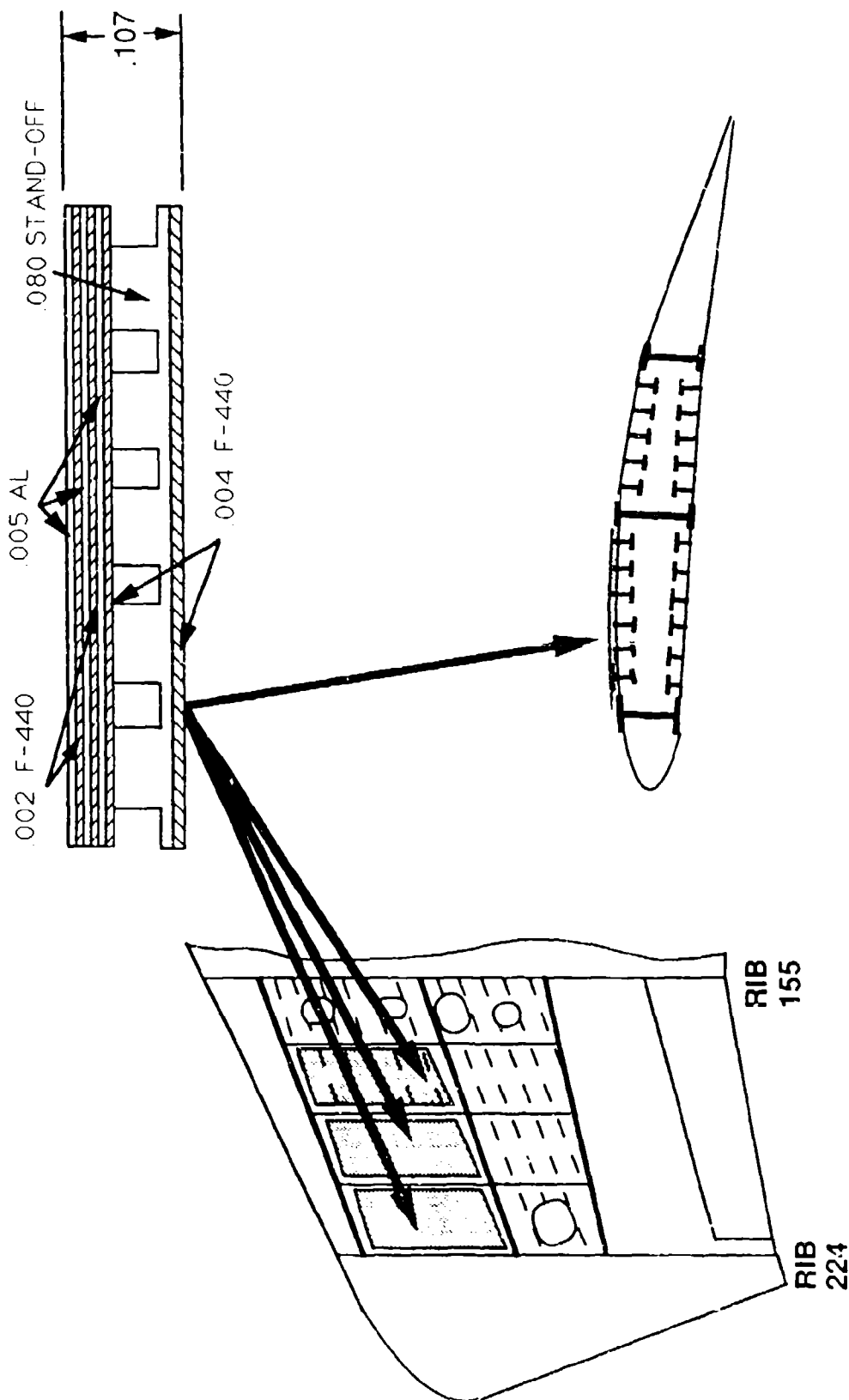


Figure A8. Test Configuration 6

F-15 UPPER OUTER WING SKIN TEST CONFIGURATION 7

S.O.D. CONF 2

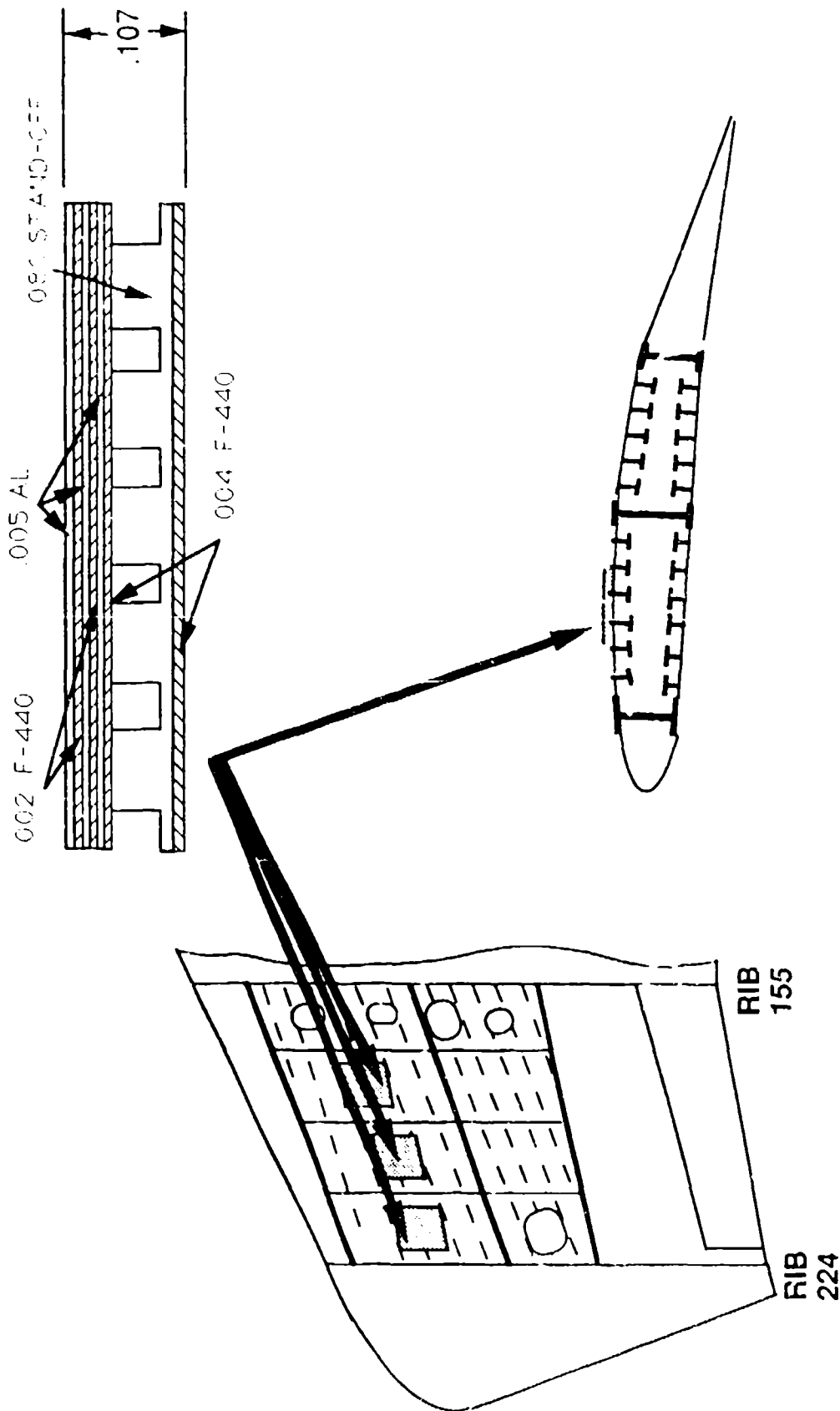


Figure A-1. Test Configuration 7

F-15 UPPER OUTER WING SKIN TEST CONFIGURATION 8

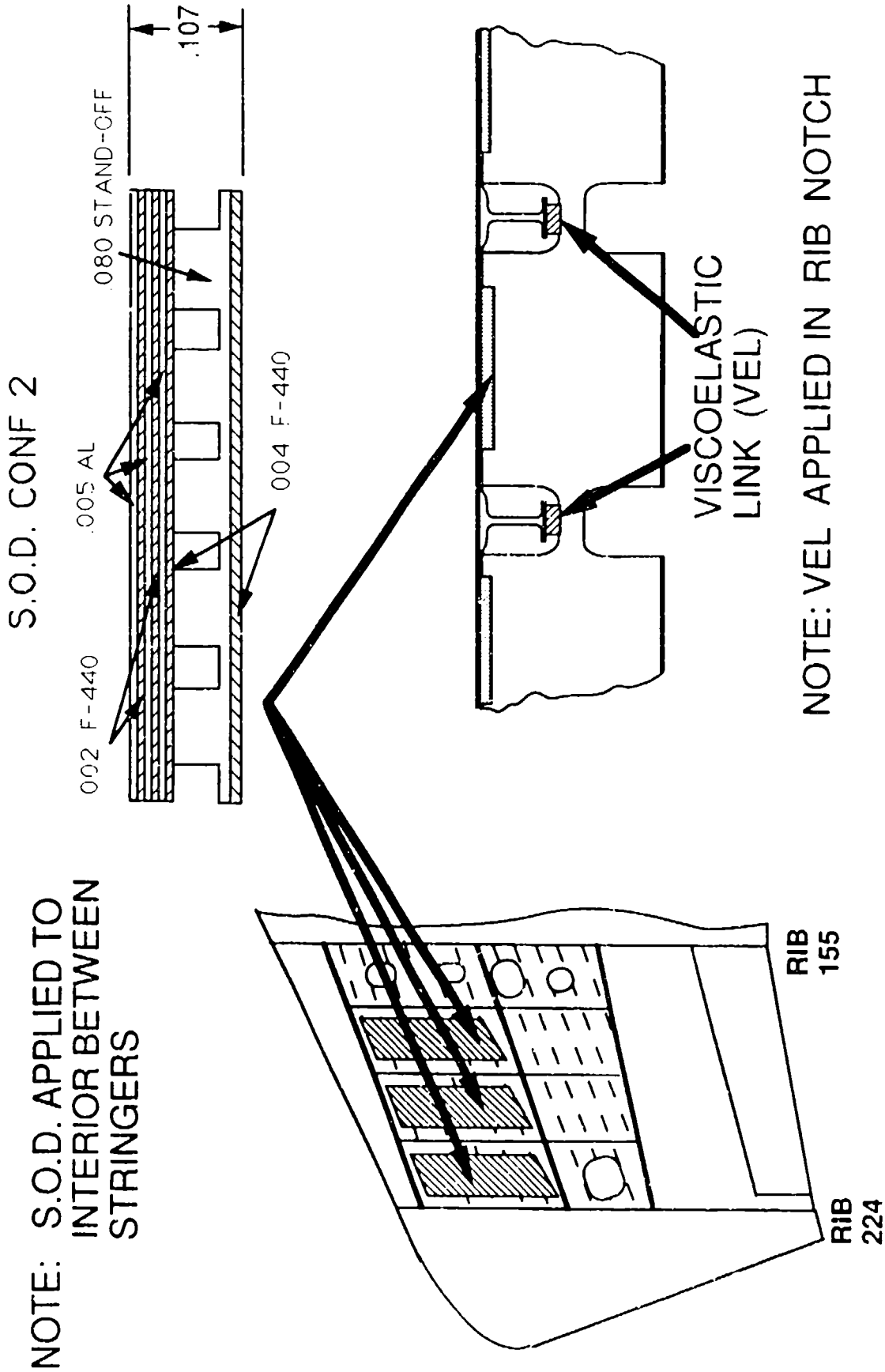


Figure A10. Test Configuration 8

F-15 UPPER OUTER WING SKIN TEST CONFIGURATION 9

NOTE: S.O.D. APPLIED TO
INTERIOR BETWEEN
STRINGERS

S.O.D. CONF 2

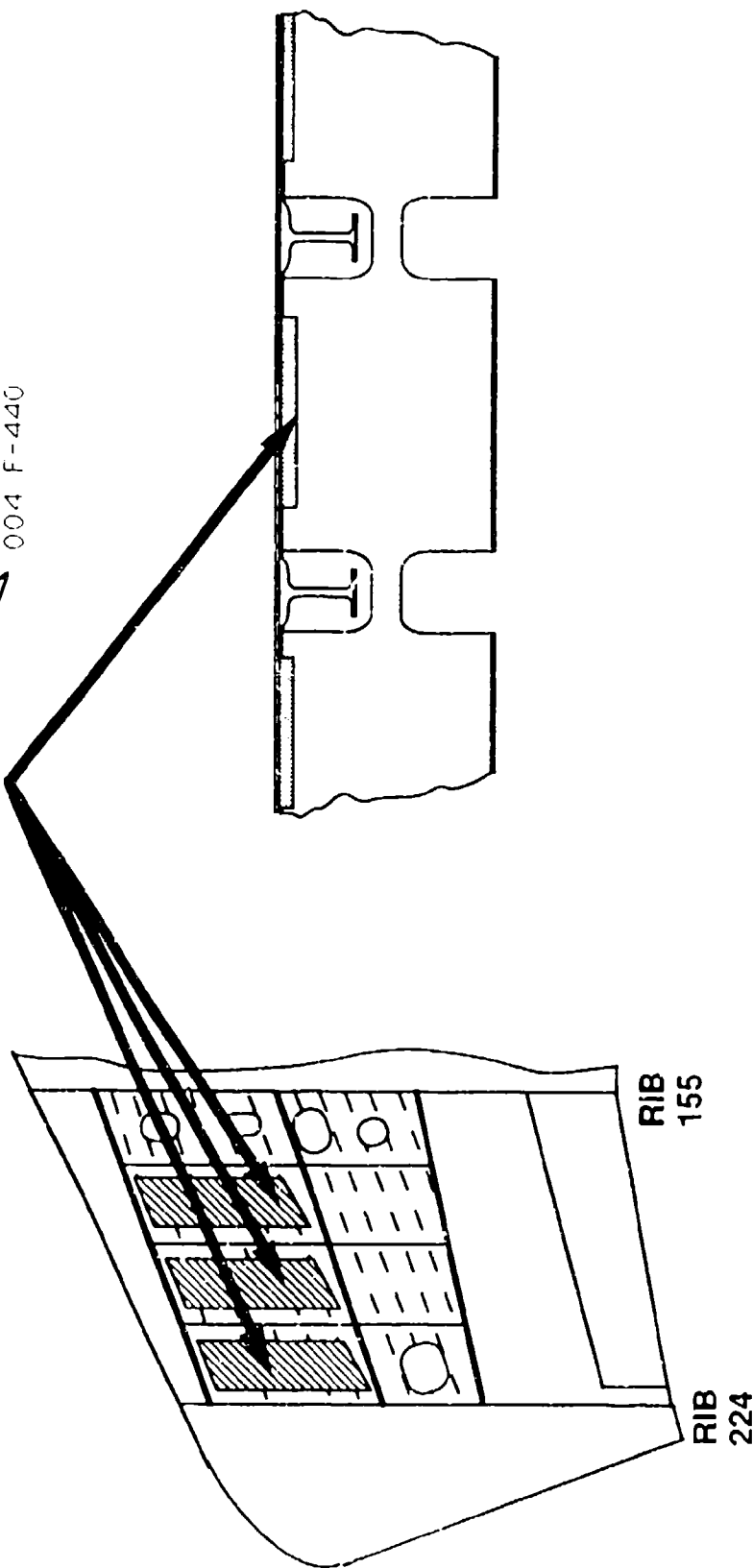
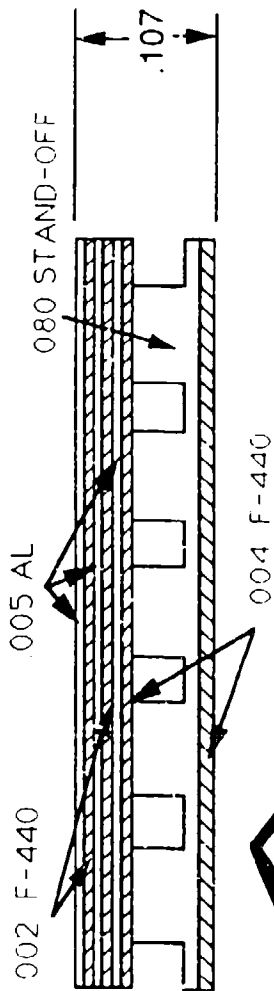


Figure A11. Test Configuration 9

F-15 UPPER OUTER WING SKIN

TEST CONFIGURATION 10

DAMPED FLOW FENCE

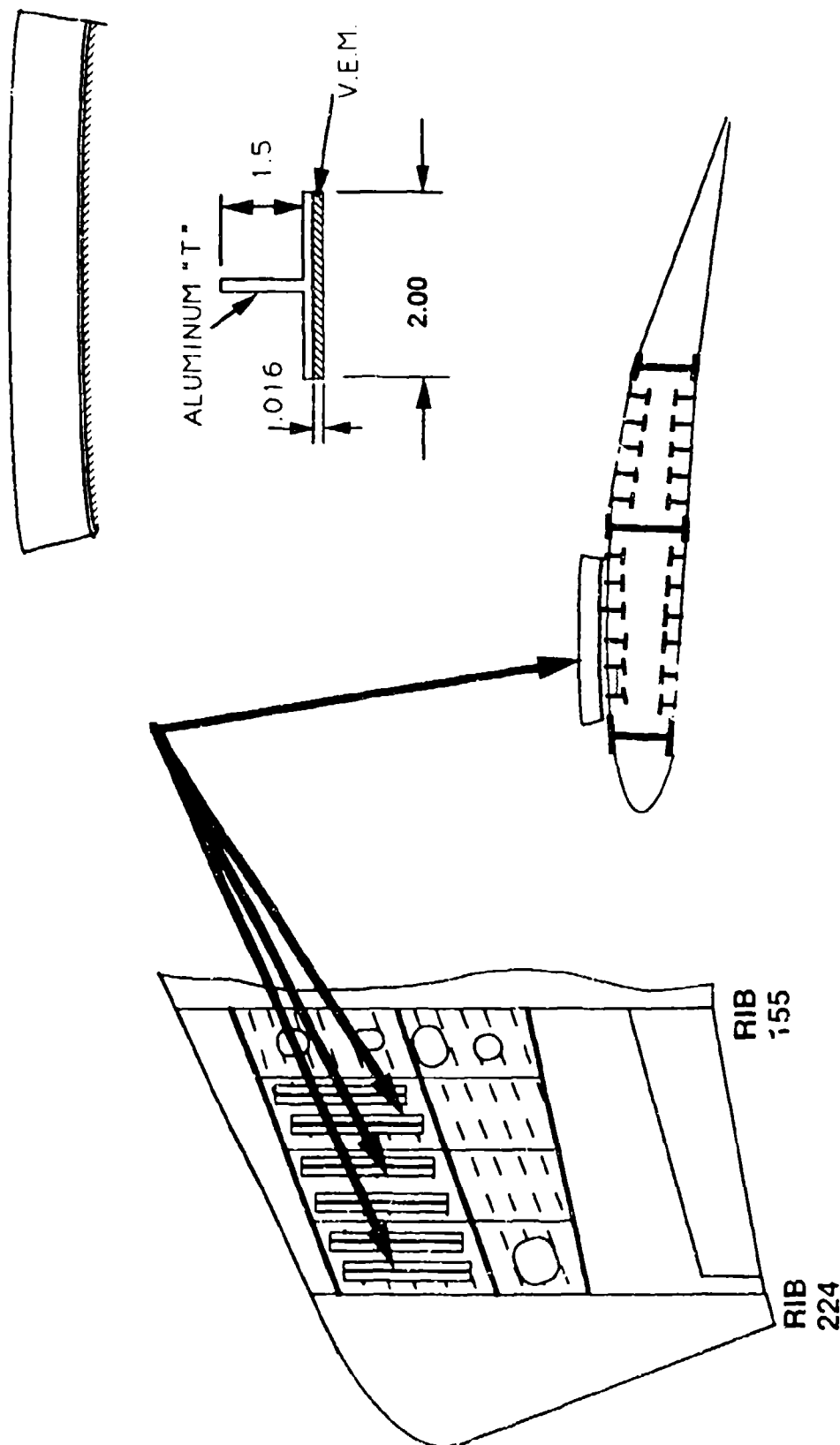


Figure A12. Test Configuration 10

F-15 UPPER OUTER WING SKIN

TEST CONFIGURATION 11

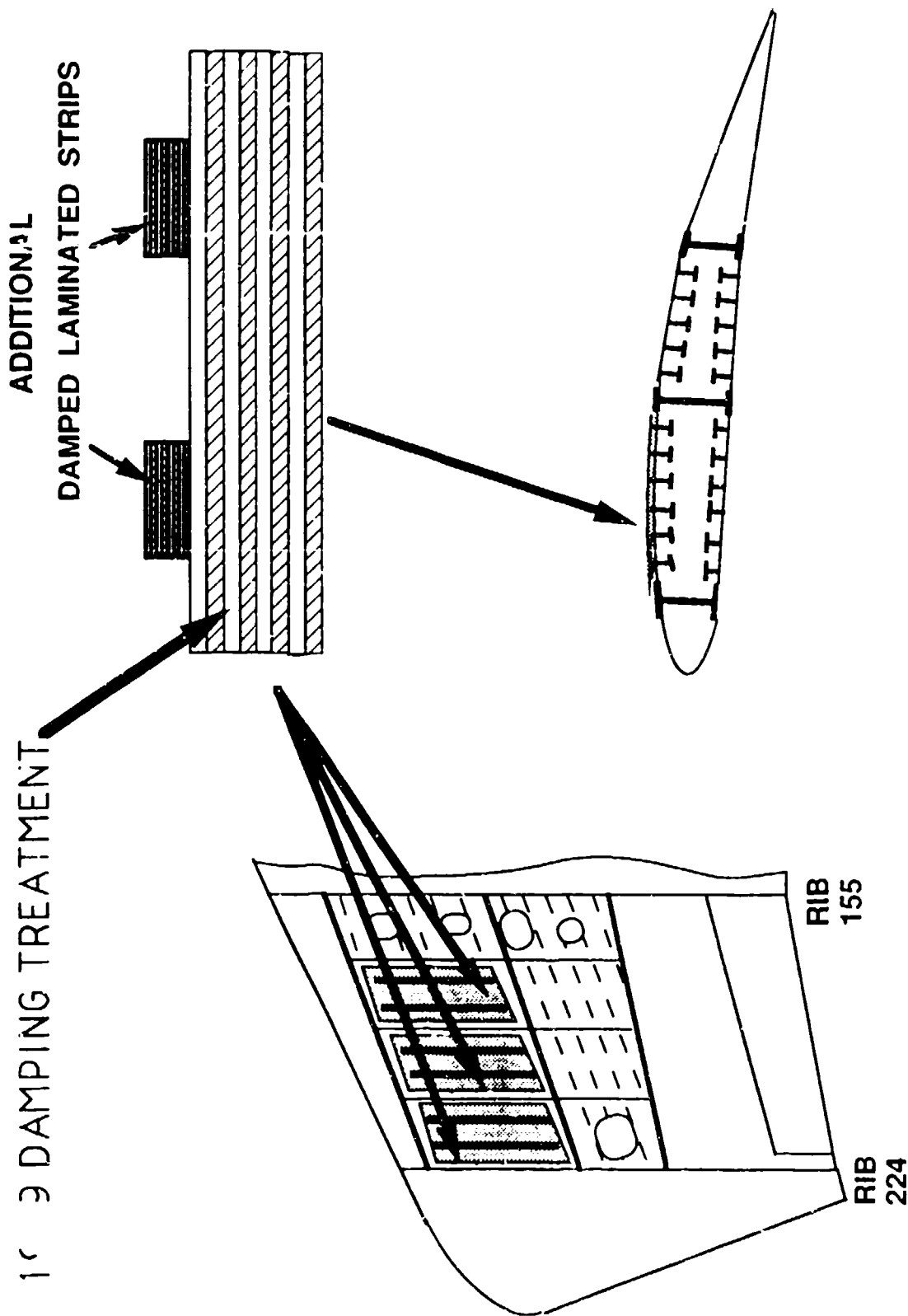
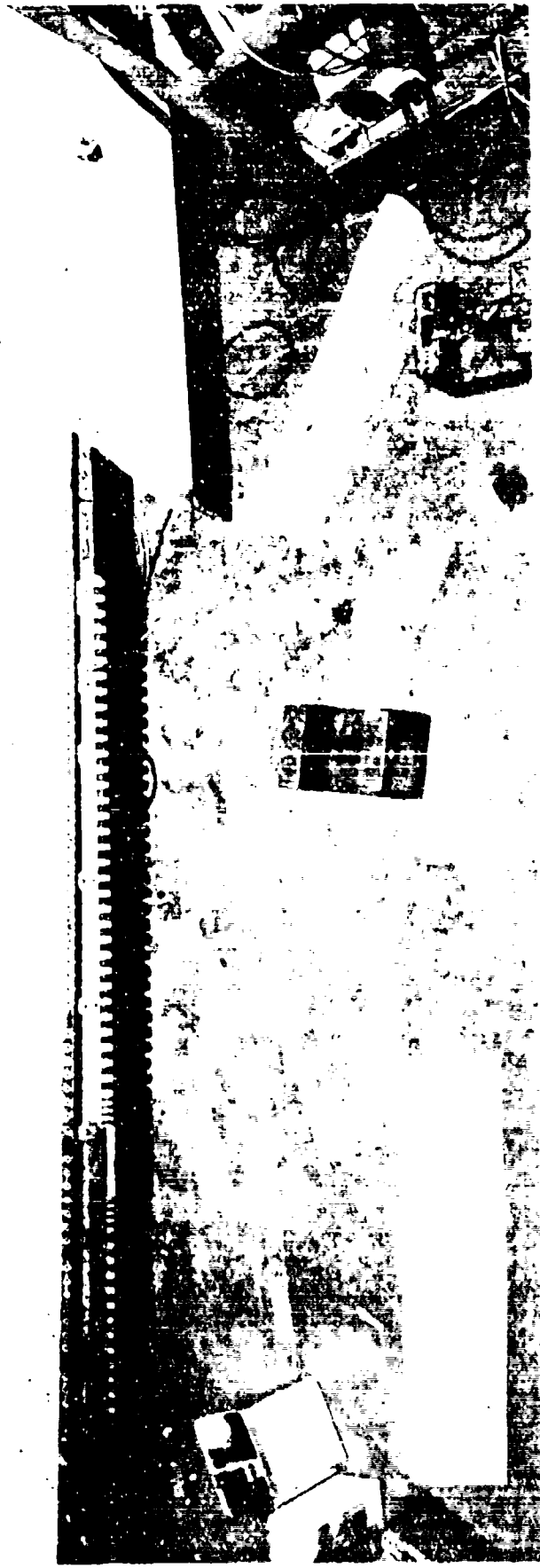


Figure A13. Test Configuration 11



TEST CONFIG NUMBER	TRANSDUCER NUMBER	300 HZ TO 400 HZ FREQUENCY BAND			
		RMS RATIO	% REDUCTION	STRINGER LIFE EXTENSION	STRINGER L. E. AVERAGE
1	15	0.88	12.47	2	4
	16	0.77	22.63	2	
	17	0.51	49.48	10	
	18	0.48	51.52	11	
2	15	0.88	12.27	2	4
	16	0.79	21.35	2	
	17	0.58	42.49	6	
	18	0.55	45.44	7	
3	15	0.73	26.82	3	5
	16	0.72	27.92	3	
	17	0.55	45.21	7	
	18	0.55	45.44	7	
4	15	0.83	16.84	2	2
	16	0.89	10.58	1	
	17	0.91	9.46	1	
	18	0.86	14.13	2	
5	15	0.62	37.63	5	7
	16	0.64	38.60	5	
	17	0.58	42.36	6	
	18	0.43	57.45	17	
6	15	0.48	51.58	11	26
	16	0.47	52.55	12	
	17	0.35	65.03	33	
	18	0.25	75.08	101	
7	15	0.52	48.02	9	13
	16	0.52	47.81	9	
	17	0.44	55.70	15	
	18	0.39	60.64	22	
8	15	0.27	72.57	74	34
	16	0.24	76.00	115	
	17	0.62	38.14	6	
	18	0.36	65.16	33	
9	15	0.27	72.57	74	21
	16	0.46	53.60	13	
	17	0.78	22.11	2	
	18	0.26	74.06	89	
10	15	0.17	83.38	388	75
	16	0.28	72.00	69	
	17	0.54	46.16	8	
	18	0.22	78.06	154	

Figure A15. Test Result for Damping
Configuration

F-15 UPPER OUTER WING SKIN LIFE EXTENSION

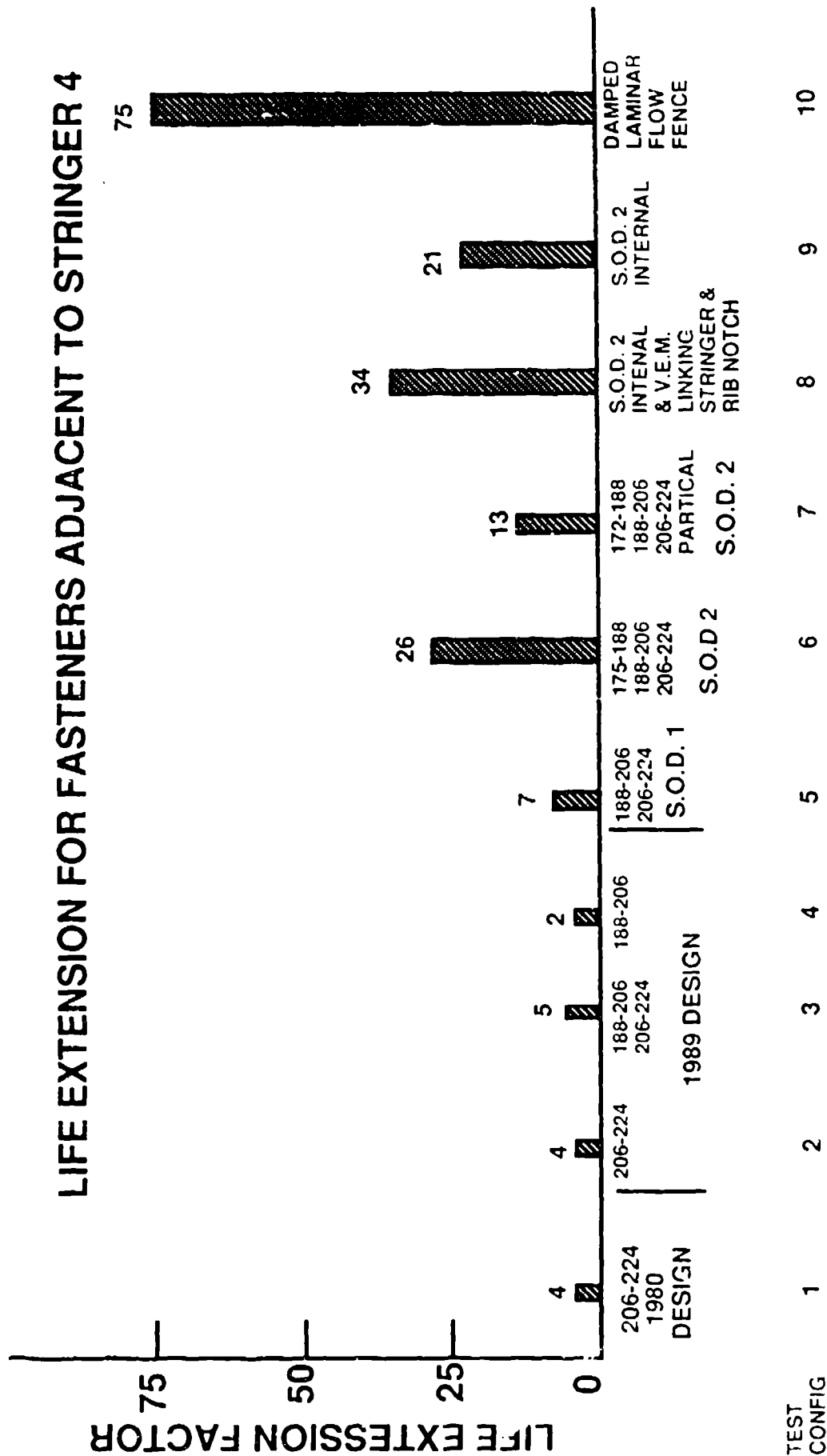
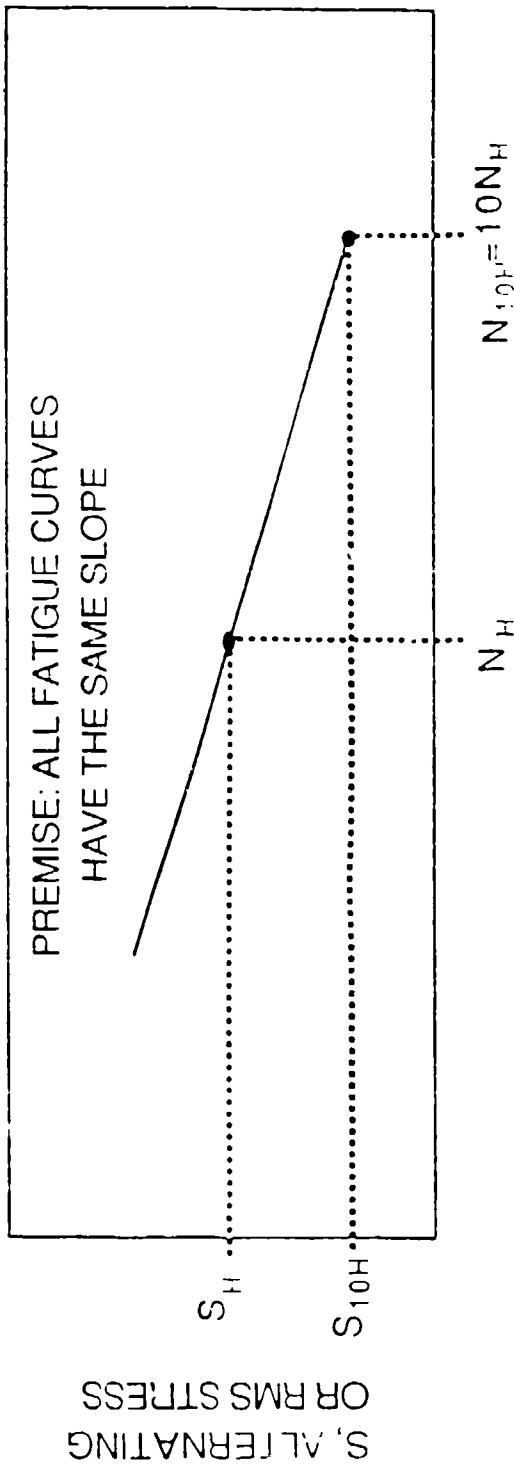


Figure A16. Life Extension Factors

METHODOLOGY FOR CALCULATION OF LIFE EXTENSION

A TYPICAL S-N CURVE

PREMISE: ALL FATIGUE CURVES
HAVE THE SAME SLOPE



% VIBRATORY STRESS
REDUCTION = $100(1 - S_d/S_u)$

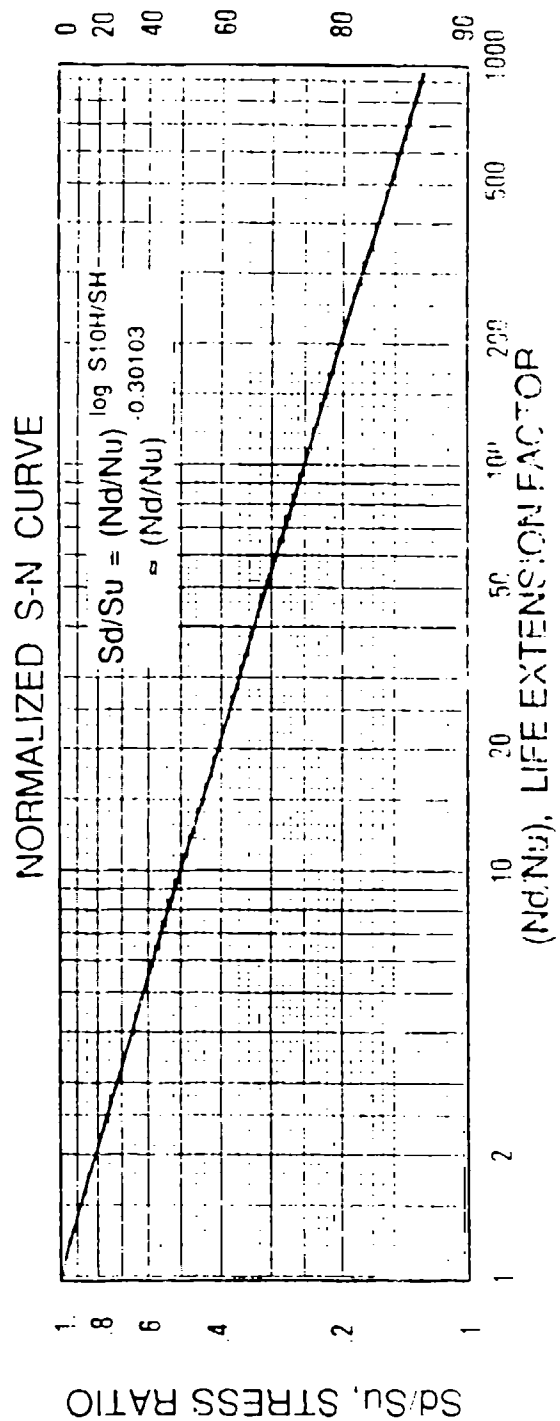


Figure 21. Typical S-N Curve

F-15 UPPER OUTER WING SKIN LIFE EXTENSION

LIFE EXTENSION FACTOR CALCULATION

$$\text{Nd/Nu} = (\text{Sd/Su})^{-3.323}$$

WHERE

Nd = DAMPED LIFE

Nu = UNDAMPED LIFE

Sd = DAMPED STRESS

Su = UNDAMPED STRESS

Figure B2. Life Extension Factor Calculation

F-15 UPPER OUTER WING SKIN

ENGINEERING JUDGEMENT IS THAT THERE WILL BE NO CORROSION ASSOCIATED WITH STAND-OFF LAYER

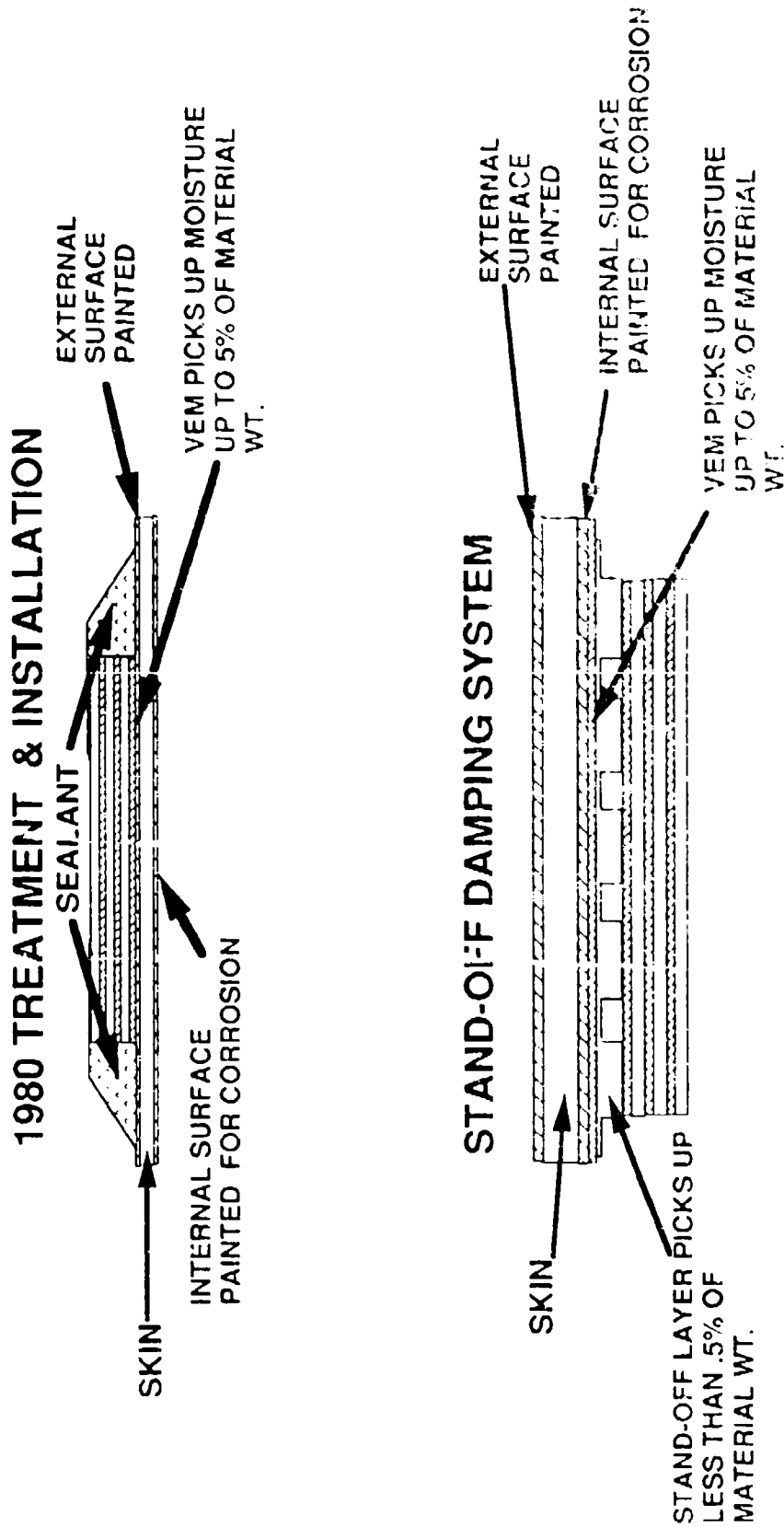


Figure 61. Damping System Cross Section

F-15 UPPER OUTER WING SKIN LIFE EXTENSION

**30 DAY HUMIDITY/CORROSION COUPON
EXPOSURE**

TEST PANEL NO. 1

BARE TEST PANEL

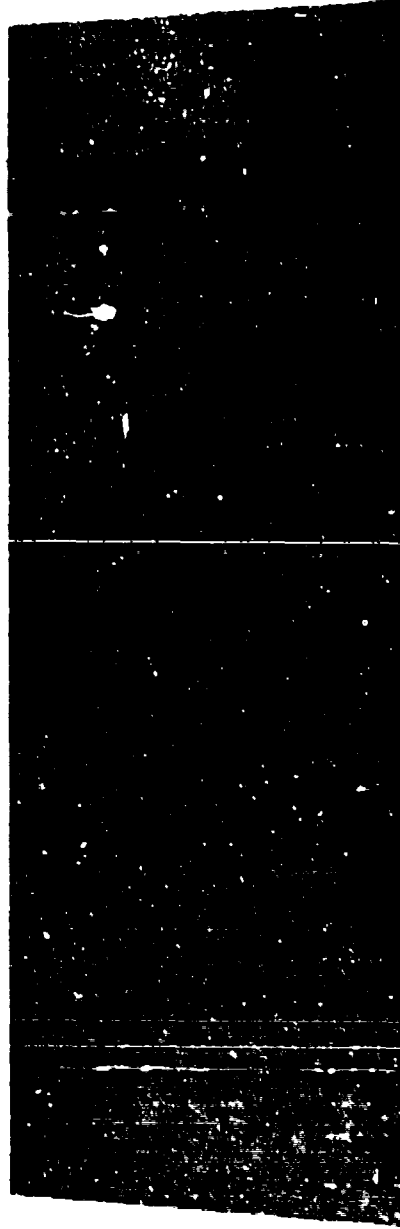


Figure 02. Bare Test Panel After Corrosion
Test

F-15 UPPER OUTER WING SKIN LIFE EXTENSION

**30 DAY HUMIDITY/CORROSION COUPON
EXPOSURE**

TEST PANEL NO. 2

1980 WING DAMPER WITH EDGE SEALANT



Figure C2. "1980 Damping Treatment" With Edge
Sealant After Corrosion Test

F-15 UPPER OUTER WING SKIN LIFE EXTENSION

**30 DAY HUMIDITY/CORROSION COUPON
EXPOSURE**

**TEST PANEL NO. 2
1980 WING DAMPER WITH EDGE SEALANT**



Figure C4. Partially Removed "1980 Damping
Treatment" With Edge Sealant After
Corrosion Test

F-15 UPPER OUTER WING SKIN LIFE EXTENSION

**30 DAY HUMIDITY/CORROSION COUPON
EXPOSURE**

TEST PANEL NO. 3

1980 WING DAMPER WITHOUT EDGE SEALANT

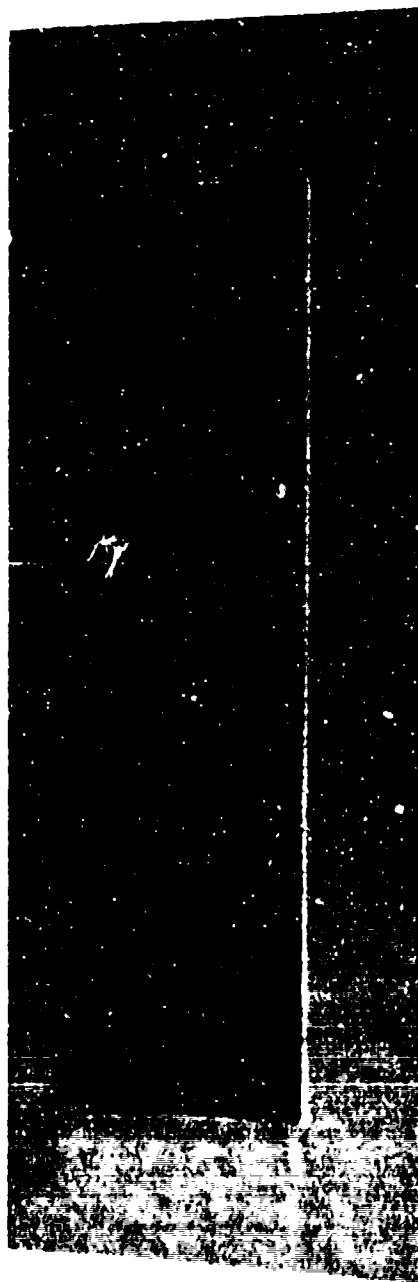


Figure C5. "1980 Damping Treatment" After
Corrosion

F-15 UPPER OUTER WING SKIN LIFE EXTENSION

**30 DAY HUMIDITY/CORROSION COUPON
EXPOSURE**

**TEST PANEL NO. 3
1980 WING DAMPER WITHOUT EDGE SEALANT**

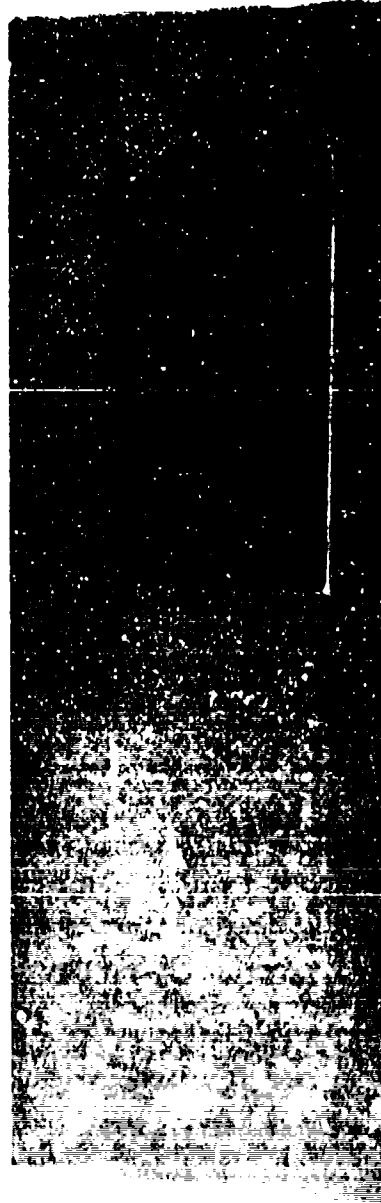


Figure C6. Partially Removed "1980 Damping
Treatment" After Corrosion Test

F-15 UPPER OUTER WING SKIN LIFE EXTENSION

**30 DAY HUMIDITY/CORROSION COUPON
EXPOSURE**

TEST PANEL NO. 4

**1990 PROPOSED WING DAMPER WITHOUT EDGE
SEALANT**

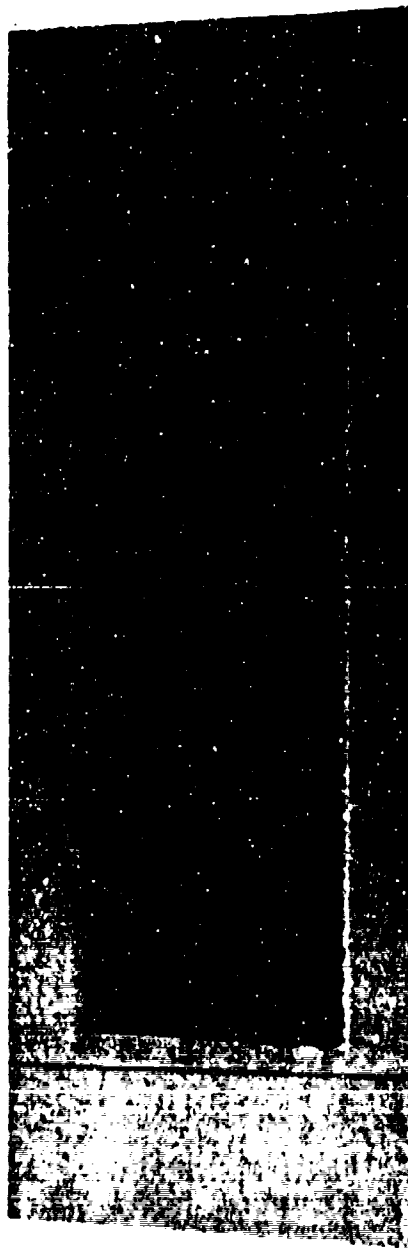


Figure C7. External Treatment After Corrosion Test

F-15 UPPER OUTER WING SKIN LIFE EXTENSION

**30 DAY HUMIDITY/CORROSION COUPON
EXPOSURE**

**TEST PANEL NO. 4
1990 PROPOSED WING DAMPER WITHOUT EDGE
SEALANT**

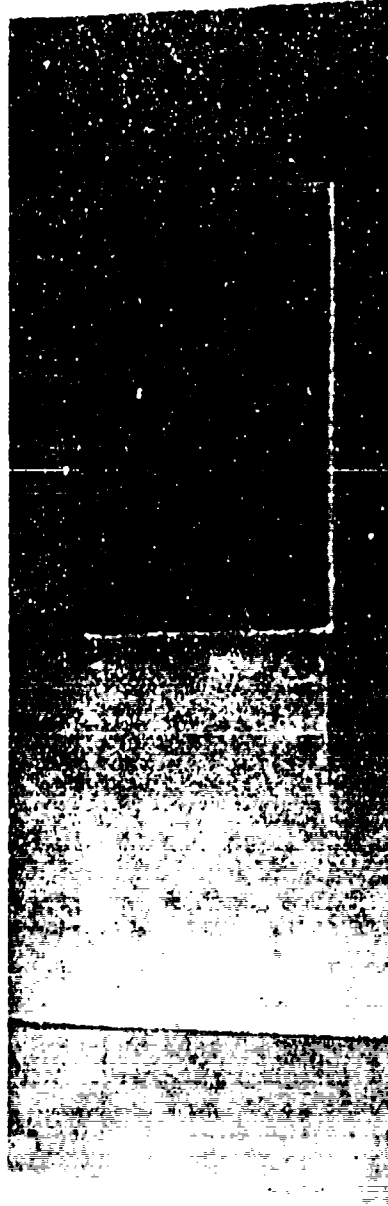


Figure C8. Partially Removed External
Treatment After Corrosion Test

F-15 UPPER OUTER WING SKIN LIFE EXTENSION

**30 DAY HUMIDITY/CORROSION COUPON
EXPOSURE**

**TEST PANEL NO. 5
1990 PROPOSED WING DAMPER WITH EDGE
SEALANT**



Figure C9. External Treatment With Edge
Sealant After Corrosion Test

F-15 UPPER OUTER WING SKIN LIFE EXTENSION

**30 DAY HUMIDITY/CORROSION COUPON
EXPOSURE**

**TEST PANEL NO. 5
1990 PROPOSED WING DAMPER WITH EDGE
SEALANT**

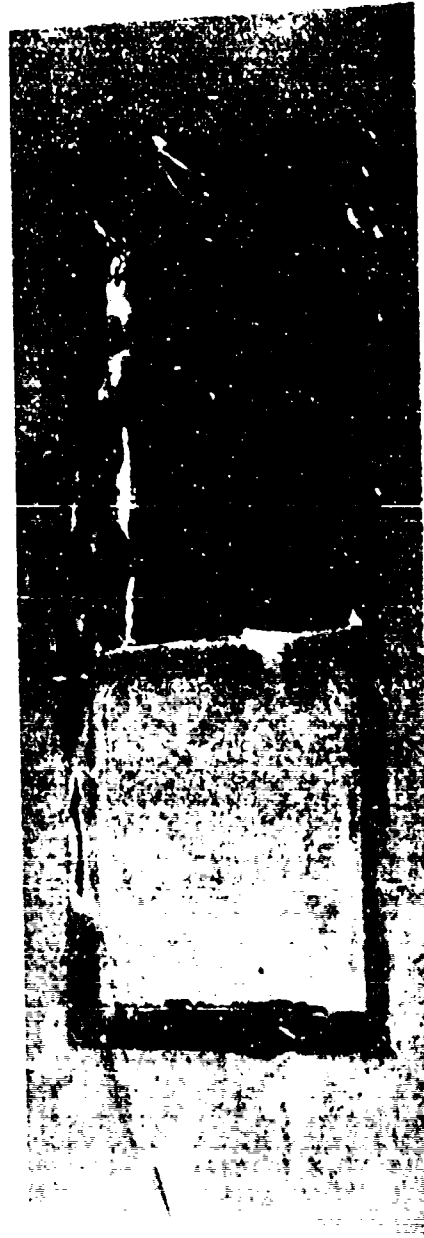


Figure C10. Partially Removed Internal
Treatment With Edge Sealant
After Corrosion Test

F-15 UPPER OUTER WING SKIN LIFE EXTENSION

**30 DAY HUMIDITY/CORROSION COUPON
EXPOSURE**

TEST PANEL NO. 6

**STAND-OFF DAMPNING SYSTEM WITHOUT EDGE
SEALANT**

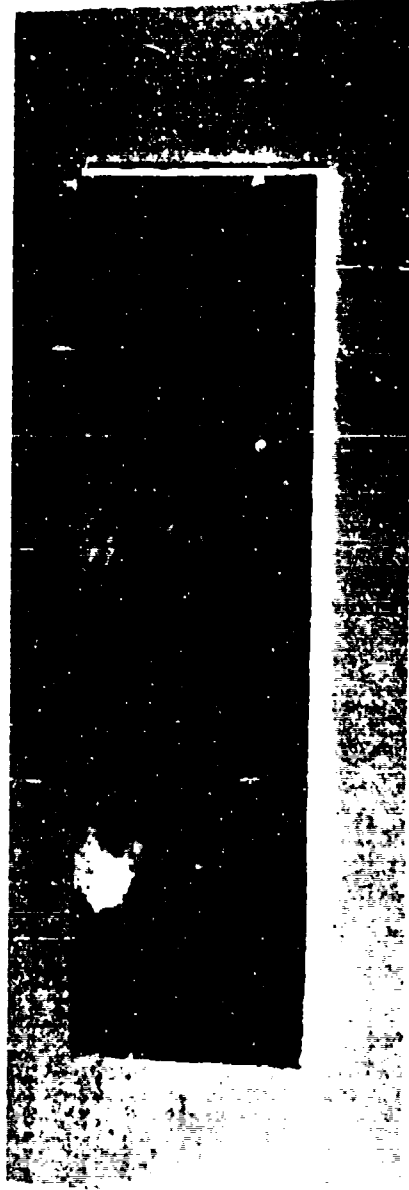


Figure 11. Internal Treatment After
Corrosion Test

F-15 UPPER OUTER WING SKIN LIFE EXTENSION

**30 DAY HUMIDITY/CORROSION COUPON
EXPOSURE**

TEST PANEL NO. 6

**STAND-OFF DAMPNING SYSTEM WITHOUT EDGE
SEALANT**

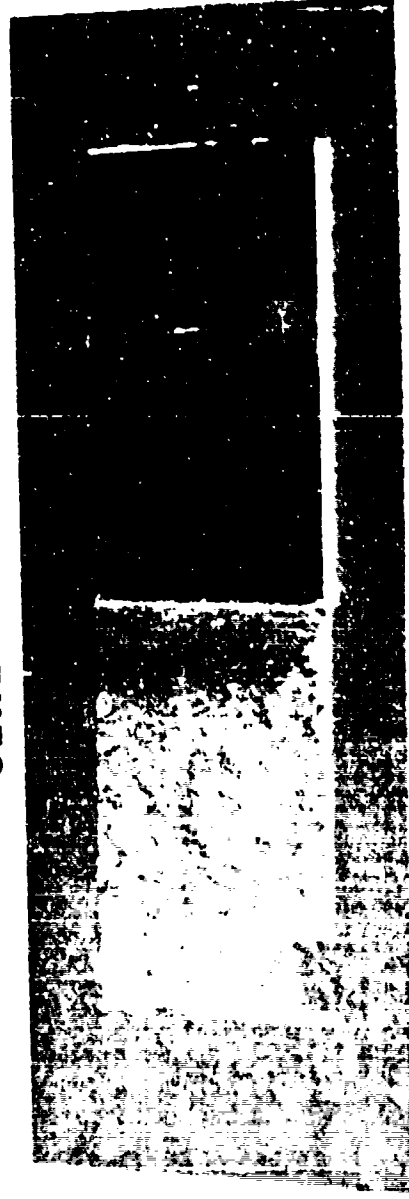


Figure C12. Partially Removed Internal
Treatment After Corrosion
Test

F-15 UPPER OUTER WING SKIN LIFE EXTENSION

**30 DAY HUMIDITY/CORROSION COUPON
EXPOSURE**

**TEST PANEL NO. 7
STAND-OFF DAMPNING SYSTEM WITH EDGE
SEALANT**



Figure C13. Internal Treatment With Edge
Sealant After Corrosion Test

F-15 UPPER OUTER WING SKIN LIFE EXTENSION

**30 DAY HUMIDITY/CORROSION COUPON
EXPOSURE**

TEST PANEL NO. 7

**STAND-OFF DAMPNING SYSTEM WITH EDGE
SEALANT**

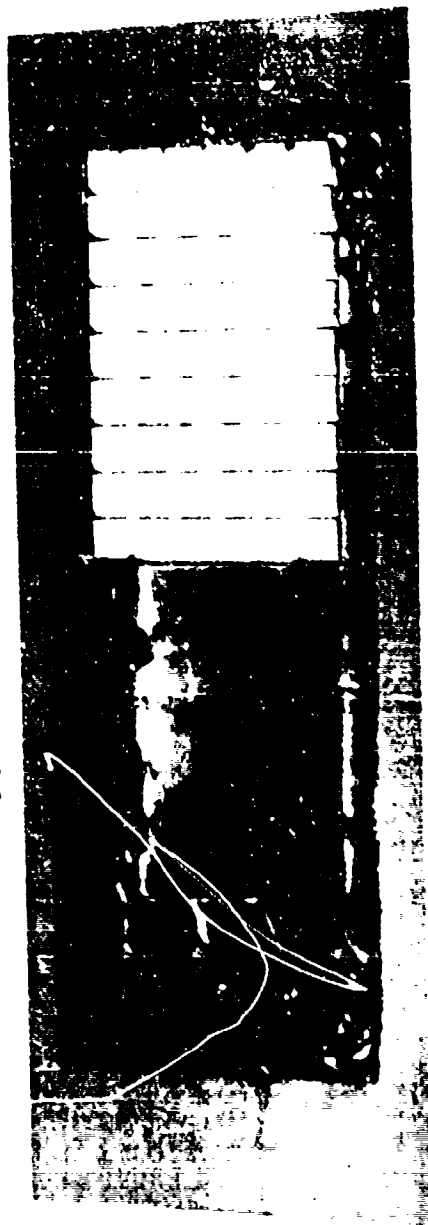


Figure C14. Exposed Stand-off Layer for
Internal Treatment With Edge
Sealant After Corrosion Test

F-15 UPPER OUTER WING SKIN LIFE EXTENSION

**30 DAY HUMIDITY/CORROSION COUPON
EXPOSURE**

TEST PANEL NO. 7

**STAND-OFF DAMPNING SYSTEM WITH EDGE
SEALANT**



Figure C15. Partially Removed Internal
Treatment With Edge Sealant

F-15 UPPER OUTER WING SKIN LIFE EXTENSION

**30 DAY HUMIDITY/CORROSION COUPON
EXPOSURE**

TEST PANEL NO. 8

VISCOELASTIC LINK

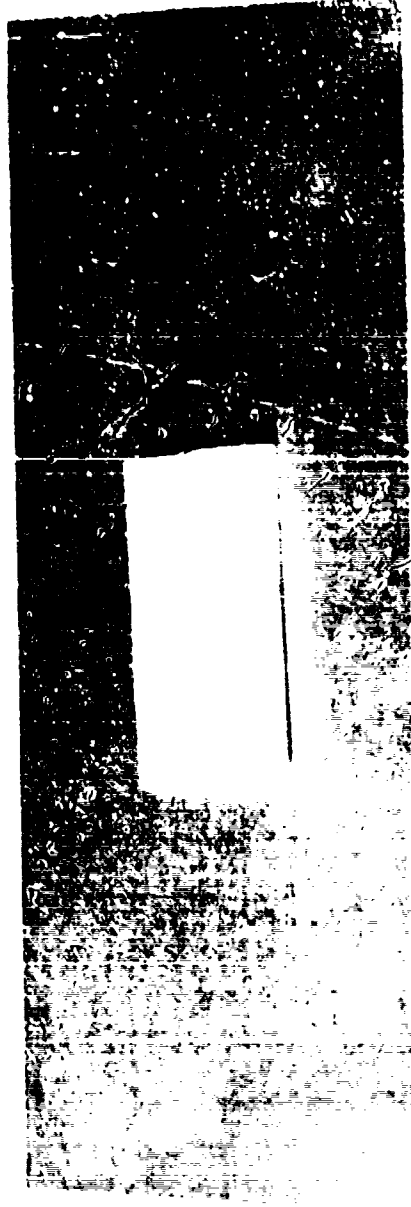


Figure 236. Viscoelastic Link After Corrosion Test

F-15 UPPER OUTER WING SKIN LIFE EXTENSION

**30 DAY HUMIDITY/CORROSION COUPON
EXPOSURE**

TEST PANEL NO. 8

VISCOELASTIC LINK

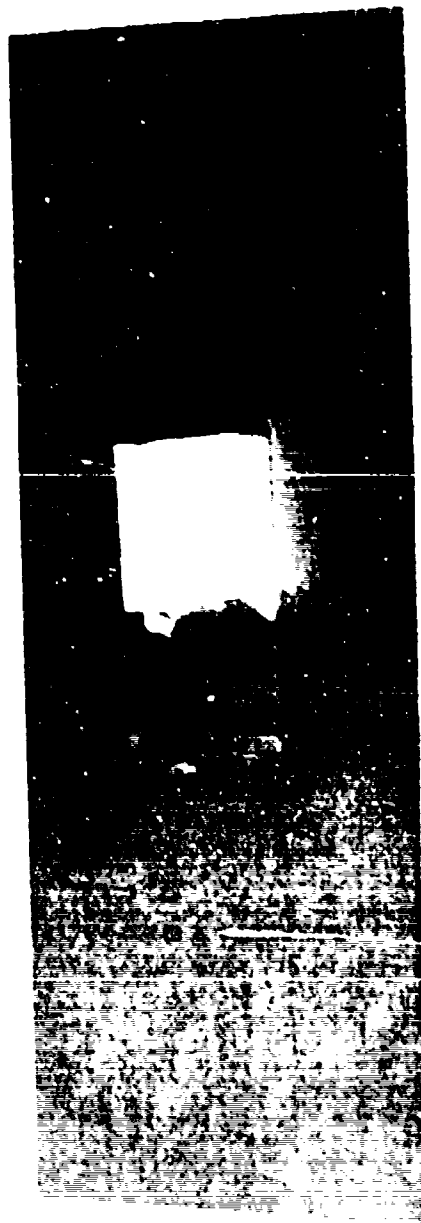


Figure C17. Partially Removed Viscoelastic
Link After Corrosion Test

F-15 UPPER OUTER WING SKIN LIFE EXTENSION

THERMAL AGING EXPERIENCED DURING FIELD SERVICE

TAKEN FROM PANEL NO. 74-140 R/H

1980 DAMPING TREATMENT



Figure Di. "1980 Damping Treatment" Exposed to
Actual Field Service

F-15 UPPER OUTER WING SKIN LIFE EXTENSION

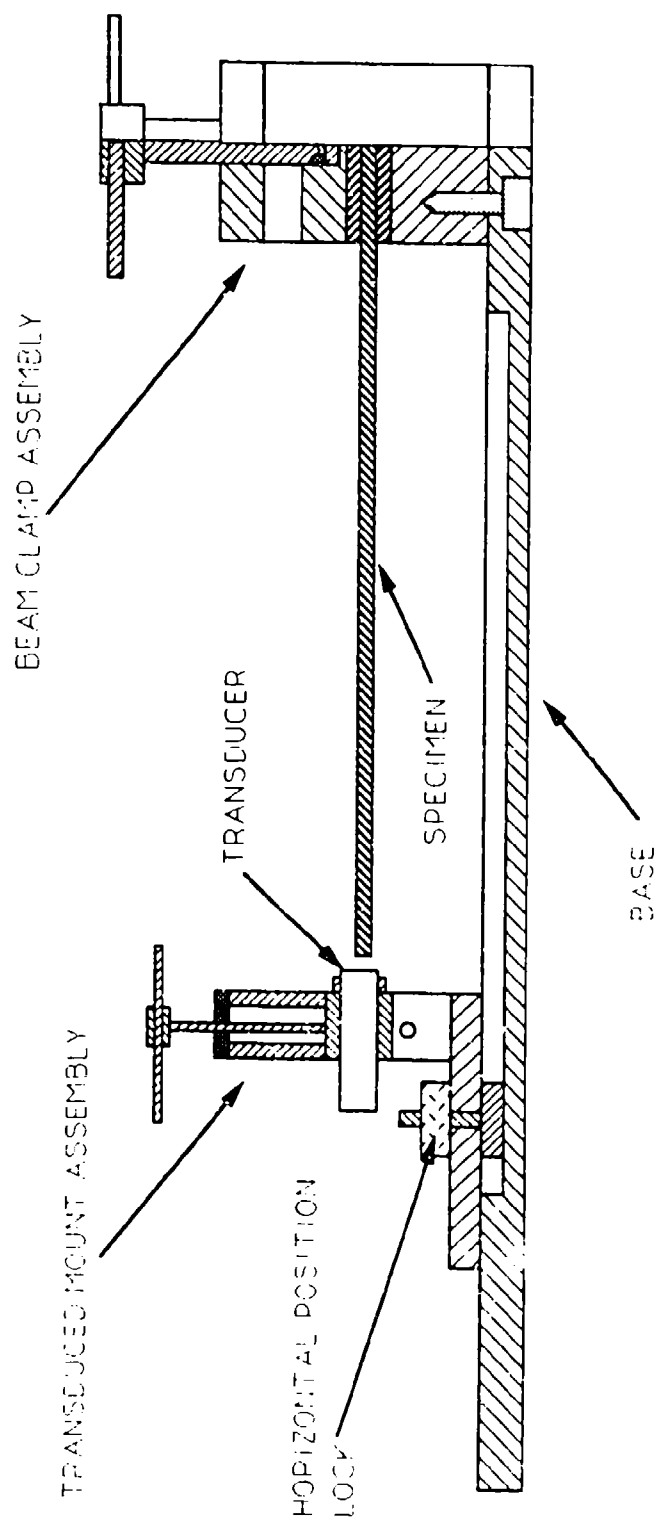
LABORATORY THERMAL AGING EVALUATION

8 HOURS @ 340 F

1980 DAMPING TREATMENT



Figure D2. "1980 Damping Treatment" Exposed
to Laboratory Thermal Aging



BEAM FIXTURE ASSEMBLY

Figure D1. Cantilever Beam Test Set-up

F-15 UPPER OUTER WING SKIN LIFE EXTENSION

HEAT AGING EFFECTS
7 HOURS @ 340 F PLUS 48 HOURS @ 270 F

1980 SYSTEM

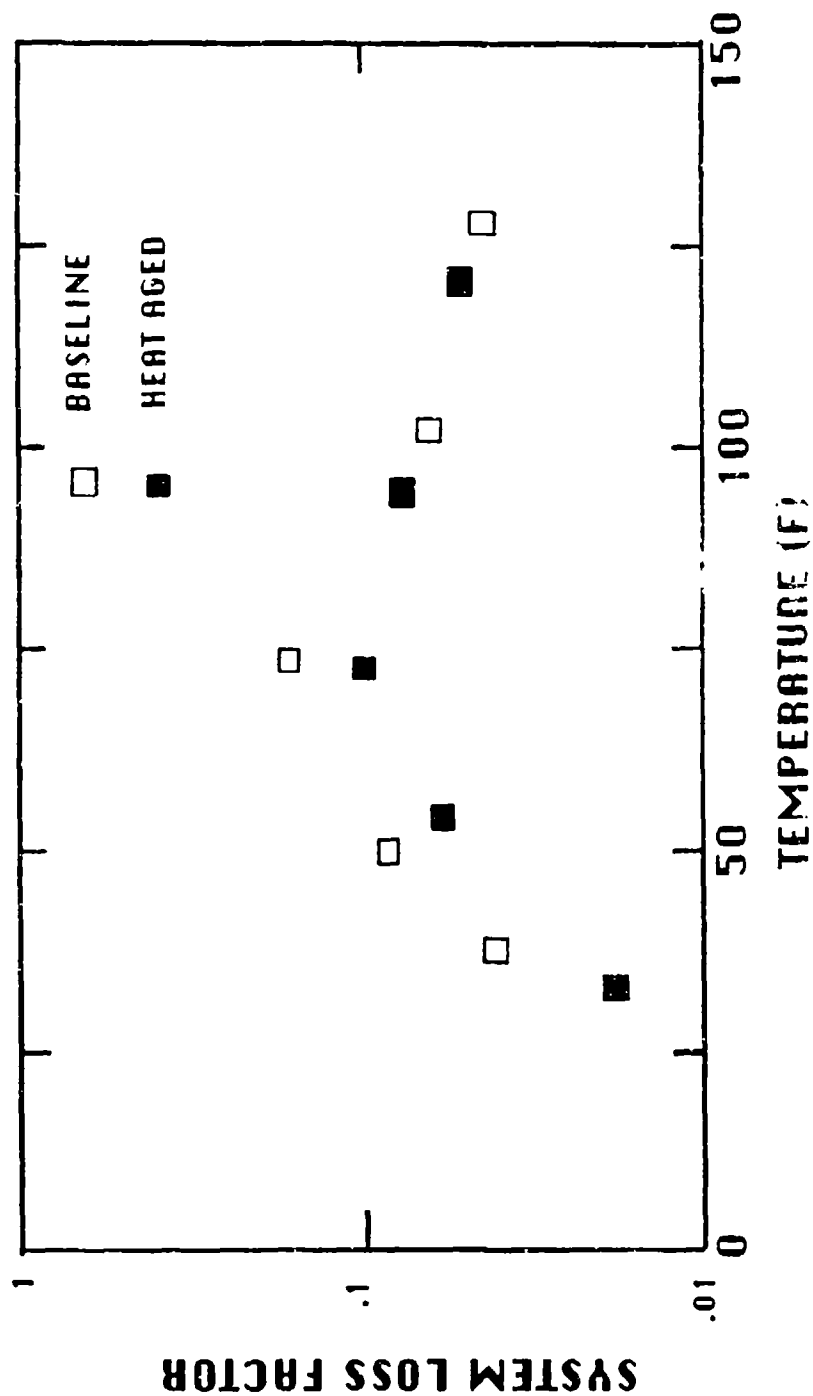


Figure 34. "1980 Damping Treatment" Thermal Aging Results

F-15 UPPER OUTER WING SKIN LIFE EXTENSION

HEAT AGING EFFECTS
7 HOURS @ 340 F PLUS 48 HOURS @ 270 F

STAND-OFF SYSTEM DESIGN II

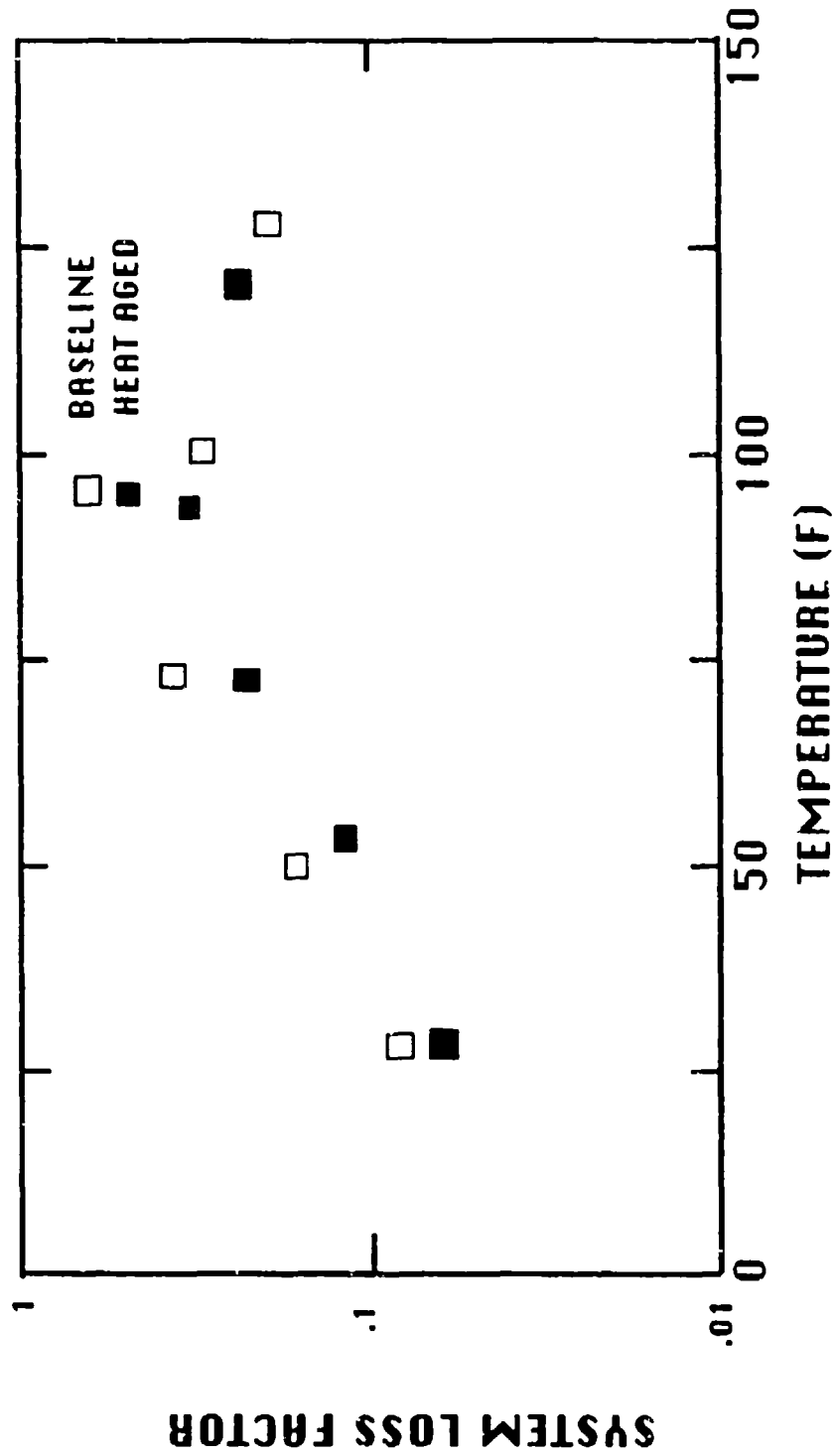


Figure D5. Stand-off Damping Treatment
Thermal Aging Results

F-15 UPPER OUTER WING SKIN LIFE EXTENSION

HEAT AGING EFFECTS
7 HOURS @ 340 F PLUS 48 HOURS @ 270 F
VISCOELASTIC LINK

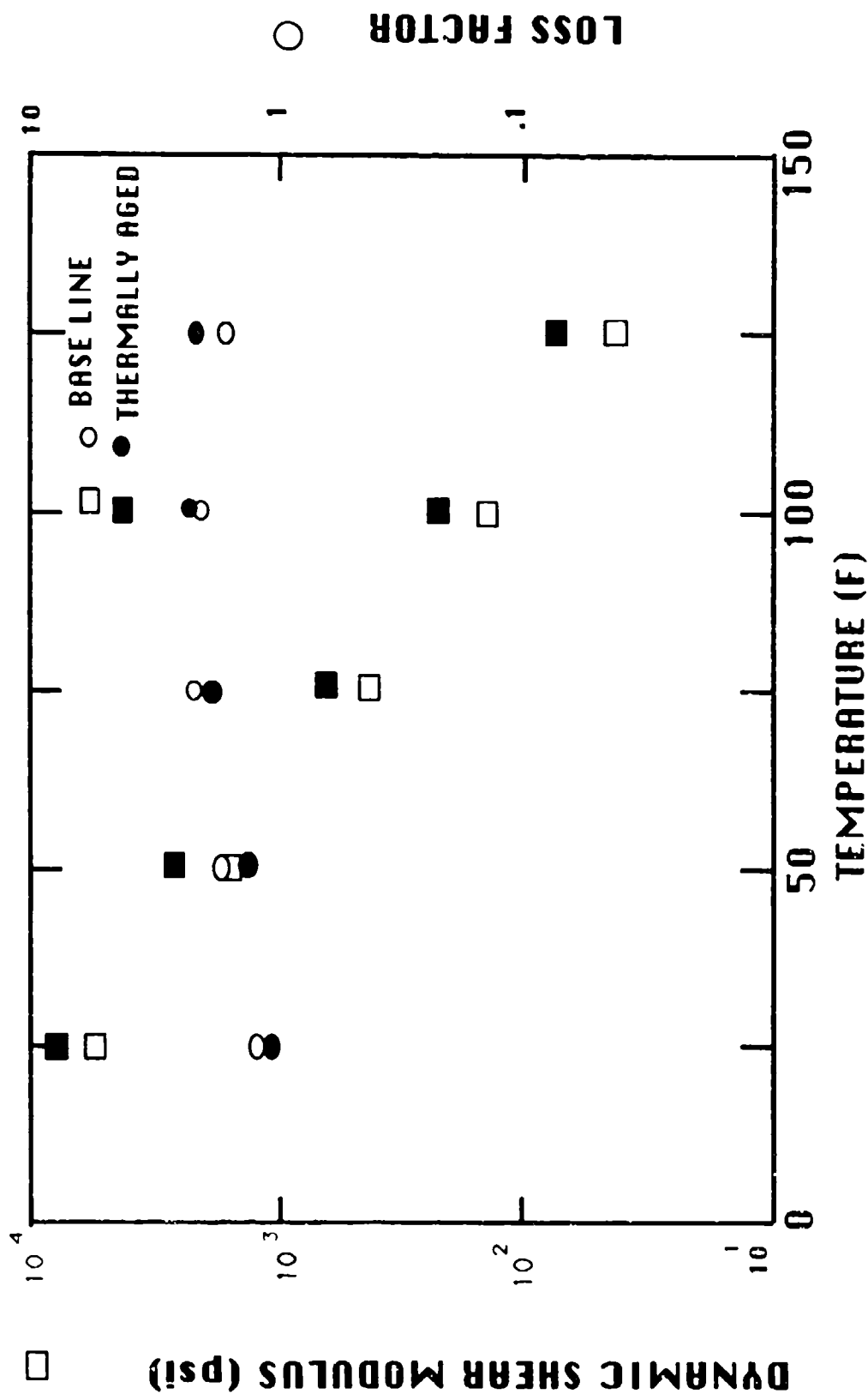


Figure D6. Viscoelastic Link Thermal Aging Results

BIBLIOGRAPHY

1. Ferman, M., Patel, S., Zimmerman, N., and Gerstenkorn, G. "A Unified Approach to Buffet Response of Fighter Aircraft Empennage," Proceedings of the AGARD Specialists' Meeting on Aircraft Dynamic Loads Due to Flow Separation, Sorrento, Italy. AGARD-CP-483, April 1990.
2. Miles, R. "The Prediction of the Damping Effectiveness of Multiple Constrained Layer Damping Treatments" Presented at Acoustical Society of America, Massachusetts Institute of Technology, June 11-15, 1979.
3. Nashif, A., Jones, D., and Henderson, J., Vibration Damping, John Wiley & Sons, 1985.
4. Parin, M., Rogers L., Moon Y., and Falugi M. "Practical Stand Off Damping Treatment for Sheet Metal," Proceedings of Damping '89, Volume II, Paper No. IBA, February 1989.